Title
Engineering of Novel Adeno-Associated Virus Vectors for Gene Therapy Applications

Author
Santiago Ortiz, Jorge Luis

Publication Date
2016

Peer reviewed|Thesis/dissertation

Engineering of Novel Adeno-Associated Virus Vectors for Gene Therapy Applications

By

Jorge Luis Santiago Ortiz

A dissertation submitted in partial satisfaction of the

requirements for the degree of

Doctor of Philosophy

in

Chemical Engineering

in the

Graduate Division

of the

University of California, Berkeley

Committee in charge:

Professor David V. Schaffer, Chair
Professor Danielle T. Tullman-Ercek
Professor Britt A. Glaunsinger

Spring 2016

Abstract

Engineering of Novel Adeno-Associated Virus Vectors for Gene Therapy Applications

by

Jorge Luis Santiago Ortiz

Doctor of Philosophy in Chemical Engineering

University of California, Berkeley

Professor David V. Schaffer, Chair

Gene therapy – the introduction of genetic material into cells and tissues of interest for a therapeutic purpose – has emerged as a very promising treatment for many diseases. Recent advances in genomics and proteomics, coupled with the advent of genome editing technologies, have generated an immense pool of potential nucleic acid cargoes that could be delivered as therapies for a wide array of diseases, ranging from monogenic disorders to cancer. However, before such therapies can be successful, a major hurdle must be overcome: the development of gene-carrying vehicles – also referred to as vectors – that can safely, efficiently, and specifically deliver those therapeutic payloads to the desired cells. The goal of this dissertation was therefore to address a major need in the field: the development of improved gene delivery vectors.

To date, more than 2,000 clinical trials employing gene transfer have taken place, establishing the safety of a number of vectors. Non-viral vectors can be easily produced at a large-scale and are amenable to the engineering of their chemical and physical properties via chemical modifications, but they suffer from a low delivery efficiency and cell toxicity. On the other hand, viral vectors harness the highly evolved mechanisms that viruses have developed to efficiently recognize and infect cells and offer several advantages that make them suitable candidates for use in gene delivery, both for therapeutic application and as tools for biological studies. In fact, gene therapy has enjoyed increasing success in clinical trials for numerous disease targets in large part due to the gene delivery capabilities viral vectors. Vectors derived from viruses have been used in the majority (over 68%) of gene therapy clinical trials to date, and the most frequently used have been based on adenovirus, retrovirus, vaccinia virus, herpesvirus, and adeno-associated virus (AAV).

AAV vectors are non-pathogenic and can transduce numerous dividing and non-dividing cell types. Because of these characteristics, AAV vectors have been utilized for gene therapy in various tissues. The amino acid composition of the viral capsid affects tropism (tissue specificity), cell receptor usage, and susceptibility to anti-AAV neutralizing antibodies – properties that influence efficacy in therapeutic gene delivery. However, AAV vectors can still encounter formidable impediments to efficacious gene delivery, including poor transduction (infection and expression of delivered gene) of some cell types, off-target transduction, difficulties with

biological transport barriers, and potential risks associated with the integration of their genetic load. Extensive engineering of the AAV capsid promises to overcome these delivery challenges and improve numerous clinically relevant properties. To this end, the overarching goal of my work in the Schaffer Laboratory, which is presented in this thesis dissertation, was to advance current gene delivery methods through the engineering and characterization of novel adeno-associated virus vectors for gene therapy and research applications.

To access new viral capsid sequences with potentially enhanced infectious properties and to gain insights into AAV's evolutionary history, we computationally designed and experimentally constructed an ancestral AAV capsid library. We performed selection for infectivity on the library, studied the resulting amino acid distribution, and characterized the selected variants, which yielded viral particles that were broadly infectious across multiple cell types. Ancestral variants displayed higher thermostability than modern (extant) natural AAV serotypes, a property that makes them promising templates for protein engineering applications, including directed evolution. Additionally, some variants displayed high in vivo infectivity on a mouse model, highlighting their potential for gene therapy.

Motivated by the success of directed evolution in the engineering of proteins with novel or enhanced properties, I worked in the engineering of AAV vectors for gene delivery to glioblastoma multiforme (GBM), a highly aggressive type of brain cancer. For this, I conducted directed evolution to select AAV variants with selective localization to and infectivity on GBM tumor cells and tumor initiating cells (TICs). Using an accurate GBM mouse model, I performed in vitro and in vivo selection, recovering viral particles that successfully trafficked to tumor cells and TICs in the brain after systemic administration to tumor-bearing animals. Following three rounds of in vivo selection, convergence was achieved upon several variants, the most abundant of which emerged from the ancestral reconstruction library. The selected variants are currently being characterized and assessed for their ability to deliver reporter and therapeutic genes, hopefully resulting in improved suppression of tumor progression compared to delivery with existing AAV serotypes. These novel vectors could enable new, potent therapies to treat GBM tumors and pave the way for engineering AAV vectors for other cancer targets.

In summary, this dissertation presents work on the development and characterization of a novel AAV capsid library, as well as on the implementation of this and of other libraries towards the engineering of novel AAV variants with selective gene delivery properties for brain tumors. The work herein presented aims to advance both the field of AAV vector engineering as a whole and the specific application of AAV vectors towards next generation cancer therapies.

Dedicated in Loving Memory of My Dear Grandmother

Carmen L. López López (1926-2015)
"Puro Amor Incondicional"

My role model to follow, who raised me and, through her unconditional love, instilled in me her core values of kindness, sacrifice, hard work, and perseveration even in the face of adversity.

Table of Contents

List of Figures

List of Tables

Acknowledgements

Graduate school has represented a tremendous professional and personal journey that, as clichéd as it sounds, can be accurately depicted by comparing it to a roller coaster – it is packed with amazing highs full of wonder, excitement, and joy, but it also comes with sometime equally powerful lows that are formidable challenges even for the toughest of skins. Accomplishing my goal of completing this degree would simply not having been possible without the contributions of many people who, in one way or the other, ensured I would reach the end.

First and foremost, I would like to thank my adviser, Professor David V. Schaffer, for giving me the opportunity to join his laboratory and work in gene therapy projects – the prospect of which was one of the biggest factors that drew me to Berkeley. From the beginning of my graduate career, Dave recognized the potential I had and did his best to promote my professional growth. I am extremely thankful to him for fostering the many collaborations I have been involved in, for his detailed feedback on manuscripts and applications, for allowing me to pursue my wish of writing a grant, and for encouraging me to pursue my desired career path. Finally, I cannot be thankful enough for his understanding of family situations and his support over them.

I would also like to thank my other two committee members, Professors Danielle Tullman-Ercek and Britt Glaunsinger. I had the amazing opportunity of learning from you both in the classroom as well as over the discussion of my research projects. Thank you for your feedback and for your time.

I would like to sincerely thank the Department of Chemical and Biomolecular Engineering, and the various people that offered assistance along the way. Rocío Sánchez, Fred Deakin, and Carlet Altamirano – thank you for your invaluable help with student affairs. The Department graciously supported me in three occasions to form part of the U.C. Berkeley recruiting team at the Ivy Plus Recruiting Fairs in Puerto Rico and I am forever thankful for its support, which allowed me to foster an interest for graduate school in many Puerto Rican students and also let me briefly visit my family in the island. The department also provided classrooms over the summer for lessons with the SMART Program in San Francisco – events I thoroughly enjoyed and enabled me to nurture my passion for teaching. Finally, the Department also nominated me for the U.C. Berkeley Dissertation Year Fellowship, which financially supported me throughout this last year of graduate school and facilitated the continuation of various research projects.

I could not have asked for a more wonderful environment than the Schaffer Laboratory, which fomented a kind, generous, diverse, and inclusive atmosphere and allowed me to feel perfectly comfortable and right at home. Noem (Wanichaya Ramey) – I don't know what I would have done without you as the lab manager. I can't thank you enough for all your help, last minute requests, support, and insightful conversations. I am so thankful for having you as a lab manager and as a friend! I would especially like to thank Dawn Spelke for so many things: being the very best of labmates; sitting next to me for over 5.5 years (I imagine that was a great test of patience!); our many science discussions, from which I learned so much by bouncing ideas back and forth regarding both your projects and mine; our conversations over lunch, coffee, dinner, and late lab nights, which I have sorely missed ever since you were finished in the lab and which have helped me grow as a person so much; but most importantly - for being the amazing friend you are, full of unconditional support and wise advice, always being there for the good, the bad, and the ugly

moments that life brings. I can't wait to be your bridesman, and I can't wait for you to be my groomswoman, either.

There are many other people in the Schaffer Laboratory I would like to thank. I had the great opportunity of having David Ojala as a collaborator within the lab. David, I couldn't have hoped for a better collaborator and co-author; thank you for such a great, productive, and enjoyable work experience. Andrew Steinsapir worked as my undergraduate student for almost four years, through which he grew to be an amazing researcher and a great friend. Thank you for your optimism, cheer, and disposition, and for being my right hand in lab for so much time. Sabrina Sun, I am excited about the prospect of having you continue follow-up studies on my projects, and of going to every last Pure Strength class I can with you. It's been great to have you as my friend and colleague! Barbara Ekerdt, I am honored to have had you as a friend, ChemE cohort mate, and labmate – you are an inspiration to us all with your courage, determination, and optimism, even in the face of adversity. You are a rockstar! Andrew Bremer, thank you for offering such interesting perspectives, and for your drive to continue making our lab and U.C. Berkeley increasingly more diverse. Riya Muckom, I am so thankful for having had you as a swimming buddy, and I look forward to more great conversations with you. Prajit Limsirichai, I want to thank you immensely for your kindness and generosity, and for always having a cheery disposition to offer a helping hand. I am very grateful for all your help throughout these years. Thom Gaj, thank you for introducing me to the world of genome editing, and for all of your insightful science advice. Maroof Adil, thank you for your assistance with various experiments, procedures, and certifications, and for being such an awesome conference travel buddy. Alyssa Rosenbloom, thank you for such great life advice and for making my tissue culture time the best in the world. Leah Byrne, thank you for your assistance and advice on AAV projects, ideas, and experiments, and for encouraging me to apply for the Ford Foundation Fellowship. Yuzhang Chen, thank you for providing your time as an undergraduate research assistant in this last and very busy year. Finally, Marc Martin Casas, honorary Schaffer lab member, thank you for friendship and for so many good conversations about graduate school, life, and of course, politics. I would like to also thank previous laboratory members that kindly offered their help and time, both within and outside of lab – Ashley Fritz, Albert Keung, Priya Shah, Siddarth Dey, Jonathan Foley, Lukasz Bugaj, Melissa Kotterman, Anthony Conway, Sisi Chen, and John Weinstein. Thank you for everything!

My experience in the Schaffer laboratory was decorated with multiple collaborations that truly embodied the multidisciplinarity that allured me about Berkeley. To my collaborators – David Ojala, John Weinstein, Oscar Westesson, Sophie Wong, Eda Altiok, Wesley Jackson, Thom Gaj, David Booth – thank you!

U.C. Berkeley is full of very special people and organizations that have contributed to my growth as a person, student, teacher, and researcher. Audrey Knowlton, thank you so much for facilitating my involvement with the Ivy Plus recruiting fairs and for requesting my financial support for them. Meltem Erol – thank you for being such a strong champion for diversity for the College of Engineering and for U.C. Berkeley as a whole, and for all of the invaluable support you have provided me. Thank you also for introducing me to Aimée Tabor, may she rest in peace, with whom I had the pleasure of working as a mentor for the summer research program (TRUST) she was running. Ira Young, thank you for your continuous help and support, and for striving to make U.C. Berkeley an ever more inclusive campus. Carlo Alesandrini, it was an honor to GSI for your

Chemical Process Design class twice; thank you for being an inspiration for a career model to follow and a great pedagogue to be.

Graduate student organizations are an invaluable asset that make U.C. Berkeley a wonderful school to be in. LAGSES, the Latino/a Association of Graduate Students in Engineering and Sciences, was a transformative instrument in my development as a graduate student, and through it I forged new and long-lasting friendships, enhanced my leadership and communication skills, and contributed to the recruitment and retention of underrepresented minority students in Berkeley. I hope to continue being involved with it as an alumni and to see it grow to even farther horizons.

My unforgettable experience in Berkeley wouldn't have been possible without the support of my friends. Boris Russ – what an honor it has been to be your friend from the very start of my stay here. Thank you so much for your support in good and bad times, for always be willing to lend an ear and give good advice, and for being an awesome gym buddy and getting me started going to the RSF. Monica Kapil, thank you for being the amazing and loving friend you have been to me, full of understanding, love, kindness, and of course, fun. I loved sharing our passion for diversity and inclusion and for good times. The bonds I have with you two, from friendship, to a devotion for family, to the understanding of what it means to have lost a loved one, united us deeply and will be forever cherished in my heart. Speaking of beloved friends, shout out to Dawn, whom I've already mentioned. Joseph Chavarria, thank you for many fun times, for great conversations, for supporting me as I had my full coming out experience in California and became fully comfortable in my own skin, and for opening your family and your country to me. Olivia Price, my sister pea from another pod, thank you for your support, your love, and your light, which always emanates from you and brightens up anywhere you go to. It was my absolute pleasure to have shown you all my island and my family.

Diana Rodríguez – you were the beacon that reinforced my path to Berkeley, from conversations back in INQU about the wonderful time you had had over your summer research experience, to guiding me over my visits to campus, to have picked me up from the airport as soon as I arrived in this new world. Thank you so much for your kindness and acceptance, for welcoming me here, for providing advice along the way, and for introducing me to some of the very best people I have met. Jessica Jiménez – together with Diana, you also formed part of my welcoming to Berkeley. I am so, so thankful for your friendship, from which I've learned and grown as a person so much. Thank you for your much needed support during my coming out, for all of our amazing brunch and sushi dates, for having patience when I am late, and for so much good work and life advice. I feel honored that you have welcomed me into your life and your blossoming family, and I can't wait to have many more good times with you, Héctor, and Maya. Amneris Miranda, Amne! I am so lucky to have met you, and so lucky to have you as my dear friend. Your kindheartedness, love, and constant support never cease to amaze me. You are my inspiration in so many aspects of life – from core values, to the proper nurturing of friendships, to the utmost devotion you have for your family. Thank you for being in my life. Steven Álvarez, thank you for your friendship, many science discussions, and many great conversations. It's been great to have you as a Stanley Hall neighbor, and I wish you the best of luck as you also finish your degree soon. David Cereceda and Celia Reina Romo – you two provided so much love, kindness, and support throughout the time in which we overlapped in Berkeley. What an amazing experience it has been to have you as friends, to have you as an inspiration for hard work, for

striving for excellence, and most importantly, for having a loving relationship. Thank you for your friendship, warmth, fun times in land and sea, and for much needed encouragement throughout my journey through grad school. I can't wait to have you on the same coast again! Finally, my dear friends from school and undergrad – Natalia, Charlie, José, Katia, Rafa, Tony, and Natalia Arzola – thank you for your friendship and for putting a smile on my face every time I have a chance to visit the island.

I am deeply thankful to my Ashby roommates, current and past: Brett Robison, Thornton Thompson, Jonathan Braverman, Jesse Niebaum, Clayton McSpadden, and Matthew Knight, for contributing to a comfortable and enjoyable place to call home. It has been great living with you and getting to know you as roommates and friends. Shout out to almost roommate Megan Hochstrasser, whose friendship I deeply cherish. I would also like to thank the ChemE class of 2010 – I loved the support and comradery that characterized our class, particularly during prelims, and thoroughly enjoyed all the fun times we had together.

I simply cannot describe with words what it means to have had the unconditional love and support of my family in all aspects of my life. To my late beloved grandmother Carmen López López, who was actually more of a mother to me and whom I referred to as mami – I am forever indebted to you for enriching my life in many more ways that I can imagine. You taught me about life, family, love, faith, and were my sturdy pillar throughout my entire life. I only wish you were still here so I could recite these words to you. You will forever live in my heart, my values, and my life. To my mother, Wanda Ortiz López, thank you for your unyielding support in every endeavor I have undertaken, for helping me in whatever I needed in every way you could, for understanding that some of us are different and accepting me as I am, and for welcoming with open arms the wonderful man I love.

Teddy Ortiz López, my uncle, godfather, but above all, father figure – I am so sincerely thankful for your love and support and your kindness, for always being there no matter what, and for representing such an excellent role model of what a good father should be like. Ivelisse Marrero Ortiz, I love you deeply as my aunt, my friend and confidant, and my second (or third, rather) mom. Thank you both for welcoming me into your loving family, where I love Yereimi and Adriana as if they were my sisters. I would also like to sincerely thank Aunt Yiyi, Uncle David, Uncle Luis and Aunt Jannette, and my dear cousins Melissa, Amalie, Gaby, José, and Brian – thank you all support for your sincere love, support, and acceptance. Finally, to my cousin Desire - I am humbled to know that you have seen me as a role model for a person and a scientist, and I am excited to see what your professional future brings. Maybe you will be the next STEM Ph.D. in our family!

Finally, AJ Habib – I can't describe how much your love and your encouragement mean to me. The joy you have brought into my life has carried me through the big and stressful roller coaster that was this last year and a half. I feel like the luckiest guy out there for being with you, and I cannot wait to find out and experience what the future has in store for us.

Chapter 1: Introduction

1.1 Gene Therapy

Gene therapy, defined as the introduction of genetic material into a target cell for therapeutic benefit, is a very promising treatment for many diseases, including monogenic diseases, cancer, cardiovascular disease, and neurodegenerative diseases. To date, more than 2,000 clinical trials employing gene transfer have taken place and in general have established that a number of vehicles or vectors are safe[1,2]. For gene therapies to be increasingly successful, however, a major hurdle must be overcome: the development of gene delivery vectors that can safely, efficiently, and specifically deliver genetic material to the target cells.

Non-viral vectors can be easily produced at a large scale and are readily amenable to engineering or enhancement of their functional properties via chemical modifications; however, they suffer from a low delivery efficiency and in some cases cell toxicity[3]. On the other hand, viral vectors harness the highly evolved mechanisms that the parental viruses have developed to efficiently recognize and infect cells and offer several advantages, which make them suitable for both therapeutic application and as tools for biological studies; however, their delivery properties can be challenging to engineer and improve. That said, viral vectors have been used in the majority (over 68%[4]) of gene therapy clinical trials, and their increasing success has been enabled in large part by the gene delivery capabilities of adeno-associated virus (AAV)[5], lentiviral vectors[6], and oncolytic viruses[7]. The first regulatory approved gene therapy product in Western nations (in the EU in 2012) uses an AAV1 vector to treat LPLD[8], and in 2015, the first recombinant viral therapy – an oncolytic herpesvirus for the treatment of melanoma – received regulatory approval in the US[7].

1.2 AAV Vectors in Gene Therapy

AAV vectors in particular have been increasingly successful due to their gene delivery efficacy, lack of pathogenicity, and strong safety profile[5]. As a result of these properties, AAV vectors have enabled clinical successes in a number of recent clinical trials that have established the promise of gene therapy in general, including for the treatment of diseases such as Leber's congenital amaurosis (LCA)[9,10], where over four Phase I and I/II clinical trials have demonstrated safety and long-term (over five years) improvement in retinal and visual function; hemophilia B, targeted in several Phase I and Phase I/II clinical trials that have shown long-term efficacy and no toxic effects[2,11]; and the Sanfilippo B syndrome, where gene expression and consequently improved cognitive development have been sustained for at least a year and are still ongoing (Pasteur Institute Phase I/II trial, unpublished). Moreover, alipogene tiparvovec (Glybera; uniQure), a gene therapy for lipoprotein lipase deficiency (LPLD) that employs an AAV vector, received regulatory approval by the European Medicines Agency in 2012[12]. AAV vectors may also offer a strong potential for the treatment of cancer, and their excellent gene delivery properties have been harnessed for *in vitro* cancer studies (i.e. cultured cells), *in vivo* pre-clinical cancer models (i.e. animal models of cancer), and cancer clinical trials under development[13].

1.3 AAV Biology

AAV is a single-stranded DNA parvovirus with a 4.7 kb genome (Figure 1.1A) composed of the *rep* and *cap* genes flanked by inverted terminal repeats (ITRs)[14]. The *rep* gene encodes non-structural proteins involved in viral replication, packaging, and genomic integration, whereas the *cap* gene codes for structural proteins (VP1, VP2, VP3) that assemble to form the viral capsid, which serves as the viral gene delivery vehicle. Additionally, an alternative open reading frame nested within the *cap* gene encodes the assembly activating protein (AAP), involved in the targeting and assembly of capsid proteins[15]. Following cellular entry through cell surface receptor-mediated endocytosis, endosomal escape, trafficking to the nucleus, uncoating, and second DNA strand synthesis, the virus can enter its replication cycle in the presence of a helper virus[16]. In the absence of a helper, however, AAV genomes can establish latency and persist as episomes[17] or in some cases integrate into host chromosomal DNA[18].

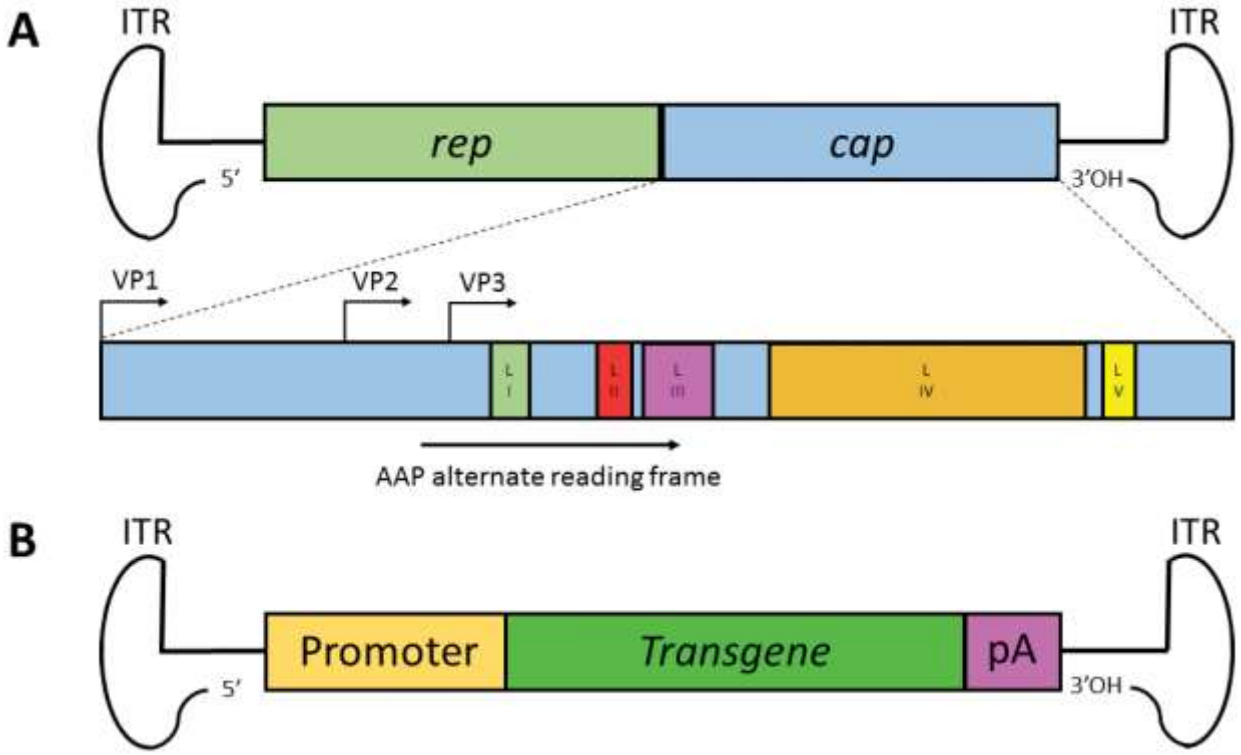

Figure 1.1: Genomic structure of AAV and AAV vectors. (A) The 4.7kb AAV genome is composed of the *rep* and *cap* genes flanked by inverted terminal repeats (ITRs). The *rep* gene codes for non-structural proteins involved in viral replication, packaging, and genomic integration, while the *cap* gene encodes the structural proteins VP1, VP2, and VP3 that assemble to form the viral capsid in a ratio of 1:1:10, respectively, in a total of 60 protein subunits. The assembly-activating protein (AAP) is translated from an alternate open reading frame. Also depicted are capsid loop domains I through V (LI-LV), which contain variable regions that influence gene delivery properties. **(B)** Recombinant AAV vectors are generated by replacing the *rep* and *cap* genes with a gene expression cassette (e.g. promoter, transgene, poly(A) tail) flanked by the ITRs. Vectors are then packaged by supplying the *rep* and *cap* genes *in trans* as well as adenoviral helper genes required for AAV replication.

1.4 AAV Vectors: Properties and Clinical Success

Recombinant AAV vectors can be generated by replacing the endogenous *rep* and *cap* genes with an expression cassette consisting of a promoter driving a transgene of interest and a poly(A) tail

(Figure 1.1B). The *rep* and *cap* genes are then provided *in trans* as helper packaging plasmids together with adenoviral helper genes needed for AAV replication[5]. Over 100 natural AAV variants have been isolated, and variations in amino acid sequences result in somewhat different tropisms (the range of cells and tissues a virus can infect)[19], though none are pathogens[20]. Recombinant vectors have been generated from a number of these serotypes[5], though vectors based on AAV-serotype 2 (AAV2) have been the most widely studied and used in preclinical models and clinical trials to date. In general, vectors based on natural AAV variants have desirable gene delivery properties: a lack of pathogenicity and immunotoxicity, which grants them a strong safety profile[20]; the ability to infect dividing and non-dividing cells with reasonable efficiency[21]; the ability to mediate stable, long-term gene expression following delivery[19]; a ~5 kb genome that can carry a broad range of cargoes[22]; access to faster expression kinetics when using self-complementary, double stranded DNA forms of the vector genome[23]; and importantly the potential for engineering and optimizing the viral capsid and thus vector delivery properties[14]. Accordingly, AAV-based vectors have been harnessed in an increasing number of clinical trials (>130 to date) for tissue targets including liver, lung, brain, eye, and muscle[5,6]. As a result of its properties, as mentioned above, AAV has enabled clinical efficacy in an increasing number of trials for various diseases[2,8,24-26].

1.5 Gene Delivery Challenges of AAV Vectors

Natural variants of AAV have enabled increasing success in human clinical trials, which have in turn provided strong momentum to the gene therapy field as a whole. That said, natural AAV serotypes have some shortcomings that render this success challenging to extend to the majority of human diseases. As has been reviewed[5], barriers for AAV and other vectors include: prior exposure of most people to natural AAVs leading to anti-AAV neutralizing antibodies that can reduce vector delivery efficiency by orders of magnitude *in vivo,* poor vector biodistribution to important tissue targets, limited spread within those tissues, an inability to target specific cells, and limited efficiency for many therapeutically relevant target cells. These concerns have motivated the engineering of AAV capsids that can more efficiently traffic to and transduce cells, as well as the engineering of genetic cargos for higher potency and selective expression.

1.6 General Developments in AAV Vector Engineering

The amino acid sequence of the proteins that constitute the viral capsid (Figure 1.2) determines an AAV vector's delivery properties, including interactions with tissue and vasculature, humoral and cellular components of the immune system, specific receptors on the target cell surface, the endosomal network following receptor-mediated internalization, the cytosol after the viral phospholipase domain enables endosomal escape, and ultimately the nucleus. Thus, engineering the AAV capsid can generate novel AAV variants with novel and enhanced delivery properties[5]. Such vector engineering efforts can be grouped into two categories: rational design, where structure-function relationships are used to guide specific capsid modifications, and directed evolution, where libraries of AAV capsids are generated using a range of mutagenesis techniques and then subjected to a selective pressure for properties of interest.

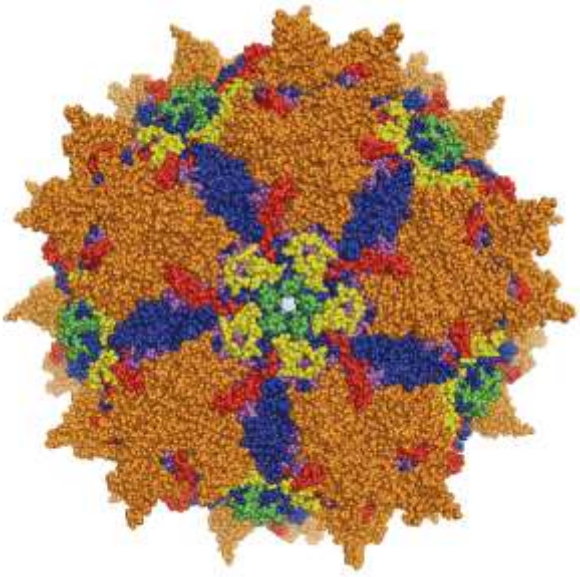

Figure 1.2: Representation of AAV2 capsid structure. Crystal structure of the AAV2 capsid[27], the most widely used and studied AAV serotype. Loop domains I through V are depicted following the same color scheme as in Figure 1.1A. Image was produced with Pymol[28].

The AAV capsid has been rationally engineered in several ways. For example, capsid surface-exposed tyrosine residues, whose phosphorylation targets the virion for ubiquitination and subsequent proteasomal degradation, have been modified via site-directed mutagenesis to phenylalanine residues to generate variants with reduced proteasomal degradation and subsequent higher gene expression[29]. Structural capsid information has also been used to generate variants with some resistance to pre-existing neutralizing antibodies by mutating surface residues that may interact with Immunoglobulin G antibodies (IgG's)[30]. As reviewed elsewhere[13], rational design has also been employed to generate variants with enhanced transduction (infection and transgene expression) in tumor cells by using site-directed mutagenesis and inserting peptides with motifs that bind to receptors highly expressed in cancer cells.

In general, however, the AAV delivery pathway from point of administration until the particle arrives in the nuclei of target cells is extremely complex, and there is often insufficient knowledge of viral structure-function relationships to enable rational design efforts. Therefore, another approach is based on the idea that evolution can generate novel and useful biological function even in the absence of detailed mechanistic knowledge. Specifically, directed evolution has been developed and implemented to generate greatly enhanced AAV variants for a variety of applications. In this approach, the AAV *cap* gene is genetically diversified to create large libraries of novel AAV variants (~10^4 - 10^8) utilizing a range of molecular approaches including DNA shuffling, random point mutagenesis, insertional mutagenesis, random peptide insertions, and most recently ancestral reconstructions[31-40]. The libraries are then subjected to a selective pressure to acquire specific, advantageous delivery properties[5], and after a suitable number of selection rounds individual AAV variants are isolated, validated, and harnessed for therapeutic gene delivery in disease models. Directed evolution has been applied[14] to create novel, optimized AAV vectors with enhanced delivery to non-permissive cells such as human airway epithelium[41], neural stem

cells[42], human pluripotent stem cells[43], retinal cells[44], and other tissues *in vitro* and *in vivo*[31,32,44-48]. AAV vectors have also been evolved for *in vivo* enhanced tissue spread and infection of non-permissive cell types[44,45]. Thus, *in vivo* directed evolution strategies could potentially be extended to engineer novel AAV vectors for enhanced gene delivery to tumors.

1.7 Scope of the Dissertation

This thesis dissertation was motivated by the continuous need for the development of improved gene delivery vehicles that are safer, more specific, and more efficient at delivering nucleic acid cargoes to cells and tissues of therapeutic interest. AAV vectors hold a great promise for gene therapy applications, and the work presented here advances the field of AAV vector development in multiple fronts. In **Chapter 2**, an ancestral reconstruction of the AAV capsid is generated as a combinatorial library that is computationally designed, synthesized, packaged, and characterized *in vitro* and *in vivo*. **Chapter 3** presents an extensive review of AAV vector developments for cancer cell-specific transduction and gene expression, and of the employment of AAV vectors for gene delivery in pre-clinical cancer models and in cancer clinical trials. Finally, in **Chapter 4**, a novel *in vivo* directed evolution strategy is developed to engineer AAV vectors for gene delivery to glioblastoma multiforme tumor cells and tumor initiating cells following systemic administration. Overall, this dissertation presents the development of novel AAV libraries and their subsequent employment in the engineering of improved vectors; it aims to enhance AAV directed evolution efforts in general and to further advance the promise of AAV for cancer applications, a field it is beginning to enter.

1.8 References

1. Simonelli, F. *et al.* Gene therapy for Leber's congenital amaurosis is safe and effective through 1.5 years after vector administration. *Mol Ther* **18**, 643-50 (2010).
2. Nathwani, A.C. *et al.* Adenovirus-associated virus vector-mediated gene transfer in hemophilia B. *N Engl J Med* **365**, 2357-65 (2011).
3. Gao, X., Kim, K.S. & Liu, D. Nonviral gene delivery: what we know and what is next. *AAPS J* **9**, E92-104 (2007).
4. Indications Addressed by Gene Therapy Clinical Trials. Vol. 2015 (The Journal of Gene Medicine, www.wiley.co.uk/genmed/clinical).
5. Kotterman, M.A. & Schaffer, D.V. Engineering adeno-associated viruses for clinical gene therapy. *Nat Rev Genet* **15**, 445-51 (2014).
6. Asokan, A., Schaffer, D.V. & Samulski, R.J. The AAV vector toolkit: poised at the clinical crossroads. *Mol Ther* **20**, 699-708 (2012).
7. Ledford, H. Cancer-fighting viruses win approval. *Nature* **526**, 622-3 (2015).
8. Gaudet, D. *et al.* Efficacy and long-term safety of alipogene tiparvovec (AAV1-LPLS447X) gene therapy for lipoprotein lipase deficiency: an open-label trial. *Gene Ther* **20**, 361-9 (2013).
9. Testa, F. *et al.* Three-year follow-up after unilateral subretinal delivery of adeno-associated virus in patients with Leber congenital Amaurosis type 2. *Ophthalmology* **120**, 1283-91 (2013).
10. Dalkara, D. & Sahel, J.A. Gene therapy for inherited retinal degenerations. *C R Biol* **337**, 185-92 (2014).
11. Ohmori, T., Mizukami, H., Ozawa, K., Sakata, Y. & Nishimura, S. New approaches to gene and cell therapy for hemophilia. *J Thromb Haemost* **13 Suppl 1**, S133-42 (2015).
12. Carpentier, A.C. *et al.* Effect of alipogene tiparvovec (AAV1-LPL(S447X)) on postprandial chylomicron metabolism in lipoprotein lipase-deficient patients. *J Clin Endocrinol Metab* **97**, 1635-44 (2012).
13. Santiago-Ortiz, J.L. & Schaffer, D.V. Adeno-associated virus (AAV) vectors in cancer gene therapy. *J Control Release* (2016).
14. Bartel, M.A., Weinstein, J.R. & Schaffer, D.V. Directed evolution of novel adeno-associated viruses for therapeutic gene delivery. *Gene Ther* **19**, 694-700 (2012).
15. Sonntag, F., Schmidt, K. & Kleinschmidt, J.A. A viral assembly factor promotes AAV2 capsid formation in the nucleolus. *Proc Natl Acad Sci U S A* **107**, 10220-5 (2010).
16. Bartlett, J.S., Samulski, R.J. & McCown, T.J. Selective and rapid uptake of adeno-associated virus type 2 in brain. *Hum Gene Ther* **9**, 1181-6 (1998).
17. Duan, D. *et al.* Circular intermediates of recombinant adeno-associated virus have defined structural characteristics responsible for long-term episomal persistence in muscle tissue. *J Virol* **72**, 8568-77 (1998).

18. Kotin, R.M. *et al.* Site-specific integration by adeno-associated virus. *Proc Natl Acad Sci U S A* **87**, 2211-5 (1990).
19. Ellis, B.L. *et al.* A survey of ex vivo/in vitro transduction efficiency of mammalian primary cells and cell lines with Nine natural adeno-associated virus (AAV1-9) and one engineered adeno-associated virus serotype. *Virol J* **10**, 74 (2013).
20. Berns, K.I. & Linden, R.M. The cryptic life style of adeno-associated virus. *Bioessays* **17**, 237-45 (1995).
21. Flotte, T.R., Afione, S.A. & Zeitlin, P.L. Adeno-associated virus vector gene expression occurs in nondividing cells in the absence of vector DNA integration. *Am J Respir Cell Mol Biol* **11**, 517-21 (1994).
22. Mancheno-Corvo, P. & Martin-Duque, P. Viral gene therapy. *Clin Transl Oncol* **8**, 858-67 (2006).
23. McCarty, D.M., Monahan, P.E. & Samulski, R.J. Self-complementary recombinant adeno-associated virus (scAAV) vectors promote efficient transduction independently of DNA synthesis. *Gene Ther* **8**, 1248-54 (2001).
24. Jacobson, S.G. *et al.* Gene therapy for leber congenital amaurosis caused by RPE65 mutations: safety and efficacy in 15 children and adults followed up to 3 years. *Arch Ophthalmol* **130**, 9-24 (2012).
25. MacLaren, R.E. *et al.* Retinal gene therapy in patients with choroideremia: initial findings from a phase 1/2 clinical trial. *Lancet* **383**, 1129-37 (2014).
26. Stroes, E.S. *et al.* Intramuscular administration of AAV1-lipoprotein lipase S447X lowers triglycerides in lipoprotein lipase-deficient patients. *Arterioscler Thromb Vasc Biol* **28**, 2303-4 (2008).
27. Xie, Q. *et al.* The atomic structure of adeno-associated virus (AAV-2), a vector for human gene therapy. *Proc Natl Acad Sci U S A* **99**, 10405-10 (2002).
28. Schrodinger, LLC. The PyMOL Molecular Graphics System, Version 1.3r1. (2010).
29. Zhong, L. *et al.* Next generation of adeno-associated virus 2 vectors: point mutations in tyrosines lead to high-efficiency transduction at lower doses. *Proc Natl Acad Sci U S A* **105**, 7827-32 (2008).
30. Lochrie, M.A. *et al.* Mutations on the external surfaces of adeno-associated virus type 2 capsids that affect transduction and neutralization. *J Virol* **80**, 821-34 (2006).
31. Koerber, J.T., Maheshri, N., Kaspar, B.K. & Schaffer, D.V. Construction of diverse adeno-associated viral libraries for directed evolution of enhanced gene delivery vehicles. *Nat Protoc* **1**, 701-6 (2006).
32. Koerber, J.T., Jang, J.H. & Schaffer, D.V. DNA shuffling of adeno-associated virus yields functionally diverse viral progeny. *Mol Ther* **16**, 1703-9 (2008).
33. Koerber, J.T. & Schaffer, D.V. Transposon-based mutagenesis generates diverse adeno-associated viral libraries with novel gene delivery properties. *Methods Mol Biol* **434**, 161-70 (2008).

34. Santiago-Ortiz, J. *et al.* AAV ancestral reconstruction library enables selection of broadly infectious viral variants. *Gene Ther* (2015).
35. Perabo, L. *et al.* Combinatorial engineering of a gene therapy vector: directed evolution of adeno-associated virus. *J Gene Med* **8**, 155-62 (2006).
36. Zinn, E. *et al.* In Silico Reconstruction of the Viral Evolutionary Lineage Yields a Potent Gene Therapy Vector. *Cell Rep* **12**, 1056-68 (2015).
37. Grimm, D. *et al.* In vitro and in vivo gene therapy vector evolution via multispecies interbreeding and retargeting of adeno-associated viruses. *J Virol* **82**, 5887-911 (2008).
38. Li, W. *et al.* Engineering and selection of shuffled AAV genomes: a new strategy for producing targeted biological nanoparticles. *Mol Ther* **16**, 1252-60 (2008).
39. Muller, O.J. *et al.* Random peptide libraries displayed on adeno-associated virus to select for targeted gene therapy vectors. *Nat Biotechnol* **21**, 1040-6 (2003).
40. Varadi, K. *et al.* Novel random peptide libraries displayed on AAV serotype 9 for selection of endothelial cell-directed gene transfer vectors. *Gene Ther* **19**, 800-9 (2012).
41. Excoffon, K.J. *et al.* Directed evolution of adeno-associated virus to an infectious respiratory virus. *Proc Natl Acad Sci U S A* **106**, 3865-70 (2009).
42. Jang, J.H. *et al.* An evolved adeno-associated viral variant enhances gene delivery and gene targeting in neural stem cells. *Mol Ther* **19**, 667-75 (2011).
43. Asuri, P. *et al.* Directed evolution of adeno-associated virus for enhanced gene delivery and gene targeting in human pluripotent stem cells. *Mol Ther* **20**, 329-38 (2012).
44. Dalkara, D. *et al.* In vivo-directed evolution of a new adeno-associated virus for therapeutic outer retinal gene delivery from the vitreous. *Sci Transl Med* **5**, 189ra76 (2013).
45. Klimczak, R.R., Koerber, J.T., Dalkara, D., Flannery, J.G. & Schaffer, D.V. A novel adeno-associated viral variant for efficient and selective intravitreal transduction of rat Muller cells. *PLoS One* **4**, e7467 (2009).
46. Dalkara, D. *et al.* AAV mediated GDNF secretion from retinal glia slows down retinal degeneration in a rat model of retinitis pigmentosa. *Mol Ther* **19**, 1602-8 (2011).
47. Koerber, J.T. *et al.* Molecular evolution of adeno-associated virus for enhanced glial gene delivery. *Mol Ther* **17**, 2088-95 (2009).
48. Maheshri, N., Koerber, J.T., Kaspar, B.K. & Schaffer, D.V. Directed evolution of adeno-associated virus yields enhanced gene delivery vectors. *Nat Biotechnol* **24**, 198-204 (2006).

Chapter 2: Reconstruction and Characterization of an Ancestral Adeno-Associated Virus (AAV) Library

This chapter is adapted from a manuscript published as

J. Santiago-Ortiz*, D. Ojala*, O. Westesson, J. Weinstein, S. Wong, A. Steinsapir, S. Kumar, I. Holmes, D. Schaffer. AAV Ancestral Reconstruction Library Enables Selection of Broadly Infectious Viral Variants. *Gene Therapy* **22**, 934-946 (2015).

* Indicates co-first authors.

2.1 Introduction

Advances in DNA sequencing, synthesis, and computational phylogenetic analyses are enabling the computational reconstruction and experimental investigation of ancestral protein variants. Following the first ancestral reconstruction study – which resurrected a functional, ancestral digestive ribonuclease from an extinct bovid ruminant using the parsimony principle[1] – reconstructions and functional analyses have been carried out on inferred ancestral proteins belonging to eubacteria, bony vertebrates, mammals, and the least common ancestor of higher primates using several inference methods, including the parsimony, consensus, Bayesian distance, and maximum likelihood methods[2]. Such ancestral reconstructions and subsequent analysis of resurrected variants have yielded insights into the conditions that led to protein evolution as well as the continuous adaption of organisms to changing environmental conditions[3].

Ancestral reconstructions have also been harnessed to incorporate additional sequence diversity into genetic libraries for protein engineering. For instance, small libraries of resurrected ancestral variants were used in evolutionary studies of protein diversification[3-5] and to generate variants that are more tolerant to deleterious mutations. Moreover, inferred ancestral sequences have been combined with extant sequences by swapping residues of interest (e.g. residues in or close to an enzyme's catalytic site) in modern sequences with those of the inferred ancestor. This residue swapping approach was used in basic evolutionary studies[6] as well as to screen for variants with properties such as increased thermostability[7], improved catalytic activity[8], novel substrate binding[9], and higher solubility[10]. Ancestral reconstruction is thus a versatile approach to explore new sequence space for engineering proteins with novel or enhanced properties, and it may likewise offer potential for gene therapy.

This approach has recently been extended to more complex, multimeric proteins including viruses. The evolutionary history of viruses is an especially interesting application given their rapid mutational rates, importance to public health, and promise for gene therapy. For example, ancestral reconstructions of viral proteins have been generated with the goal of developing vaccine candidates against HIV-1 and influenza virus[11,12], and to study the functionality and properties of the resurrected variants of HIV-1, influenza, and coxsackievirus[13,14]. These studies demonstrated that viral reconstructions could recapitulate properties of modern variants, including immunogenicity, packaging, tropism, and cell receptor dependencies. These properties are key to the viral life cycle, and they are also important properties for viruses used as gene therapy vectors.

Adeno-associated virus (AAV) vectors are highly promising for gene therapy. AAVs are non-pathogenic[15] and can transduce numerous dividing and non-dividing cell types, leading to long term expression in the latter[16]. AAV vectors have accordingly been utilized for gene therapy in various tissues, including liver, lung, brain, eye, and muscle[17,18]. Furthermore, Glybera, the first gene therapy product approved in the European Union in 2012, employs an AAV1 vector[19]. The amino acid composition of the viral capsid, encoded by the *cap* gene, affects AAV tropism, cell receptor usage, and susceptibility to anti-AAV neutralizing antibodies[20]. These key properties in turn impact efficacy in therapeutic gene delivery, which is often limited by poor transduction of numerous cell types, off-target transduction, difficulties with biological transport barriers, and neutralization by pre-existing anti-AAV antibodies[18]. However, extensive engineering of the AAV capsid, via modification of the *cap* gene, promises to improve numerous clinically relevant properties[18].

Given the functional diversity of natural AAV serotypes, availability of numerous genetic sequences, and demonstrated clinical efficacy of recombinant vectors, AAV is an intriguing candidate for ancestral reconstruction, which could further our understanding of its evolutionary history and plasticity. Interesting questions include whether reconstructed variants exhibit higher or lower infectivity on a range of cell types, and whether they are relatively specific for particular cells – an attractive feature for many clinical applications – or are instead promiscuous, as are many extant serotypes. Finally, ancestral sequences and libraries may be useful starting materials for directed evolution studies[8,21], especially considering that such AAVs likely gave rise to the modern serotypes with their divergent biological properties and tropism.

Motivated by these questions, we conducted ancestral reconstruction of the AAV capsid. Acknowledging and taking advantage of the inherent ambiguity in reconstructing sequences containing highly divergent residues, we synthesized the inferred ancestral capsid not as a single "best guess" sequence, but rather as a large combinatorial library of candidate sequences incorporating degenerate residues at positions of low confidence. We then explored whether phenotypic selection of this ancestral sequence space using five cell lines representative of different tissues would lead to highly infectious variants, and whether these would be promiscuous – i.e. broadly infectious particles - or exhibit specific tropisms. The ancestral library was found to be fit, with packaging and transduction efficiencies that were on par with extant serotypes, and genetically selected variants were found to be broadly infectious on different cell lines. Furthermore, putative ancestral clones exhibited strong *in vivo* gene delivery efficiency, underscoring the potential of such vectors for gene therapy applications.

2.2 Results

Ancestral AAV sequence reconstruction

The goals of ancestral sequence reconstruction are, given a set of extant DNA sequences, to generate a phylogenetic tree and sequence alignment that relates these sequences, and to infer the sequences of ancestral variants at different ancestral nodes. Accurate sequence reconstruction is challenging due to ambiguity in the evolutionary relationships between extant variants (which affects the phylogenetic tree-building step) as well as sequence divergence at highly variable residues (which affects the sequence alignment and ancestral reconstruction steps).

As a starting point, we reconstructed the phylogeny of human, macaque and rhesus monkey AAV *cap* sequences retrieved from Genbank (n=52)[22]. We used MrBayes[23], which conducts Bayesian Markov chain Monte Carlo (MCMC) simulation of tree space, to estimate the confidence values at each internal node (shown in curly braces in Figs. 2.1a and A.1). This approach generated a phylogenetic tree relating extant sequences, which is essentially a hypothesis concerning the evolutionary history of AAVs. Each branch on this tree depicts the evolutionary direction that diversified the sequences, and each internal node represents a 'splitting' event where two AAV lineages diverged.

With many ancestral nodes to choose from (full tree in Fig. A.1), we selected node 27 (Fig. 2.1a) based on its high confidence value (1.00), which minimizes one potential source of uncertainty (at the level of phylogenetic relationships between entire sequences) and thus improves confidence in the finer-grained downstream reconstruction of individual amino acids' evolutionary histories. This node is also the ancestor of serotypes with demonstrated clinical efficacy (AAV1, Glybera), biomedical interest (AAV6[24]), or relative resistance to neutralizing antibodies (AAV7[25]).

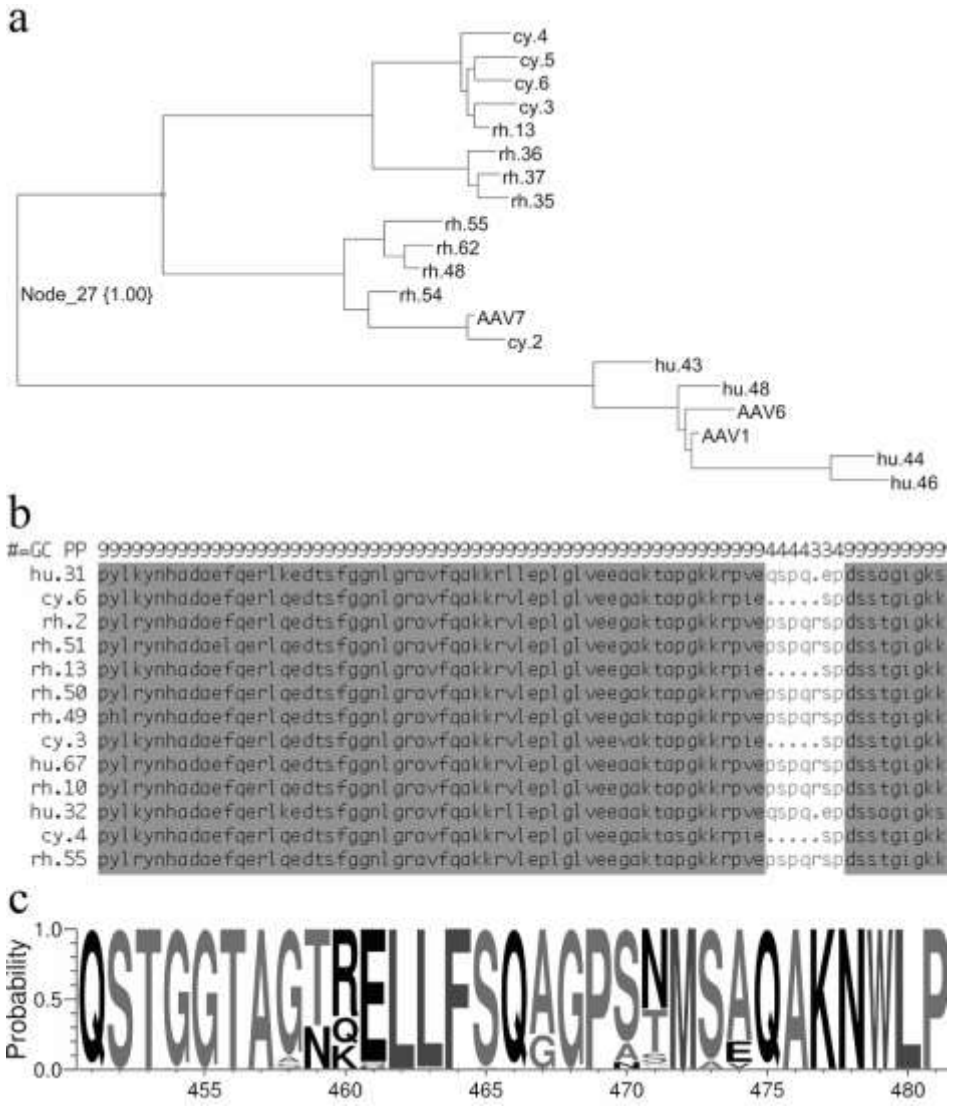

Figure 2.1. Ancestral AAV sequence reconstruction. a) A phylogenetic tree relating a subset of extant AAV variants at node 27. Curly braced numbers indicate clade posterior probabilities[23]. The phylogenetic tree graphic was generated in Dendroscope[26]. b) A multiple sequence alignment of a subset of AAV variants with column-specific confidence annotated along the top with single digits. Confidence ranges from above 0.9 (shaded grey) to 0.3-0.4 (shaded white). c) A distribution of predicted ancestral amino acid sequences for node 27, residues 451-481. The character height of each amino acid is proportional to its posterior probability.

We then used the Markov chain Monte Carlo alignment sampler HandAlign[27] to explore alignment space and predict the ancestral sequence of the most likely alignment at node 27. HandAlign generates a multiple sequence alignment, arranging the sequences of different variants in aligned 'columns' such that residues grouped in a column share a common ancestor (Fig. 2.1b). It also performs the ancestral reconstruction simultaneously with the alignment, and accounts for sequence insertions, deletions, and character substitutions. Figure 2.1c shows the distribution of predicted amino acids as a sequence logo, with character heights proportional to posterior probabilities. The majority of amino acid positions could be predicted with high confidence (≥ 0.90) and thus represented residues highly conserved during evolution. However, as is common in ancestral reconstruction, other positions were less evolutionarily conserved and could thus be predicted with lower probabilities.

Position	Residue 1	% Freq.	Residue 2	% Freq.	Residue 3	% Freq.
264	T	55	Q	25	A	20
266	A	63	S	37		
268	S	70	A	30		
448	S	71	A	29		
459	T	69	N	31		
460	R	63	Q	20	K	17
467	A	75	G	25		
470	S	85	A	15		
471	N	60	T	32	S	8
474	A	83	E	16		
495	S	75	T	25		
516	D	91	N	9		
533	D	86	E	14		
547	Q	81	E	11	T	8
551	A	50	K	50		
555	T	54	A	46		
557	E	86	D	14		
561	M	62	L	28	I	10
563	S	80	N	19		
577	E	50	Q	50		
583	S	86	D	8	A	6
593	A	45	Q	39	V	16
596	A	81	T	19		
661	A	71	E	19	T	10
662	V	53	T	26	A	22
664	T	66	S	34		
665	P	64	A	26	Q	10
710	T	87	A	13		
717	N	69	D	31		
718	N	60	S	40		
719	E	79	D	21		
723	S	68	T	32		

Table 1. Variable positions synthesized in ancestral AAV library.

A DNA library was designed based on these results, and residues above the 0.90 confidence value were fixed, whereas those below this confidence level were varied by introducing the two or three most likely amino acids (above a threshold value of 0.08), such that the fraction of library members containing each amino acid at a given position reflects the probability of that amino acid appearing

in the sequence reconstructions. The locations, identities, and synthesis frequencies of the 32 variable residues are presented in Table 2.1, and the most likely full ancestral *cap* amino acid sequence is shown in Fig. A.2 and aligned with extant serotypes in Fig. A.3. The ancestral *cap* library was synthesized (GeneArt, Life Technologies), and analysis of 61 sequenced clones from this library revealed that the amino acid frequencies at variable positions were not significantly different from the theoretical probabilities from the library ($P < 0.001$, see Materials and Methods), highlighting the correctness of the library synthesis.

Phenotypic selection of ancestral AAV library

Given the inherent probabilistic uncertainty of ancestral reconstruction, rather than investigating many possible, candidate ancestral sequences one by one, we selected the library as a whole for functional clones. Specifically, after validating the initial synthesized distribution of amino acids at the 32 variable positions, we probed how those positions would change when subjected to selective pressure for packaging and infectivity, which are key factors for successful viral replicative fitness during the natural evolution of AAV. The ancestral library was cloned into an AAV packaging plasmid, and viral particles were produced by transfection into human embryonic kidney 293T cells as previously described [28]. The viral genomic titer was comparable to levels obtained when packaging libraries based on extant AAV serotypes (data not shown), indicating that the ancestral library can support robust packaging titers.

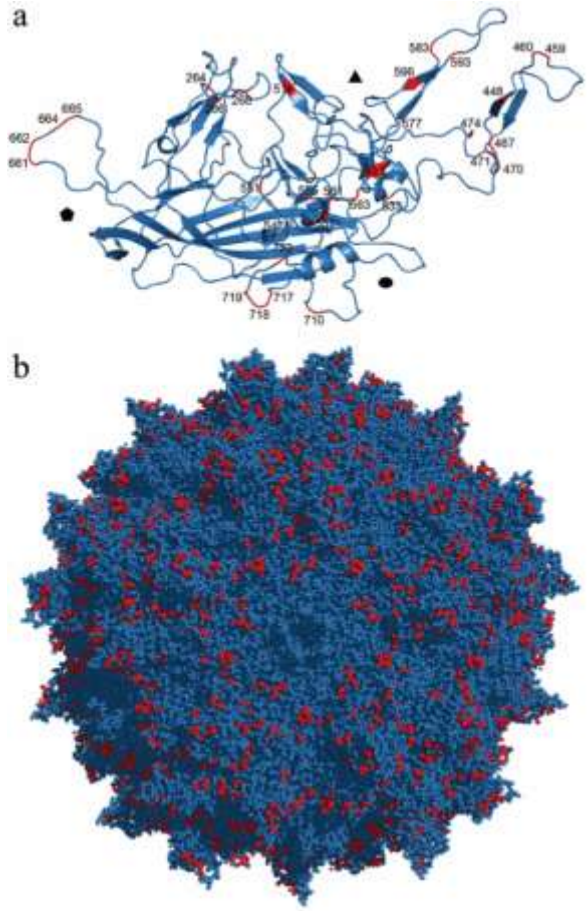

Figure 2.2. Variable residues mapped to the crystal structure of homologous AAV1, the closest AAV relative with an available structure. A three-dimensional molecular model of the AAV1 capsid was generated in PyMOL[29]. An amino acid alignment of the ancestral AAV sequence with AAV1 was used to map the highlighted residues to the a) individual asymmetric unit and b) full biological assembly.

The amino acid distribution at variable positions was only slightly altered by one round of packaging, and we hypothesized that additional selective pressure for infectivity could reveal more about the significance of each variable position. We chose five cell lines representative of different tissues to conduct rounds of selection: C2C12 mouse myoblast cells, IB3-1 human lung epithelial cells, B16-F10 mouse skin melanoma cells, human embryonic kidney 293T cells, and L0 human glioblastoma (GBM) tumor-initiating cells. Briefly, for each round 1 x 10^5 of each cell type were infected with iodixanol-purified, replication-competent AAV libraries at an initial genomic multiplicity of infection (MOI) of 5,000, and successful virions were recovered by superinfecting the cells with adenovirus type 5 two days later. Six rounds of selection were conducted on each cell line, resulting in five independently selected pools, and the stringency of selection was increased during subsequent rounds by decreasing the genomic MOI (Table A.1).

Amino acid	Theoretical distribution	Synthesized library	Post-packaging	C2C12 round 6	293T round 6	IB3 round 6	GBM round 6	B16 round 6
264	T, 55%	T, 53%	A, 52%	Q, 86%	A, 79%	A, 71%	A, 79%	Q, 50%
266	A, 63%	A, 54%	S, 57%	S, 100%	S, 86%	S, 100%	S, 86%	A, 56%
268	S, 70%	S, 72%	S, 87%	S, 100%	S, 100%	S, 100%	S, 100%	S, 100%
448	S, 71%	S, 56%	A, 52%	S, 79%	S, 64%	S, 57%	A, 57%	S, 56%
459	T, 69%	T, 79%	T, 61%	N, 100%	T, 100%	T, 100%	T, 100%	T, 88%
460	R, 63%	R, 79%	R, 78%	R, 86%	R, 93%	R, 100%	R, 93%	R, 88%
467	A, 75%	A, 79%	A, 61%	G, 86%	A, 93%	G, 79%	A, 64%	A, 75%
470	S, 85%	S, 96%	S, 87%	A, 79%	S, 77%	S, 93%	S, 79%	S, 94%
471	N, 60%	N, 67%	N, 83%	N, 100%	N, 79%	T, 71%	N, 86%	N, 50%
474	A, 83%	A, 94%	A, 87%	A, 100%	A, 100%	A, 100%	A, 100%	A, 100%
495	S, 75%	S, 89%	S, 87%	S, 100%	S, 67%	S, 100%	S, 50%	S, 81%
516	D, 91%	D, 98%	D, 100%	D, 100%	D, 100%	D, 100%	D, 100%	D, 88%
533	D, 86%	D, 90%	D, 87%	E, 79%	D, 93%	D, 86%	D, 100%	D, 88%
547	Q, 81%	Q, 79%	Q, 83%	Q, 93%	Q, 93%	Q, 100%	Q, 100%	Q, 100%
551	A, 50%	A, 58%	A, 64%	A, 100%	A, 67%	A, 100%	A, 100%	A, 100%
555	T, 54%	T, 52%	T, 59%	T, 79%	A, 60%	A, 57%	A, 71%	A, 56%
557	E, 86%	E, 80%	E, 86%	D, 79%	E, 67%	E, 64%	E, 57%	E, 75%
561	M, 62%	M, 75%	M, 68%	M, 93%	M, 93%	M, 64%	M, 57%	M, 75%
563	S, 80%	S, 65%	S, 73%	S, 79%	S, 87%	N, 86%	S, 50%	S, 69%
577	E, 50%	E, 55%	Q, 59%	Q, 100%	Q, 60%	Q, 100%	Q, 100%	Q, 88%
583	S, 86%	S, 80%	S, 77%	S, 100%	S, 73%	S, 100%	S, 100%	S, 81%
593	A, 45%	Q, 49%	Q, 45%	Q, 79%	A, 60%	V, 86%	A, 71%	Q, 44%
596	A, 81%	A, 69%	A, 68%	T, 93%	A, 80%	T, 64%	T, 79%	T, 56%
661	A, 71%	A, 82%	A, 82%	A, 100%	A, 64%	A, 64%	A, 57%	A, 100%
662	V, 53%	V, 69%	V, 68%	V, 93%	V, 57%	T, 71%	V, 64%	V, 69%
664	T, 66%	T, 87%	T, 82%	S, 71%	S, 50%	T, 93%	T, 86%	T, 88%
665	P, 64%	P, 65%	P, 77%	P, 100%	P, 79%	P, 93%	P, 71%	P, 100%
710	T, 87%	T, 90%	T, 100%	T, 100%	T, 100%	T, 100%	T, 100%	T, 100%
717	N, 69%	N, 81%	N, 77%	N, 100%	N, 100%	N, 79%	N, 79%	N, 100%
718	N, 60%	N, 83%	N, 59%	S, 79%	S, 93%	N, 57%	S, 57%	S, 94%
719	E, 79%	E, 63%	E, 82%	E, 100%	E, 64%	E, 100%	E, 100%	E, 100%
723	S, 68%	S, 79%	S, 77%	S, 100%	T, 57%	S, 86%	T, 71%	S, 81%

Figure 2.3. Dominant amino acids at variable positions after six rounds of selection. A heat map was generated based on the frequency of the most common amino acid at each position in the different libraries. The dominant amino acid and frequency at each position were determined based on sequencing results from individual clones n = 61 (synthesized library), n = 23 (post-packaging), and n=14 (for each ancestral library after selection on respective cell lines).

To assess the progression of selection at each variable position, clones were sequenced (*n = 14)* from each library after initial viral packaging (hereafter referred to as post-packaging), after three rounds of selection, and after six rounds of selection. This analysis revealed a range of outcomes for each variable position across the different cell lines. Figure 2.2 shows the positions of the variable amino acids mapped onto the crystal structure of AAV1 (the most homologous serotype with a solved structure), and Figure 2.3 depicts the dominant amino acid at each of these positions for each selected pool as a heat map, with darker shades representing higher convergence. As expected, selection for infection of cell lines led to increased convergence, and Figure 2.4 shows the percentage change in amino acid frequency in rounds 6 relative to post-packaging (increases in blue, decreases in red, and change of amino acid in yellow). Some amino acid positions approached full convergence to the same residue across all cell lines; other positions were divergent, or even acquired specific identities unique to only one cell line. The majority of residues unique to one cell line are located on the surface of the capsid, and they could for example play a role in altering the affinity of capsid interactions with cell surface receptors.

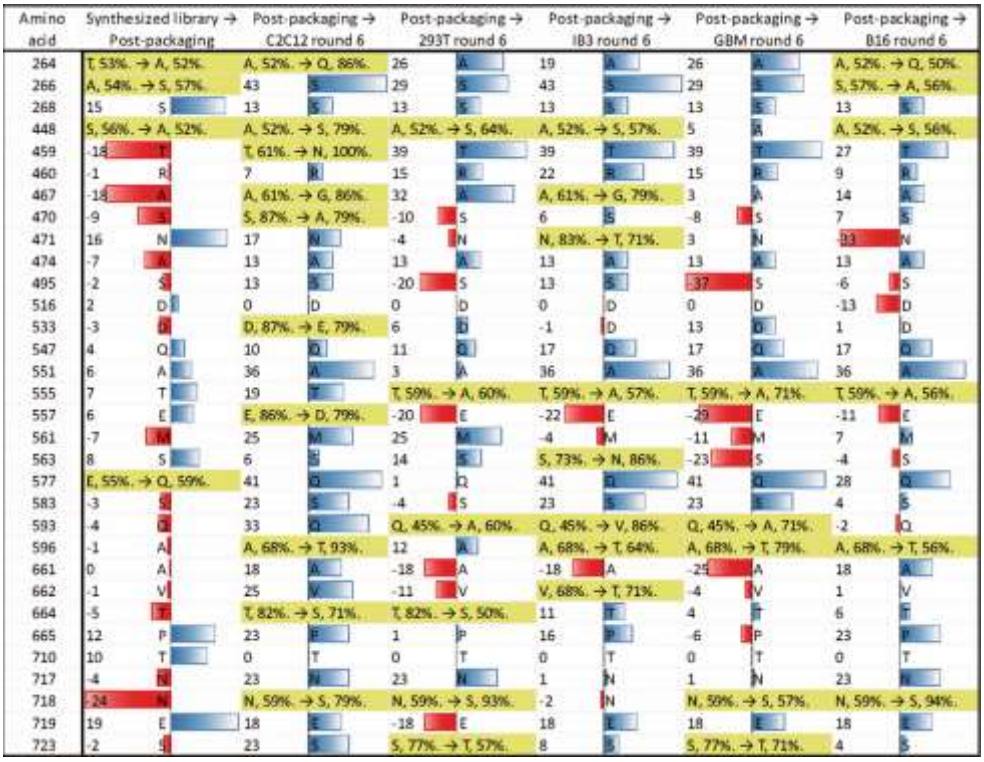

Figure 2.4. Change in amino acid frequency at variable positions after six rounds of selection. The percent change in amino acid frequency between the post-packaging library and evolved libraries after six rounds of selection on each cell line was calculated. If the identity of the dominant amino acid did not change, the increase (blue) or decrease (red) in frequency is displayed. If selection resulted in a change in amino acid identity at that position, the new amino acid and frequency is shown (yellow).

To determine whether the changes in amino acid frequencies imparted by phenotypic selection were statistically significantly different from the initial synthesized distribution, we conducted Bayesian Dirichlet-multinomial model comparison tests (as described in Materials and Methods) to calculate the posterior probability that the two sets of variable amino acids come from different

distributions. This analysis identified several amino acid positions that are significantly different after selection ($P < 0.05$, shown in green), and many more that are moderately different ($P < 0.5$, shown in yellow) (Fig. 2.5).

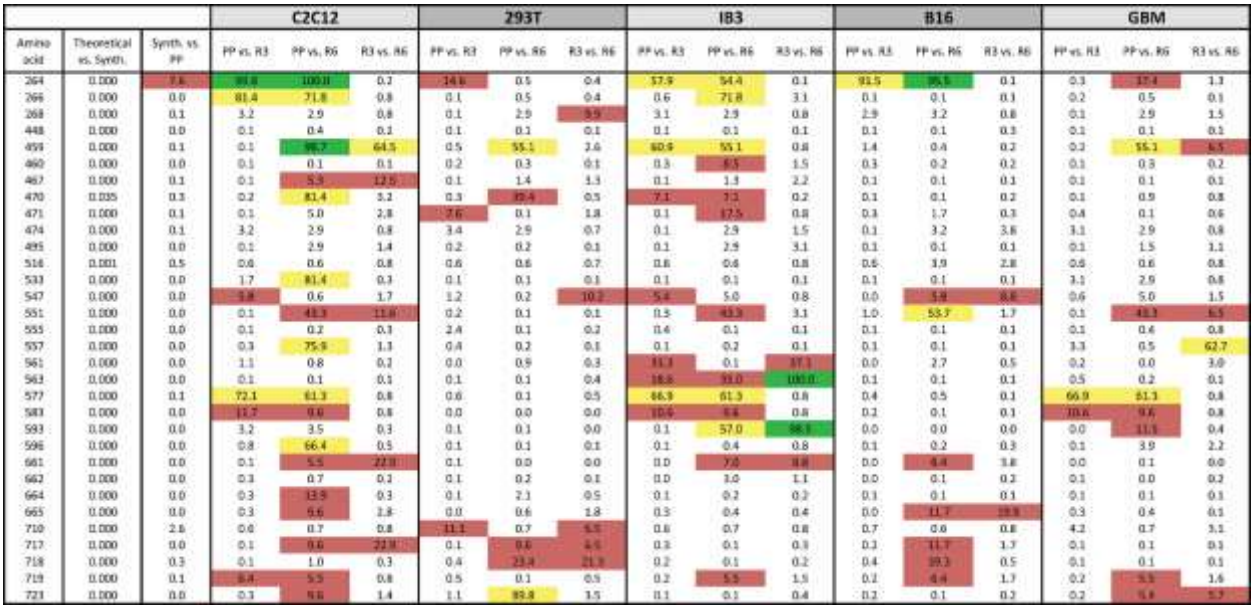

			C2C12			293T			IB3			B16			GBM		
Amino acid	Theoretical vs. Synth.	Synth. vs. PP	PP vs. R3	PP vs. R6	R3 vs. R6	PP vs. R3	PP vs. R6	R3 vs. R6	PP vs. R3	PP vs. R6	R3 vs. R6	PP vs. R3	PP vs. R6	R3 vs. R6	PP vs. R3	PP vs. R6	R3 vs. R6
264	0.000	7.6	91.8	100.0	0.2	14.6	0.5	0.4	57.9	54.4	0.1	91.5	95.5	0.1	0.3	17.4	1.3
266	0.000	0.0	81.4	71.8	0.8	0.1	0.5	0.4	0.6	71.8	3.1	0.3	0.1	0.1	0.2	0.5	0.1
268	0.000	0.1	3.2	2.9	0.8	0.1	2.9	3.9	3.1	2.9	0.8	2.9	3.2	0.8	0.1	2.9	1.5
448	0.000	0.0	0.1	0.4	0.1	0.1	0.1	0.1	0.1	0.1	0.1	0.1	0.1	0.3	0.1	0.1	0.1
459	0.000	0.1	0.1	98.7	64.5	0.5	55.1	2.6	60.9	55.1	0.8	1.4	0.4	0.2	0.2	55.1	6.5
460	0.000	0.0	0.1	0.1	0.1	0.2	0.3	0.1	0.3	6.5	1.5	0.3	0.2	0.2	0.1	0.3	0.2
467	0.000	0.1	0.1	5.3	12.5	0.1	1.4	1.3	0.1	1.3	2.2	0.1	0.1	0.1	0.1	0.1	0.1
470	0.035	0.3	0.2	81.4	3.2	0.3	39.4	0.5	7.1	7.1	0.2	0.1	0.1	0.2	0.1	0.9	0.8
471	0.000	0.1	0.1	5.0	2.8	7.6	0.1	1.8	0.1	17.5	0.8	0.3	1.7	0.3	0.4	0.1	0.6
474	0.000	0.1	3.2	2.9	0.8	3.4	2.9	0.7	0.1	2.9	1.5	0.1	3.2	3.8	3.1	2.9	0.8
495	0.000	0.0	0.1	2.9	1.4	0.2	0.2	0.1	0.1	2.9	3.1	0.1	0.1	0.1	0.1	1.5	1.1
516	0.001	0.5	0.6	0.6	0.8	0.6	0.6	0.7	0.8	0.6	0.8	0.6	3.9	2.8	0.6	0.6	0.8
533	0.000	0.0	1.7	81.4	0.3	0.1	0.1	0.1	0.1	0.1	0.1	0.1	0.1	0.1	3.1	2.9	0.8
547	0.000	0.0	5.8	0.6	1.7	1.2	0.2	10.2	5.4	5.0	0.8	0.0	5.8	8.8	0.6	5.0	1.5
551	0.000	0.0	0.1	43.3	11.8	0.2	0.1	0.1	0.3	43.3	3.1	1.0	53.7	1.7	0.1	43.3	6.5
555	0.000	0.0	0.1	0.2	0.3	2.4	0.1	0.2	0.4	0.1	0.1	0.1	0.1	0.1	0.1	0.4	0.8
557	0.000	0.0	0.3	75.9	1.3	0.4	0.2	0.1	0.1	0.2	0.1	0.1	0.1	0.1	3.3	0.5	62.7
561	0.000	0.0	1.1	0.8	0.2	0.0	0.9	0.3	31.3	0.1	17.1	0.0	2.7	0.5	0.2	0.0	3.0
563	0.000	0.0	0.1	0.1	0.1	0.1	0.1	0.4	18.6	33.0	100.0	0.1	0.1	0.1	0.5	0.2	0.1
577	0.000	0.1	72.1	61.3	0.8	0.6	0.1	0.5	66.9	61.3	0.8	0.4	0.5	0.1	66.9	61.3	0.8
583	0.000	0.0	11.7	9.6	0.8	0.0	0.0	0.0	10.6	8.6	0.8	0.2	0.1	0.1	10.6	9.6	0.8
593	0.000	0.0	3.2	3.5	0.3	0.1	0.1	0.0	0.1	57.0	98.3	0.0	0.0	0.0	0.0	11.5	0.4
596	0.000	0.0	0.8	66.4	0.5	0.1	0.1	0.1	0.1	0.4	0.8	0.1	0.2	0.3	0.1	3.9	2.2
661	0.000	0.0	0.1	5.5	22.9	0.1	0.0	0.0	0.0	7.0	9.8	0.0	0.8	3.8	0.0	0.1	0.0
662	0.000	0.0	0.3	0.7	0.2	0.1	0.2	0.1	0.0	1.0	1.1	0.0	0.1	0.2	0.1	0.0	0.2
664	0.000	0.0	0.3	13.9	0.3	0.1	2.1	0.5	0.1	0.2	0.2	0.1	0.1	0.1	0.1	0.1	0.1
665	0.000	0.0	0.3	9.6	2.8	0.0	0.6	1.8	0.3	0.4	0.4	0.0	11.7	19.9	0.3	0.4	0.1
710	0.000	2.6	0.6	0.7	0.8	11.1	0.7	5.5	0.6	0.7	0.8	0.7	0.6	0.8	4.2	0.7	3.1
717	0.000	0.0	0.1	9.6	22.9	0.1	0.6	4.5	0.3	0.1	0.3	0.3	11.7	1.7	0.1	0.1	0.1
718	0.000	0.3	0.1	1.0	0.3	0.4	23.4	21.9	0.2	0.1	0.2	0.4	19.3	0.5	0.1	0.1	0.1
719	0.000	0.1	8.4	5.5	0.8	0.5	0.1	0.5	0.2	5.5	1.5	0.1	8.4	1.7	0.2	5.5	1.6
723	0.000	0.0	0.3	9.6	1.4	1.1	99.8	3.5	0.1	0.1	0.4	0.2	0.1	0.2	0.2	5.8	5.7

Figure 2.5. Identification of key variable residues by Bayesian Dirichlet-multinomial model comparison tests. A comparison of the two sets of variable amino acids was conducted to identify positions that changed significantly during selection. The posterior probability that the two sets of amino acids come from two different probability distributions was calculated assuming probability parameters that are Dirichlet-distributed with low pseudocounts to reflect sparse observed sequences. Results colored green indicate a >95% chance that the sets came from different distributions, yellow a >50% chance, red a >5% chance, and no color a <5% chance. Synth, synthesized library; PP, post-packaging; R3, round three of selection; R6, round six of selection.

Transduction efficiency of evolved ancestral libraries

Phenotypic selection could conceivably lead to specific infectivity of a given cell line or may alternatively increase overall infectivity but in a promiscuous manner across all cell types. We investigated these possibilities by evaluating the transduction efficiency of evolved ancestral libraries on the cell line panel. The degree of convergence for each amino acid position after six rounds of selection is shown in Figure 2.3. Selection did not drive full convergence to a single sequence, potentially due to the presence of neutral positions that conferred no selective advantage. Therefore, rather than packaging individual clones, the libraries selected on each cell line were each packaged as a pool of recombinant virus (at a low ratio of AAV helper plasmid per producer cell to minimize mosaic capsids), resulting in five distinct round 6 ancestral libraries; results thus represent overall or average library infectivities. High titer, iodixanol-purified recombinant AAV (rAAV) encoding the green fluorescent protein (GFP) was produced for the ancestral libraries, as well as for natural serotypes AAV1-6, 8, and 9 for comparison of transduction efficiency and tropism. Infection at a genomic MOI of 2,000 (or 32,000 for C2C12s) revealed a range of properties (Fig. 2.6). Functionally selected ancestral libraries mediated high delivery efficiencies most comparable to AAV1 and AAV6 and generally superior to AAV4, AAV5, AAV8, and AAV9. Ancestral libraries were especially successful in infecting C2C12 and GBM cell lines

relative to natural serotypes. Importantly, we observed a large increase in infectivity when comparing the synthesized vs. the round 6 ancestral libraries, suggesting phenotypic selection of advantageous amino acids at the variable positions. Interestingly, the libraries in general displayed broad infectivity across all cell lines, indicating that this reconstructed ancestral pool contains promiscuous AAVs, a property known to be advantageous for natural evolutionary adaptability [30,31].

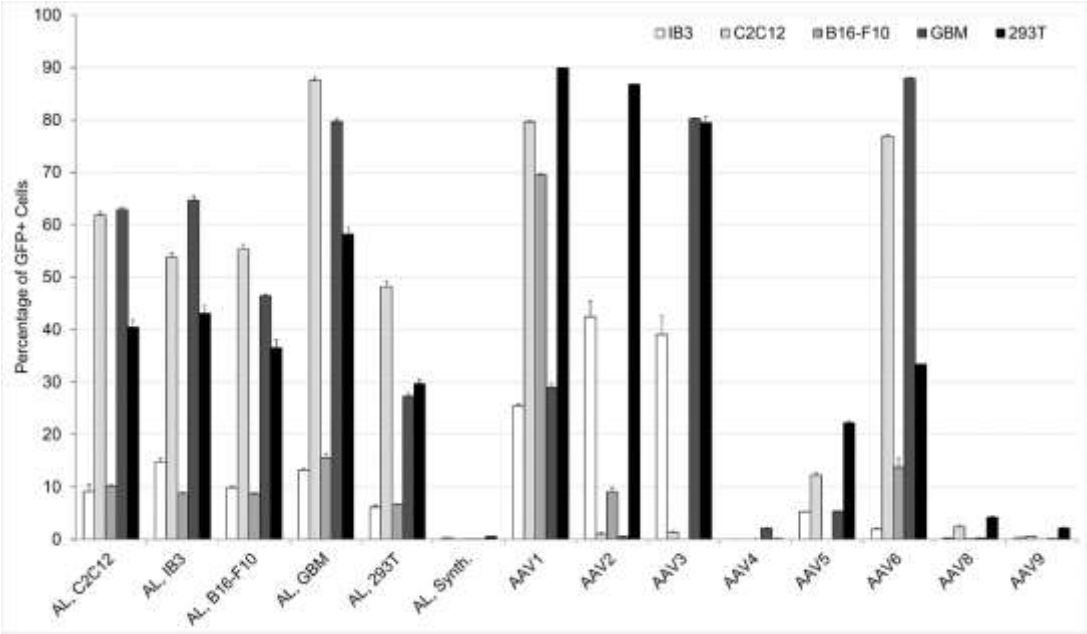

Figure 2.6. Transduction efficiency of ancestral libraries benchmarked against natural AAV serotypes. After six rounds of selection, viral genomic DNA was recovered from ancestral libraries and packaged as rAAV scCMV-GFP along with wild type AAV 1-6, 8, and 9. Cell lines were infected at a genomic multiplicity of infection (MOI) of 2,000 (293T, IB3, B16-F10, GBM) or 32,000 (C2C12). The fraction of GFP expressing cells was quantified by flow cytometry 72 hours later. Data are presented as mean ± SEM, n = 3. AL, ancestral library.

Characterization of the thermostability of candidate ancestral AAV variants

High thermostability and enhanced tolerance to mutations are also properties that could confer an evolutionary advantage to ancestral viral capsids[3,7,32]. We benchmarked the thermostability of AAV variants selected from our reconstructed pool against the natural serotypes AAV1, AAV2, AAV5, and AAV6 by assaying their transduction efficiency after heat treatment. Specifically, for initial analysis we chose the ancestral library selected on C2C12 cells and a representative variant from this library, C7. Virions packaged with self-complementary CMV-GFP were treated for 10 minutes at different temperatures using a thermal gradient before being cooled down to 37°C and used to infect 293T cells. We normalized the resulting fraction of GFP expressing cells after treatment at each temperature to the sample incubated at 37° (Fig. 2.7).

Ancestral variants displayed higher thermostability than natural serotypes and showed moderate transduction levels even at the highest treatment temperature, 78°C, which ablated transduction by natural serotypes. The obtained thermostabilities confirm those previously reported for natural

serotypes[33], which showed that AAV5 is more stable than AAV1 and that AAV2 is less stable than both. Enhanced thermostability of the ancestral variants in general could enable a higher tolerance to destabilizing mutations, and consequently a higher evolutionary adaptability.

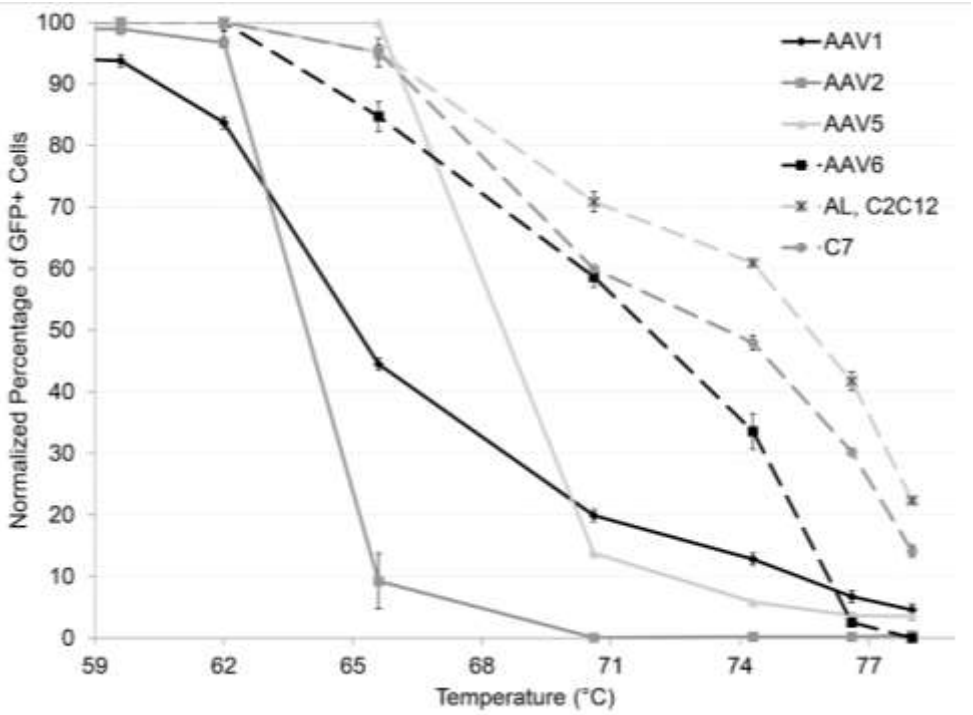

Figure 2.7. Candidate ancestral variants display higher thermostability than natural serotypes. The thermostability of the ancestral library selected on C2C12 cells and of the representative ancestral variant C7 was characterized and compared to that of natural serotypes 1, 2, 5, and 6. Virions packaged with scCMV-GFP were incubated at temperatures ranging from 59.6°C to 78°C for 10 minutes before being cooled down to 37°C and used to infect 293T cells. The fraction of GFP expressing cells was quantified by flow cytometry 72 hours later. Data are presented, after being normalized to the fraction of GFP expressing cells after incubation at 37°, as mean ± SEM, *n*=3.

Characterization of ancestral AAV glycan dependencies and susceptibility to neutralizing antibodies

Our *in vitro* transduction experiments demonstrated the broad infectivity of reconstructed variants. Given that ancestral node 27 gave rise to AAV1 and AAV6, we were interested in determining whether the candidate ancestral clones shared the same glycan dependencies, or if those evolved later. AAV1 and AAV6 utilize both alpha 2,3 and alpha 2,6 N-linked sialic acids as their primary receptor, and AAV6 has moderate affinity for heparan sulfate proteoglycans[24]. To probe heparan sulfate proteoglycan (HSPG) usage, we transduced parental CHO-K1 cells and the pgsA CHO variant line deficient in HSPG. To examine sialic acid dependence we transduced parental Pro5 CHO cells presenting glycans with both N- and O-linked sialic acids, a Lec2 CHO variant cell line deficient in all N- and O-linked sialic acids, and a Lec1 line deficient in complex and hybrid type N-glycans including sialic acids[34] (Fig. 2.8b). Interestingly, candidate ancestral AAVs exhibited no dependence on HSPG or N- and O-linked sialic acids (Fig. 2.8a). We also verified that selected individual clones exhibited similar transduction behavior as the evolved libraries (Fig. A.6).

We next examined whether ancestral AAVs were neutralized by antibodies against a broad range of contemporary AAVs, in particular human intravenous immunoglobulin (IVIG) that contains polyclonal antibodies against extant serotypes due to natural exposure across the human population. *In vitro* incubation with IVIG strongly reduced transduction of ancestral libraries and the AAV1 control (Fig. A.7), indicating that this ancestral pool is not highly serologically distinct from its progeny. Additional capsid engineering may be necessary to address this clinically relevant problem.

a

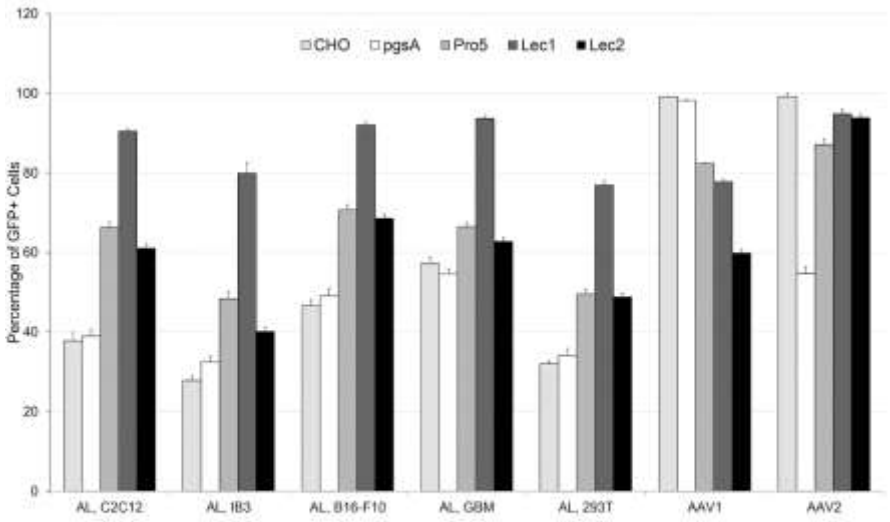

b

Cell line	Biochemical defect	Glycosylation phenotype	N-glycans	O-GalNAc glycans
Pro5	N/A	Full complement of complex N-glycans capped with sialic acid residues		
Lec1	Loss of N-acetylglucosyl transferase-I activity	N-glycans terminate in mannose, no complex or hybrid N-glycans		
Lec2	Unable to transport CMP-sialic acid into Golgi	N-glycans terminate in galactose, all glycans lack sialic acid		
CHO-K1	N/A	Full complement of heparan sulfate proteoglycans		
pgsA	Loss of xylosyltransferase	Lacks heparan sulfate proteoglycans		

sialic acid ○ galactose ● mannose ■ N-acetylglucosamine □ N-acetylgalactosamine

glucosamine ◇ iduronic acid

Figure 2.8. Glycan dependency of candidate ancestral AAV variants. a) After six rounds of selection, the transduction efficiency of ancestral libraries carrying scCMV-GFP was quantified by flow cytometry 72 hours after infection at a genomic MOI of 2,000 (Pro5, Lec1, Lec2) and 50,000 (CHO-K1, pgsA). The CHO-K1/pgsA comparison examines heparan sulfate proteoglycan dependence, while Pro5/Lec1 and Pro5/Lec2 probe sialic acid dependence. Data are presented as mean ± SEM, $n = 3$. b) Glycans present on CHO glycosylation mutants. AL, ancestral library.

Characterization of ancestral variants in vivo in mouse gastrocnemius muscle

Upon finding that the ancestral AAV libraries exhibited efficiencies comparable to or in some cases higher than extant serotypes on a panel of cell lines from representative tissues, we next probed *in vivo* infectivity. Based on the high transduction efficiencies of candidate ancestral AAVs on the most nonpermissive cell line (C2C12 mouse myoblasts), we chose to evaluate *in vivo* transduction of mouse gastrocnemius muscle. In particular, individual ancestral variant clones from the selected viral pools (Table A.2) that were closest to the consensus sequences of libraries evolved on C2C12 (clones C4, C7) and glioblastoma cells (clone G4) were chosen, based on the efficiency of these two libraries in transducing C2C12 myoblasts *in vitro*. In addition, these variants were benchmarked against AAV1, given its clinical efficacy in muscle-targeted gene therapy [35].

We generated recombinant AAV vectors expressing firefly luciferase under the control of the hybrid CAG (CMV early enhancer/chicken β-actin/splice acceptor of β-globin gene) promoter. A volume of 30 µl DNase-resistant genomic particles (5×10^{10} vg) was injected into each gastrocnemius muscle of BALB/c mice, and after six weeks, mice were sacrificed and tissue luciferase activities analyzed (Fig. 9). Ancestral reconstruction variants yielded 19-31 fold higher transgene expression than AAV1 in gastrocnemius muscle, with variant C7 yielding the highest expression. Interestingly, variant C7 was the most abundant sequence (71%) in the round 6 ancestral library selected on C2C12 cells. These results demonstrate that candidate ancestral AAVs also exhibit high infectivity *in vivo*, and even offer the potential to exceed the performance of the best contemporary natural serotypes in gene therapy applications.

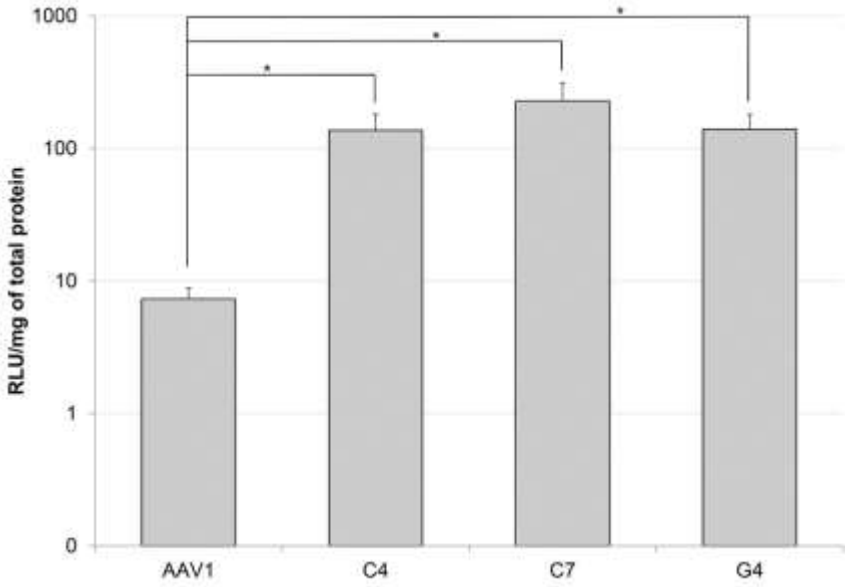

Figure 2.9. Evaluation of gastrocnemius muscle transduction. Luciferase activity measured in relative light units (RLU) per mg protein was determined in gastrocnemius tissue homogenate 48 days after intramuscular administration of 5 x 10^{10} viral particles of ancestral clones C4, C7, G4, or AAV1 in adult mice. Controls injected with phosphate-buffered saline displayed no activity (data not shown). *, statistical difference of $P < 0.05$ by two-tailed Student's t-test.

2.3 Discussion

Ancestral sequence reconstruction offers unique opportunities to study fundamental biological questions of virus evolution and fitness, including the characterization of ancestral sequence space relative to extant serotypes, the importance of mutational tolerance or evolutionary conservation, and the comparative advantages of promiscuous versus selective tropism. The primary challenge of ancestral reconstruction is to accurately infer an ancestral sequence despite uncertainty arising from sequence divergence within hypervariable regions of extant variants. We have combined sophisticated computational and library synthesis approaches to address this uncertainty and thereby generate a functional ancestral AAV library. We then studied the biological properties of this library to learn more about the evolutionary behavior of AAV and the gene therapy potential of reconstructed ancestral variants.

The posterior probability that an AAV ancestral sequence accurately reflects the actual ancestral virus is the product of the probabilities that each of the amino acids in the capsid protein is correctly predicted. At positions of high evolutionary convergence the posterior probability nears 1.0, yet there are many sites that diverged during evolution and thus cannot be predicted with such high confidence. Our library synthesis approach addressed this concern by introducing the two or three most likely amino acids at the 32 lowest confidence positions in the AAV *cap* protein. Interestingly, the majority of positions varied in our ancestral library have not been previously described in studies of the functional importance of single mutations to the AAV capsid[36,37]. Unlike previous ancestral reconstructions of enzymes and other proteins, which utilized single best guess ancestral sequences [11,38], or which sampled only a small fraction of library variants due to the low throughput of enzymatic assays [8,39], our massively parallel phenotypic selection enabled screening of a large library (and is limited only by the transformation efficiency of electrocompetent bacteria).

The selection strategy applied pressure for efficient packaging and transduction of cell types representing a variety of tissues. By comparing the frequencies of amino acids selected at variable positions to the theoretical ancestral sequence prediction, one can gain insights into both the accuracy of our sequence reconstruction as well as the functional role of each residue in AAV biology. Comparison of sequences from the synthesized library with those recovered after initial library packaging suggested that one round of packaging imposed no statistically significant changes on the amino acid distribution at variable positions (except for a low 0.076 probability change in preference from a threonine to an alanine at residue 264). However, with selection for infectivity on a range of cell types specific positions begin to diverge, and differences between round six and post-packaging sequences were more significant than between round three and post-packaging sequences, likely because six rounds enabled a larger cumulative effect of positive selection. Genetic drift may also play a role, but is unlikely to be the main driving force given that

the time to fixation by genetic drift increases with population size [40], and a large number of virions ($>10^8$) was used in each sequential round of selection.

By comparing the ancestral libraries after six rounds of selection with the post-packaging library, we identified several trends in the level of convergence of the amino acid residues, suggesting these positions may have potential roles in modulating properties like capsid stability and infectivity. Some amino acid positions approached full convergence to the same residue across all cell lines (268, 460, 474, 516, 547, 583, 665, 710, 717, 719); these positions are distributed throughout the capsid and may for example be important for core viral functions such as capsid stability, uncoating, or endosomal escape. Others showed more divergent outcomes across different cell lines (264, 467, 593, 664, 723) and may be neutral with respect to overall fitness. Finally, some positions (459, 470, 471, 533, 555, 596, 662, 718) acquired identities specific to a given cell line and may confer an infectious advantage on each respective cell line.

Positions 264 and 459 showed the strongest evidence of change due to selection ($P < 0.05$). Position 459 is prominently exposed on loop IV of the AAV capsid surface. Position 264 is positioned on loop I of the capsid and has been identified as a key determinant of muscle tropism in the rationally engineered variant AAV2.5[41]. There is also suggestive evidence of selection at positions 266, 470, 533, 551, 557, 577, 596, and 723 in various libraries ($P < 0.5$). Position 533 has been previously described as a key contributor to infectivity and glycan dependence in our previously evolved variant ShH10, a vector differing by only four amino acids from AAV6 but exhibiting unique tropism in the retina[34]. Additionally, Lochrie et al.[42] examined several other of these positions in their thorough mutational analysis of the AAV2 serotype, though AAV2 lies in a different phylogenetic clade than ancestral node 27. The characterization of these variable positions is therefore novel, and lessons learned may inform targeted mutagenesis efforts to improve the fitness of extant variants.

The assembly-activating protein (AAP), which is involved in directing capsid proteins to the nucleolus and in assembly of the viral capsid in this organelle[20], is translated from an alternative open reading frame (ORF) with a non-canonical CTG start codon present within the *cap* gene. This alternate ORF is also present in the ancestral reconstruction of the AAV capsid at node 27 (Fig. A.2b). Three of the variable residues (positions 264, 266, and 268) are present within the AAP ORF, and the putative ancestral AAP sequence is otherwise conserved across the reconstruction. As discussed above, residue 264 is among the positions that showed strong and statistically significant changes after six rounds of packaging and infection on the cell line panel, and it is possible that both capsid and AAP may have undergone functional selective pressure during this process.

The *in vitro* transduction results also demonstrate the importance of utilizing a library approach coupled with selection. A single or small number of best guess sequences could likely include deleterious amino acids that significantly impact fitness. Indeed, our data show that the synthetized ancestral AAV library evaluated prior to rounds of selection reproducibly exhibited dramatically lower infectivity than libraries subjected to selective pressure. This is not surprising, given that numerous directed evolution studies demonstrate that even single point mutations can significantly alter enzyme activity or virus infectivity by several orders of magnitude [36,43-45].

Interestingly, despite differences in amino acid composition at variable positions, the ancestral libraries selected for infecting a number of individual cell lines subsequently demonstrated broad tropism across all of these cell lines. Such promiscuity may have been rewarded during the natural evolution of AAVs, since the ability to replicate in different cell and tissue types enhances virus spread. In fact, most natural AAV serotypes exhibit broad tropism[46,47], indicating that promiscuity continues to be a valued trait for natural evolution.

Such broad tropism, however, has important implications for gene therapy. In cases where disease pathologies affect multiple tissues and cell types (e.g. lysosomal storage disorders), broader infectivity could be an advantageous trait. Expanded tropism may also be useful for infecting cell types refractory to infection by most AAV serotypes, or for *ex vivo* treatments of homogeneous cell populations where off-target infectivity is not a concern. However, in the majority of gene therapy applications it is desirable to limit transgene expression to a target tissue for several important reasons, including risks associated with off-target expression of the transgene, off-target transduction leading to higher immune presentation and reaction, and higher overall dosages needed to overcome vector dilution into multiple tissues. This is true not only when vector is delivered via routes that lead to intentional exposure to multiple tissues (e.g. intravascular delivery) but also for local injection into multiple tissues in which vector leakage into circulation can lead to widespread distribution to multiple organs. For example, biodistribution studies have shown the spread of AAV vectors to sites distant from the target tissue after injecting viral particles through the hepatic artery, intramuscularly, or into the putamen of the brain[48-50].

To address concerns with off-target transgene expression, strategies for controlling gene and protein expression including cell type specific promoters [51] and microRNA elements[52,53] are being explored to restrict expression to target cells. These approaches are promising, but would not address immune presentation of the capsid protein. Therefore, the optimal scenario is one in which selective AAV tropism is engineered through modification of the capsid protein. Directed evolution can generate vectors capable of targeted gene delivery[34], and evolution for enhanced AAV infectivity of a given target cell in general can enable a reduction in vector dose and thereby reduce the level of off-target transduction. Ancestral variants may be promising starting points for such directed evolution efforts given their high infectivity and representation of a capsid protein sequence space that is different from and complementary to extant serotypes.

High thermostability may also be an advantageous property for AAV engineering. Ancestral sequences have been correlated with increased thermostability in multiple studies [3,7,32], and in fact, enriching for seemingly neutral mutations that resemble an ancestral sequence has been shown to increase protein kinetic and thermodynamic stability and to improve the probability of acquiring new function mutations[54]. This work lends additional evidence of the correlation between ancestral sequences and thermostability by demonstrating that candidate ancestral AAV variants are more thermostable than contemporary serotypes.

We also characterized the glycan dependencies of ancestral variants and found that previously studied AAV glycan dependencies including N- and O-linked sialic acids, heparan sulfate proteoglycans, and galactose were not utilized. It is conceivable that these dependences may have arisen more recently in the evolution along these AAV lineages.

In addition, we found that ancestral libraries were as susceptible to neutralizing antibodies as AAV1, suggesting that this ancestral reconstruction pool exhibits immunogenic properties similar to current serotypes. Multiple antigenic regions have been mapped on natural AAV serotypes, including AAV1, AAV2, AAV5, and AAV8 [55]. Given that AAV1 is a descendant of the node 27 ancestral reconstruction, we aligned known AAV1 epitopes [56] with the ancestral reconstruction sequence. Mapped antigenic regions corresponding to AAV1 residues 496-499, 583, 588-591, and 597 were conserved in the ancestral reconstruction. Additionally, the ancestral sequence is identical to several known AAV2 antigenic regions including residues 272-281, 369-378, and 562-573[57]. Such conserved regions may contribute to the observed susceptibility of ancestral variants to neutralizing antibodies.

Interestingly, previous studies have also demonstrated cross-seroreactivity between ancestral and extant viral capsids. In particular, antiserum against extant viruses has been shown to neutralize reconstructed ancestral variants [14], and ancestral viruses can elicit neutralizing antibodies that protect against currently circulating strains, a property that has been exploited for the development of vaccine candidates [11,12]. Neutralizing antibodies may therefore pose a significant clinical challenge for ancestral vectors. Further capsid engineering under a strong selective pressure for evading neutralizing antibodies may enable selection of combinations of mutations that promote antibody evasion [58]. For example, there are variable residues in the ancestral reconstruction that map to antigenic regions corresponding to AAV1 residues 456-459, 494, 582, and 593-595, and to antigenic regions in other serotypes [56]. Mutations in these regions could disrupt the binding of antibodies to capsid epitopes, and could potentially be combined with other mutagenesis strategies to engineer variants with enhanced antibody evasion properties [58].

Ancestral AAVs demonstrated efficient *in vitro* gene transfer to C2C12 mouse myoblast cells comparable to AAV1, a current gold standard for muscle transduction, yet utilized a different receptor for cell entry. This distinction may contribute to their efficient *in vivo* infectivity, which impressively reached 19-31 fold higher levels of expression than AAV1 in mouse gastrocnemius muscle. If the improved expression observed with ancestral reconstruction vectors is reproducible in human muscle tissue, ancestral variants will be auspicious candidates for clinical translation.

In summary, our results indicate that a library of AAV variants representing sequence space around a key ancestral node is rich in broadly infectious variants with potential in gene therapy applications. We have taken initial steps in characterizing this sequence space by varying the amino acids at the lowest confidence positions identified by ancestral sequence reconstruction, followed by phenotypic selection to yield highly functional sets of amino acids at these locations. Sequence analysis of variable residues revealed a variety of outcomes ranging from highly conserved residues to more neutral positions that are pliable to change. Selected variants were promiscuous in their infectivity but showed promise as recombinant vectors *in vitro* and *in vivo*, and the putative mutational tolerance and evolvability of this library could be further harnessed in directed evolution studies to overcome gene therapy challenges such as targeted gene delivery and immune evasion.

2.4 Materials and Methods

Ancestral reconstruction

AAV *cap* sequences (n=52) from Genbank [22], including those from human and non-human primate origin, were incorporated in this analysis, starting from lists of AAV sequences published in previous phylogenetic analyses [59,60]. The MrBayes package [23] was used to perform Bayesian Markov chain Monte Carlo (MCMC) simulation of tree space and estimate the confidence values at each internal node. We then used the Markov chain Monte Carlo alignment sampler HandAlign [27] to explore alignment space and estimate regional confidence for the most likely alignment at node 27, discarding all but the sequences descended from this node. HandAlign generates a multiple sequence alignment, arranging the sequences of different variants in aligned 'columns' such that residues grouped in a column share a common ancestor. Each alignment column was modeled as a realization of the standard phylogenetic continuous-time Markov process of character evolution, using amino acid and empirical codon substitution rate matrices that were estimated from databases of aligned protein-coding sequence [61]. HandAlign performs the reconstruction simultaneously with the alignment, and accounts for sequence insertions, deletions, and character substitutions. The codon-level model was used to account for the possibility of synonymous substitutions with a phenotype at the DNA level; we also checked for the possibility of dual selection in overlapping reading frames ("overprinted" genes), by reconstructing both ancestral reading frames at the codon level. Neither of these subtle effects appeared significant enough to warrant prioritizing synonymous (silent, DNA-level) variants over the many non-synonymous amino acid variants.

Library construction and vector packaging

The reconstructed ancestral AAV *cap* sequence was synthesized (GeneArt, Life Technologies) with a library size of 5.6×10^{11}, greater than the theoretical diversity of 2.5×10^{11}. The library was digested with *Hin*d III and *Not* I, and ligated into the replication competent AAV packaging plasmid pSub2. The resulting ligation reaction was electroporated into *E. coli* for plasmid production and purification. Replication competent AAV was then packaged and purified by iodixanol density centrifugation as previously described[58,62]. DNase-resistant genomic titers were obtained via quantitative real time PCR using a Bio-Rad iCycler (Bio-Rad, Hercules, CA) and Taqman probe (Biosearch Technologies, Novato, CA)[62].

Cell culture

C2C12 mouse myoblast, B16-F10 skin melanoma cells, CHO-K1, pgsA, Pro5, Lec1, and Lec2 cells were obtained from the Tissue Culture Facility at the University of California, Berkeley. IB3-1 lung epithelial and human embryonic kidney 293T cells were obtained from American Type Culture Collection (Manassas, VA). Unless otherwise noted all cell lines were cultured in Dulbecco's Modified Eagle's medium (DMEM, Gibco) at 37 °C and 5% CO_2. L0 human glioblastoma tumor initiating cells were kindly provided by Dr. Brent Reynolds (University of Florida, Gainesville), and propagated in neurosphere assay growth conditions [63] with serum-free media (Neurocult NS-A Proliferation kit, Stem Cell Technologies) that contained epidermal growth factor (EGF, 20 ng/ml, R&D), basic fibroblast growth factor (bFGF, 10 ng/ml, R&D), and heparin (0.2% diluted in phosphate buffered saline, Sigma). IB3-1 cells were cultured in DMEM/F-12 (1:1) (Invitrogen, Carlsbad, CA). CHO-K1 and pgsA cells were cultured in F-12K medium (ATCC), and Pro5, Lec1, and Lec2 cells were cultured in MEM α nucleosides (Gibco).

Except for GBM culture, all media were supplemented with 10% fetal bovine serum (Invitrogen) and 1% penicillin/streptomycin (Invitrogen).

Library selection and evolution

All cell lines were seeded in 6-well tissue culture plates at a density of 1 x 10^5 cells per well. One day after seeding, cells were infected with replication competent AAV libraries. After 24 hours of exposure, cells were superinfected with adenovirus serotype 5 (Ad5). Approximately 48 hours later, cytopathic effect was observed, and virions were harvested by three freeze/thaw steps followed by treatment with Benzonase nuclease (1 unit/mL) (Sigma-Aldrich) at 37 °C for 30 minutes. Viral lysates were then incubated at 56°C for 30 minutes to inactivate Ad5. The viral genomic titer was determined as described above. To analyze *cap* sequences, AAV viral genomes were extracted after packaging and rounds 3 and 6 of selection, amplified by PCR, and sequenced at the UC Berkeley DNA Sequencing Facility.

Statistical analysis of variable positions in evolved ancestral libraries

A comparison of the two sets of amino acids at each variable amino acid position was conducted to identify variable positions whose library proportions had changed significantly during selection. The posterior probability that the two sets of variable amino acids come from two different probability distributions was calculated assuming probability parameters that are Dirichlet-distributed with low pseudocounts to reflect sparse observed counts. For comparison of the synthesized and theoretical library, post-synthesis amino acid frequencies distributed via a Dirichlet-multinomial were compared with the theoretical probabilities from the library distributed by a multinomial.

In vitro transduction analysis

After six rounds of selection, ancestral library viral genomes were cloned into the pXX2 recombinant AAV packaging plasmid. To benchmark the infectivity of rAAV ancestral libraries against a panel of natural AAV serotypes, vectors were packaged with a self-complementary CMV-GFP cassette using the transient transfection method previously described[58,62]. Cell lines (293T, C2C12, IB3-1, B16-F10, CHO-K1, pgsA, Pro5, Lec1, and Lec2) were seeded in 96-well plates at a density of 15,000 cells per well. One day after seeding, cells were infected with rAAV at a genomic MOI of 2,000 (293T, C2C12, IB3-1, B16-F10, GBM), 10,000 (Pro5, Lec1, Lec2), 32,000 (C2C12), or 50,000 (CHO-K1, pgsA) (n = 3). To analyze antibody evasion properties, ancestral rAAV libraries were incubated at 37°C for 1 hour with serial dilutions of heat inactivated IVIG (Gammagard), and then used to infect HEK293T cells at a genomic MOI of 2000 (n = 3).

To characterize thermostability, virions packaged with self-complementary CMV-GFP were diluted with DMEM supplemented with 2% FBS and incubated at temperatures ranging from 59.6°C to 78°C for 10 minutes in a thermocycler (Bio-Rad) before being cooled down to 37°C and used to infect 293T cells at genomic MOIs ranging from 1,500-16,000; MOIs were adjusted to ensure an adequate number of GFP-positive cells for analysis. For all studies, the fraction of GFP-expressing cells 72 hours post-infection was quantified with a Guava EasyCyte 6HT flow cytometer (EMD/Millipore) (UC Berkeley Stem Cell Center, Berkeley, CA).

In vivo animal imaging and quantification of luciferase expression

High-titer rAAV CAG-Luciferase vectors were purified by iodixanol gradient and then concentrated and exchanged into PBS using Amicon Ultra-15 centrifugal filter units (Millipore). To study skeletal muscle transduction 5×10^{10} rAAV-Luc DNase-resistant genomic particles were injected in a volume of 30 µl into each gastrocnemius muscle of 7-week-old female BALB/c mice (Jackson Laboratories, $n = 3$) as previously described [58]. Six weeks after injection, animals were sacrificed, and gastrocnemius muscle was harvested and frozen. Luciferase activity was determined and normalized to total protein as previously described[62]. All animal procedures were approved by the Office of Laboratory Animal Care at the University of California, Berkeley and conducted in accordance with NIH guidelines on laboratory animal care.

2.5 Acknowledgements

The authors are grateful to Professor Brent Reynolds (University of Florida) for kindly providing the L0 human glioblastoma tumor-initiating cells.

2.6 Funding

This work was supported by the National Institutes of Health grant [R01EY022975]. DSO is supported by a National Science Foundation Graduate Fellowship, and JSO is supported by a National Science Foundation Graduate Fellowship and a UC Berkeley Graduate Division Fellowship. IH and OW were supported by the National Human Genome Research Institute grant [HG004483].

Conflict of interest statement. DVS, DSO, and JSO are inventors on patents involving AAV directed evolution.

2.7 References

1. Stackhouse, J., Presnell, S.R., McGeehan, G.M., Nambiar, K.P. & Benner, S.A. The ribonuclease from an extinct bovid ruminant. *FEBS Lett* **262**, 104-6 (1990).
2. Cole, M.F. & Gaucher, E.A. Utilizing natural diversity to evolve protein function: applications towards thermostability. *Curr Opin Chem Biol* **15**, 399-406 (2011).
3. Gaucher, E.A., Govindarajan, S. & Ganesh, O.K. Palaeotemperature trend for Precambrian life inferred from resurrected proteins. *Nature* **451**, 704-7 (2008).
4. Ortlund, E.A., Bridgham, J.T., Redinbo, M.R. & Thornton, J.W. Crystal structure of an ancient protein: evolution by conformational epistasis. *Science* **317**, 1544-8 (2007).
5. Ugalde, J.A., Chang, B.S. & Matz, M.V. Evolution of coral pigments recreated. *Science* **305**, 1433 (2004).
6. Afriat-Jurnou, L., Jackson, C.J. & Tawfik, D.S. Reconstructing a missing link in the evolution of a recently diverged phosphotriesterase by active-site loop remodeling. *Biochemistry* **51**, 6047-55 (2012).
7. Watanabe, K., Ohkuri, T., Yokobori, S. & Yamagishi, A. Designing thermostable proteins: ancestral mutants of 3-isopropylmalate dehydrogenase designed by using a phylogenetic tree. *J Mol Biol* **355**, 664-74 (2006).
8. Alcolombri, U., Elias, M. & Tawfik, D.S. Directed evolution of sulfotransferases and paraoxonases by ancestral libraries. *J Mol Biol* **411**, 837-53 (2011).
9. Chen, F. *et al.* Reconstructed evolutionary adaptive paths give polymerases accepting reversible terminators for sequencing and SNP detection. *Proc Natl Acad Sci U S A* **107**, 1948-53 (2010).
10. Gonzalez, D. *et al.* Ancestral mutations as a tool for solubilizing proteins: The case of a hydrophobic phosphate-binding protein. *FEBS Open Bio* **4**, 121-7 (2014).
11. Kothe, D.L. *et al.* Ancestral and consensus envelope immunogens for HIV-1 subtype C. *Virology* **352**, 438-49 (2006).
12. Ducatez, M.F. *et al.* Feasibility of reconstructed ancestral H5N1 influenza viruses for cross-clade protective vaccine development. *Proc Natl Acad Sci U S A* **108**, 349-54 (2011).
13. Rolland, M. *et al.* Reconstruction and function of ancestral center-of-tree human immunodeficiency virus type 1 proteins. *J Virol* **81**, 8507-14 (2007).
14. Gullberg, M. *et al.* Characterization of a putative ancestor of coxsackievirus B5. *J Virol* **84**, 9695-708 (2010).
15. Berns, K.I. & Linden, R.M. The cryptic life style of adeno-associated virus. *Bioessays* **17**, 237-45 (1995).
16. Ellis, B.L. *et al.* A survey of ex vivo/in vitro transduction efficiency of mammalian primary cells and cell lines with Nine natural adeno-associated virus (AAV1-9) and one engineered adeno-associated virus serotype. *Virol J* **10**, 74 (2013).
17. Asokan, A., Schaffer, D.V. & Samulski, R.J. The AAV vector toolkit: poised at the clinical crossroads. *Mol Ther* **20**, 699-708 (2012).
18. Kotterman, M.A. & Schaffer, D.V. Engineering adeno-associated viruses for clinical gene therapy. *Nat Rev Genet* **15**, 445-51 (2014).
19. Gaudet, D. *et al.* Efficacy and long-term safety of alipogene tiparvovec (AAV1-LPLS447X) gene therapy for lipoprotein lipase deficiency: an open-label trial. *Gene Ther* **20**, 361-9 (2013).
20. Sonntag, F., Schmidt, K. & Kleinschmidt, J.A. A viral assembly factor promotes AAV2 capsid formation in the nucleolus. *Proc Natl Acad Sci U S A* **107**, 10220-5 (2010).
21. Khersonsky, O. *et al.* Directed evolution of serum paraoxonase PON3 by family shuffling and ancestor/consensus mutagenesis, and its biochemical characterization. *Biochemistry* **48**, 6644-54 (2009).
22. Benson, D.A. *et al.* GenBank. *Nucleic Acids Res* **42**, D32-7 (2014).

23. Huelsenbeck, J.P. & Ronquist, F. MRBAYES: Bayesian inference of phylogeny. *Bioinformatics* **17**, 754-755 (2001).
24. Wu, Z., Miller, E., Agbandje-McKenna, M. & Samulski, R.J. Alpha2,3 and alpha2,6 N-linked sialic acids facilitate efficient binding and transduction by adeno-associated virus types 1 and 6. *J Virol* **80**, 9093-103 (2006).
25. Gao, G.P. *et al.* Novel adeno-associated viruses from rhesus monkeys as vectors for human gene therapy. *Proc Natl Acad Sci U S A* **99**, 11854-9 (2002).
26. Huson, D.H. & Scornavacca, C. Dendroscope 3: an interactive tool for rooted phylogenetic trees and networks. *Syst Biol* **61**, 1061-7 (2012).
27. Westesson, O., Barquist, L. & Holmes, I. HandAlign: Bayesian multiple sequence alignment, phylogeny and ancestral reconstruction. *Bioinformatics* **28**, 1170-1 (2012).
28. Koerber, J.T., Maheshri, N., Kaspar, B.K. & Schaffer, D.V. Construction of diverse adeno-associated viral libraries for directed evolution of enhanced gene delivery vehicles. *Nat Protoc* **1**, 701-6 (2006).
29. Schrodinger, LLC. The PyMOL Molecular Graphics System, Version 1.3r1. (2010).
30. Bloom, J.D., Romero, P.A., Lu, Z. & Arnold, F.H. Neutral genetic drift can alter promiscuous protein functions, potentially aiding functional evolution. *Biol Direct* **2**, 17 (2007).
31. Aharoni, A. *et al.* The 'evolvability' of promiscuous protein functions. *Nat Genet* **37**, 73-6 (2005).
32. Thornton, J.W. Resurrecting ancient genes: experimental analysis of extinct molecules. *Nat Rev Genet* **5**, 366-75 (2004).
33. Rayaprolu, V. *et al.* Comparative analysis of adeno-associated virus capsid stability and dynamics. *J Virol* **87**, 13150-60 (2013).
34. Klimczak, R.R., Koerber, J.T., Dalkara, D., Flannery, J.G. & Schaffer, D.V. A novel adeno-associated viral variant for efficient and selective intravitreal transduction of rat Muller cells. *PLoS One* **4**, e7467 (2009).
35. Hauck, B. & Xiao, W. Characterization of tissue tropism determinants of adeno-associated virus type 1. *J Virol* **77**, 2768-74 (2003).
36. Vandenberghe, L.H. *et al.* Naturally occurring singleton residues in AAV capsid impact vector performance and illustrate structural constraints. *Gene Ther* **16**, 1416-28 (2009).
37. Wu, Z. *et al.* Single amino acid changes can influence titer, heparin binding, and tissue tropism in different adeno-associated virus serotypes. *J Virol* **80**, 11393-7 (2006).
38. Thornton, J.W., Need, E. & Crews, D. Resurrecting the ancestral steroid receptor: ancient origin of estrogen signaling. *Science* **301**, 1714-7 (2003).
39. Voordeckers, K. *et al.* Reconstruction of ancestral metabolic enzymes reveals molecular mechanisms underlying evolutionary innovation through gene duplication. *PLoS Biol* **10**, e1001446 (2012).
40. Lanfear, R., Kokko, H. & Eyre-Walker, A. Population size and the rate of evolution. *Trends Ecol Evol* **29**, 33-41 (2014).
41. Bowles, D.E. *et al.* Phase 1 gene therapy for Duchenne muscular dystrophy using a translational optimized AAV vector. *Mol Ther* **20**, 443-55 (2012).
42. Lochrie, M.A. *et al.* Mutations on the external surfaces of adeno-associated virus type 2 capsids that affect transduction and neutralization. *J Virol* **80**, 821-34 (2006).
43. Schmidt, D.M. *et al.* Evolutionary potential of (beta/alpha)8-barrels: functional promiscuity produced by single substitutions in the enolase superfamily. *Biochemistry* **42**, 8387-93 (2003).
44. Asuri, P. *et al.* Directed evolution of adeno-associated virus for enhanced gene delivery and gene targeting in human pluripotent stem cells. *Mol Ther* **20**, 329-38 (2012).
45. Varadarajan, N., Gam, J., Olsen, M.J., Georgiou, G. & Iverson, B.L. Engineering of protease variants exhibiting high catalytic activity and exquisite substrate selectivity. *Proc Natl Acad Sci U S A* **102**, 6855-60 (2005).

46. Zincarelli, C., Soltys, S., Rengo, G. & Rabinowitz, J.E. Analysis of AAV serotypes 1-9 mediated gene expression and tropism in mice after systemic injection. *Mol Ther* **16**, 1073-80 (2008).
47. Wu, Z., Asokan, A. & Samulski, R.J. Adeno-associated virus serotypes: vector toolkit for human gene therapy. *Mol Ther* **14**, 316-27 (2006).
48. Schenk-Braat, E.A., van Mierlo, M.M., Wagemaker, G., Bangma, C.H. & Kaptein, L.C. An inventory of shedding data from clinical gene therapy trials. *J Gene Med* **9**, 910-21 (2007).
49. Toromanoff, A. *et al.* Safety and efficacy of regional intravenous (r.i.) versus intramuscular (i.m.) delivery of rAAV1 and rAAV8 to nonhuman primate skeletal muscle. *Mol Ther* **16**, 1291-9 (2008).
50. Ciron, C. *et al.* Human alpha-iduronidase gene transfer mediated by adeno-associated virus types 1, 2, and 5 in the brain of nonhuman primates: vector diffusion and biodistribution. *Hum Gene Ther* **20**, 350-60 (2009).
51. Gray, S.J. *et al.* Optimizing promoters for recombinant adeno-associated virus-mediated gene expression in the peripheral and central nervous system using self-complementary vectors. *Hum Gene Ther* **22**, 1143-53 (2011).
52. Qiao, C. *et al.* Liver-specific microRNA-122 target sequences incorporated in AAV vectors efficiently inhibits transgene expression in the liver. *Gene Ther* **18**, 403-10 (2011).
53. Geisler, A. *et al.* microRNA122-regulated transgene expression increases specificity of cardiac gene transfer upon intravenous delivery of AAV9 vectors. *Gene Ther* **18**, 199-209 (2011).
54. Bershtein, S., Goldin, K. & Tawfik, D.S. Intense neutral drifts yield robust and evolvable consensus proteins. *J Mol Biol* **379**, 1029-44 (2008).
55. Tseng, Y.S. & Agbandje-McKenna, M. Mapping the AAV Capsid Host Antibody Response toward the Development of Second Generation Gene Delivery Vectors. *Front Immunol* **5**, 9 (2014).
56. Gurda, B.L. *et al.* Capsid antibodies to different adeno-associated virus serotypes bind common regions. *J Virol* **87**, 9111-24 (2013).
57. Wobus, C.E. *et al.* Monoclonal antibodies against the adeno-associated virus type 2 (AAV-2) capsid: epitope mapping and identification of capsid domains involved in AAV-2-cell interaction and neutralization of AAV-2 infection. *J Virol* **74**, 9281-93 (2000).
58. Maheshri, N., Koerber, J.T., Kaspar, B.K. & Schaffer, D.V. Directed evolution of adeno-associated virus yields enhanced gene delivery vectors. *Nat Biotechnol* **24**, 198-204 (2006).
59. Gao, G. *et al.* Clades of Adeno-associated viruses are widely disseminated in human tissues. *J Virol* **78**, 6381-8 (2004).
60. Takeuchi, Y., Myers, R. & Danos, O. Recombination and population mosaic of a multifunctional viral gene, adeno-associated virus cap. *PLoS One* **3**, e1634 (2008).
61. Westesson, O. & Holmes, I. Developing and applying heterogeneous phylogenetic models with XRate. *PLoS One* **7**, e36898 (2012).
62. Koerber, J.T., Jang, J.H. & Schaffer, D.V. DNA shuffling of adeno-associated virus yields functionally diverse viral progeny. *Mol Ther* **16**, 1703-9 (2008).
63. Deleyrolle, L.P. *et al.* Determination of somatic and cancer stem cell self-renewing symmetric division rate using sphere assays. *PLoS One* **6**, e15844 (2011).

Chapter 3: Adeno-Associated Virus (AAV) Vectors in Cancer Gene Therapy

This chapter is adapted from a manuscript published as

Santiago-Ortiz, J.L. & Schaffer, D.V. Adeno-associated virus (AAV) vectors in cancer gene therapy. *J Control Release* (2016).

3.1 Introduction

Cancer, a large group of diseases characterized by the unregulated proliferation and spread or metastasis of abnormal cells, collectively represents a major worldwide healthcare problem. In the U.S. alone more than 1.5 million cases are diagnosed each year, and cancer overall has a 5-year relative survival rate of 68%, making it the second leading cause of death after heart disease[1]. Standard treatments include surgery, chemotherapy, and radiotherapy; however, these are often incapable of completely eradicating a malignancy[2] and can be accompanied by serious side effects[3]. Thus, there is a strong unmet medical need for the development of novel therapies that offer improved clinical efficiency and longer survival times in patients afflicted with disease.

Gene therapy is a very promising treatment for many diseases including cancer. To date, more than 2,000 clinical trials employing gene transfer have taken place, establishing the safety of a number of vectors[4,5]. Furthermore, the majority (64%, n=1,415[6]) of gene therapy clinical trials to date have targeted cancer – including lung, skin, neurological, and gastrointestinal tumors – and have utilized a variety of therapeutic strategies such as anti-angiogenic factors, tumor suppressors, immunostimulation, and oncolytic viruses. In 2015, the first recombinant viral therapy for cancer – an oncolytic herpesvirus for the treatment of melanoma – received regulatory approval in the U.S.[7].

For cancer gene therapies to be increasingly successful, however, a major hurdle must be overcome: the development of gene delivery vectors that can safely, efficiently, and specifically deliver genetic material to the target cells. Viral vectors have been used in the majority (over 68%[6]) of gene therapy clinical trials, and the most frequently used have been based on adenovirus, retrovirus, vaccinia virus, herpesvirus, and AAV[8]. As discussed in Chapter 1, AAV vectors in particular have been increasingly successful due to their gene delivery efficacy, lack of pathogenicity, and strong safety profile[9]. As a result of these properties, AAV vectors have enabled clinical successes in a number of recent clinical trials that have established the promise of gene therapy in general.

AAV vectors may also offer a strong potential for the treatment of cancer, and as presented in this review, their excellent gene delivery properties have been harnessed for *in vitro* cancer studies, *in vivo* pre-clinical cancer models, and more recently cancer clinical trials under development. For oncology applications, AAV vectors can transduce a wide variety of cancer primary cells and cell lines[10-12] and have the capacity to carry highly potent therapeutic payloads for cancer including anti-angiogenesis genes, suicide genes, immunostimulatory genes, and DNA encoding smaller

nucleic acids (e.g. shRNAs, siRNAs) for post-transcriptional regulation of oncogenes[13]. AAVs therefore offer a strong potential as gene delivery vehicles for cancer gene therapy and have consequently been employed in numerous preclinical cancer models and in early stage clinical trials for cancer.

3.2 Rational Design of the AAV Capsid for Cancer-Specific Transduction

Natural variants of AAV have enabled increasing success in human clinical trials, but as discussed in Chapter 1, they also have some shortcomings that render this success challenging to extend to the majority of human diseases, including cancer. These concerns have motivated the engineering of AAV capsids that can more efficiently traffic to and transduce cancer cells, as well as the engineering of genetic cargos for higher potency and selective expression.

Changes in protein expression patterns [14] and subsequent presentation of tumor-specific antigens [15,16] in cancer tissues may enable the preferential targeting of AAV gene delivery vehicles to tumor tissues [17,18]. For example, Grifman *et al.* [19] targeted aminopeptidase N (or CD13), a membrane-bound enzyme that is highly expressed in cancerous tissue and vessels and has consequently been explored for targeted cancer therapies [20]. Specifically, they modified the AAV2 capsid, whose primary receptor for cellular entry is heparin sulfate proteoglycan (HSPG), by introducing a NGR peptide motif, which binds to CD13 [17], either in replacement of antigenic loops of AAV2 (residues T448-T455 and N587-A591) or after residues 449 and 588 of the capsid (Figures 3.1B, 3.1C). Mutant viruses with the NGR motif exhibited reduced affinity for heparin, suggesting a tropism different from AAV2, and transduced the sarcoma cell lines KS1767 and RD (which express CD13 at high levels) 10- to 20-fold better than wild-type AAV2, demonstrating the selectivity of these vectors.

Integrins, which contribute to tumor progression and metastasis, are also highly expressed in tumor cells and tumor vasculature [21] and have accordingly also been harnessed for selective tumor transduction. AAV2 vectors have been modified by inserting a 4C-RGD peptide [22], whose RGD motif selectively binds to αvβ3 and αvβ5 integrins [17], into different sites of the *cap* gene. Mutant vectors with the RGD insertion after residues 584 and 588 of VP3 (Figures 3.1B, 3.1C) retained infectivity, and the A5884C-RGD mutant was shown to bind to integrin and to mediate increased *in vitro* and *in vivo* gene delivery to integrin-expressing tumor cells. A5884C-RGD- mediated gene delivery was 40-fold higher on K562 human chronic myelogenous leukemia cells, 13-fold higher on Raji human lymphoblast-like cells, and 6-fold higher on SKOV-3 human ovarian adenocarcinoma cells, compared to wild-type AAV2.

Additionally, designed ankyrin repeat proteins (DARPins) targeting cancer-associated receptors have been fused to AAV2 capsid proteins for enhanced selectivity to cancer cells [23]. DARPin 9.29, which specifically binds to HER2/*neu*, a receptor overexpressed in cancer cells, was fused to VP2 and then used to package AAV2 particles whose affinity for HSPG had been ablated through site-directed mutagenesis. The resulting vectors (Her2-AAV) transduced cells in a HER2-dependent manner, showing selectivity for HER2-expressing cells and only weakly transducing cells not expressing the receptor. Moreover, systemically administered Her2-AAV vectors localized to subcutaneous tumors of $HER2^+$ SK-OV-3 cells in mice, compared to a lack of tumor cell transduction of AAV2 vectors, which instead localized primarily to the liver.

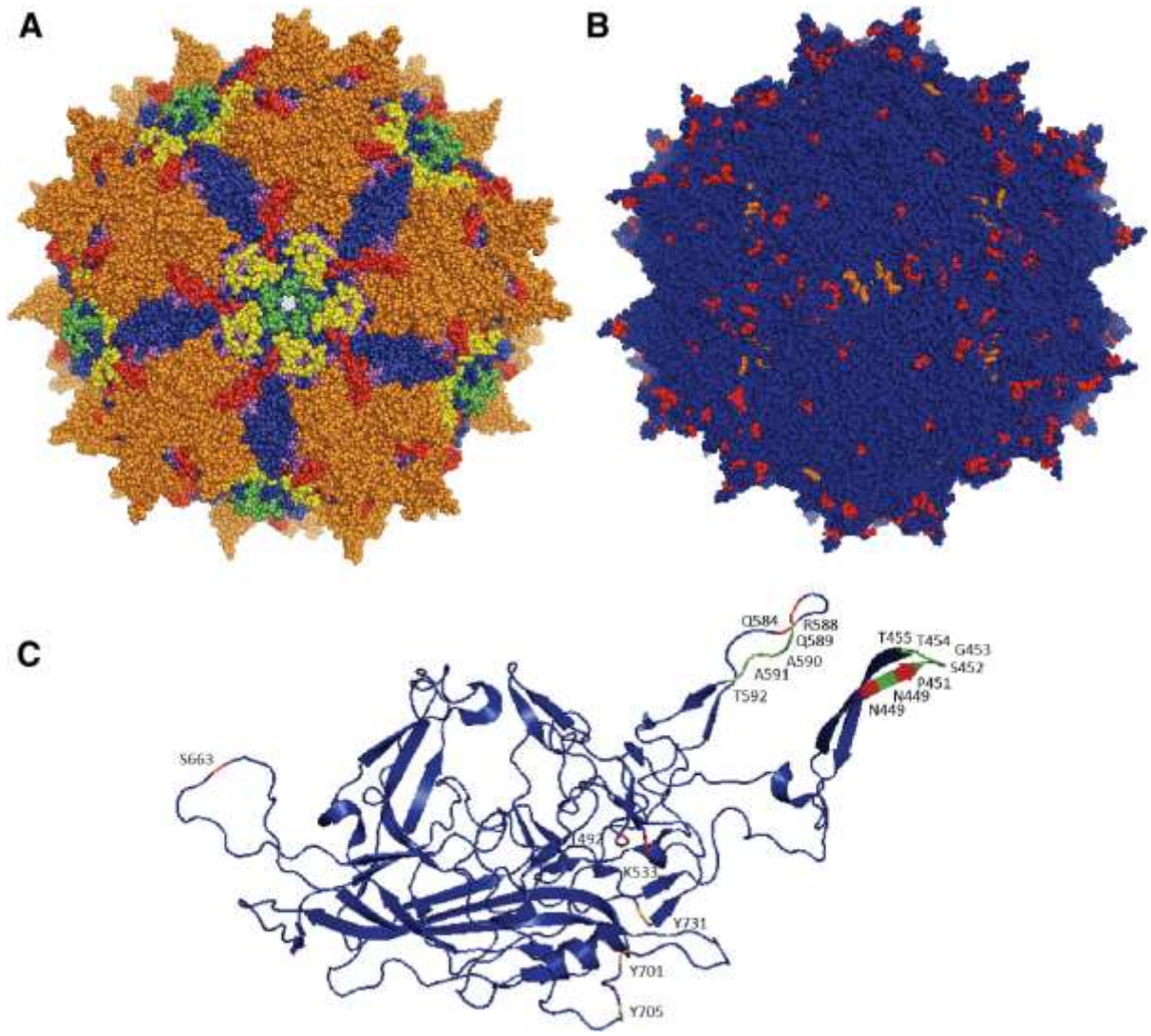

Figure 3.1: Representation of AAV2 capsid structure and individual monomeric protein. (A) Crystal structure of the AAV2 capsid[24], the most widely used and studied AAV serotype. **(B)** Residues that have been mutated to engineer vectors for transduction of cancer cells are mapped onto the AAV2 crystal structure and depicted in orange (tyrosine to phenylalanine mutations) or red (other mutations). **(C)** Mutated residues are similarly depicted in the individual VP3 monomer structure. Additionally, residues that have been removed to insert protein-binding peptides [58] are depicted in green. Images were produced with Pymol[25].

AAV5 has also been engineered by inserting homing peptides for integrins, sialyl Lewis X (sLex), and tenascin C (TnC), which are overexpressed in many cancer tumors [26]. Mutants with RGD peptides infected integrin-expressing cells 5-fold better than AAV5, and both integrin- and TnC-targeting AAVs preferentially transduced cells presenting these molecules while showing very low transduction of cells negative for these antigens. Mutants with the sLex-targeting peptide did not transduce sLex-expressing cells.

Cheng *et al.* [27] studied the effects of mutating surface-exposed tyrosine residues to phenylalanines on AAV3. Three of the single-residue mutants – Y701F, Y705F, and Y731F (corresponding

residues in AAV2 depicted in Figures 3.1B, 3.1C) – showed 1.5-, 2.2-, and 8.8-fold enhanced transduction, respectively, of Huh7 hepatocellular carcinoma (HCC) cells and 2.3-, 3.3-, and 9.1-fold enhanced transduction, respectively, of Hep293TT human hepatoblastoma tumor cells compared to wild-type AAV3. A double mutant, Y705F+Y731F, showed further increased transduction (11-fold higher) on Huh7 cells. This double mutant, when administered intra-tumorally or systemically to a mouse xenograft model of human liver tumors, also showed enhanced transduction, as reported by fluorescence microscopy, compared to AAV3. Additional studies with AAV3 have mutagenized serine, threonine, and lysine residues to valine, glutamate, and arginine residues, respectively, in addition to changing tyrosine residues to phenylalanines (corresponding residues in AAV2 depicted in Figures 2B, 2C) [28]. Mutants S663V+T492V+K533R, S663V+T492V+K533R, and S663V+T492V had transduction efficiencies over 10-fold higher than wild-type AAV3 on Huh7 cells. Some of these mutants also showed 2- and 8-fold enhanced transduction on HepG2 and Hep293TT cells, respectively, and the S663V+T492V mutant showed 2-fold higher transduction than the Y705+731F mutant in mouse xenografts of these cells lines.

There has also been a strong interest in AAV delivery to immune cells. In particular, given that cancers can develop resistance mechanisms against both drugs and the immune system, cancer research efforts have also focused on stimulating the adaptive immune system to mount a T cell-mediated anti-tumor response. Immunotherapy offers important potential advantages over traditional therapies, including selectivity for tumor cells and the generation of memory T cells that protect against recurring tumors [29]. This has motivated the engineering of viral vectors with enhanced infectivity for dendritic cells (DCs), antigen-presenting cells that can prime T cells and generate an anti-tumor cytotoxic T lymphocyte (CTL) immune response. Surface-exposed serine and threonine residues in AAV6 (corresponding residues in AAV2 depicted in Figures 3.1B, 3.1C) have been mutated to valine residues for enhanced *in vitro* transduction efficiency on monocyte-derived DCs (moDCs) [30]. Mutants T492V, S663V, and T492V+S663V showed enhanced infectivity, with the double mutant showing 5-fold higher transduction. This T492V+S663V mutant was used to transduce moDCs with human prostate-specific antigen (hPSA), which led to and a 3-fold higher hPSA expression in moDCs and a 1.3-fold stronger CTL response against human prostate adenocarcinoma cells compared to wild-type AAV6 gene delivery, underscoring the utility of enhanced AAV vectors that can be used for cancer immunotherapy, particularly if delivery can be achieved *in vivo*.

Additionally, AAV vectors have been modified by inserting protease recognition sequences on the capsid such that protease cleavage is required for complete viral transduction [31]. Specifically, short sequences encoding negatively charged amino acids, which serve as “locks” by interfering with virus-receptor interactions, were flanked by protease cleavage sites recognized by matrix metalloproteinases (MMPs) and genetically inserted into surface-exposed regions near the heparin binding domain of the AAV2 capsid. Inactivated or “locked” vectors had reduced heparin affinity and infectivity, and treatment with MMPs restored heparin binding and allowed efficient transduction. MMPs are highly expressed in most cancers compared to normal tissue [32], so such protease-responsive AAV vectors could provide enhanced selectivity towards cancerous tissues, as other studies that have exploited high levels of MMP expression for selective viral gene delivery have demonstrated [33].

3.3 Directed Evolution for the Engineering of Cancer-Specific Transduction

As described above, directed evolution and library selection are alternative approaches that can generate highly efficient vectors, even in the absence of mechanistic knowledge underlying a particular gene delivery barrier. Michelfelder *et al.* [34] employed an *in vitro* selection scheme to identify variants from an AAV2-based random peptide insertion library that had high infectivity on tumor cells. In this case, analogous to the rational approach, the selected AAV variants shared the RGDXXXX amino acid motif and exhibited over 15-fold higher transduction than wild-type AAV2 vectors on PymT breast cancer cells. The investigators also performed an *in vivo* selection, in which they administered the AAV library to tumor-bearing mice, harvested tumor tissue, and then recovered the peptide sequences of viral particles that had successfully infected tumor cells. Selected mutants had peptide sequences rich in serine and glycine residues. Dominant clones displayed 40- to 200-fold higher *in vivo* transduction of breast tumor tissue compared to wild-type vectors and interestingly also showed enhanced cardiac tropism; however, the liver tropism of the mutants was comparable or only moderately lower than that of wild-type vectors.

A DNA shuffled library of AAV serotypes 1, 2, 5, 9, rh8, and rh10 was selected for transduction of U87 human glioma cells and generated infectious mutants after seven rounds of *in vitro* selection [35]. One of the selected clones, AAV-U87R7-C5, had a chimeric *cap* gene with contributions from serotypes 1, 2, rh.8 and rh.10. This mutant transduced U87 cells and a panel of other glioma cells moderately better than AAV2.

3.4 Payload Engineering for Cancer-Specific Expression

In addition to tissue specificity and high transduction efficiency, AAV vectors for cancer gene delivery may also have regulatory elements that promote tissue-selective gene expression, a feature particularly important when off-target transduction with a cytotoxic or immunostimulatory factor is a potential risk. Promoters that are tissue-specific, tumor-specific, or tumor microenvironment-specific have been explored to restrict transcription of the delivered transgene to a cancerous tissue of interest [36]. For instance, the promoter for C-X-C chemokine receptor type 4 (CXCR4), which is overexpressed in many cancer tissues, was implemented to restrict AAV-mediated transgene expression to primary and metastatic breast cancer [37]. AAV2 vectors encoding firefly luciferase under the control of either the CMV promoter or the CXCR4 promoter were directly delivered to subcutaneous or liver-localized MCF-7 (a human breast cancer cell line) xenografts in mice, and the ratio of expression levels between tumor tissue and muscle was determined. Off-target luminescence in muscle from control CMV vectors was 4- to 21-fold higher than in tumor tissue. In contrast, expression from CXCR4 vectors was selective for tumor tissue, with off-target muscle luminescence levels of only 10%-50% relative to tumor luminescence. Systemic administration via a splenic port of CXCR4 vectors to tumor-bearing mice resulted in luminescence levels at the tumor site that were five-fold higher than in tumor-free mice, confirming selectivity for tumor tissue.

The human telomerase reverse transcriptase (hTERT) promoter has been widely used as a cancer-selective promoter, though its *in vivo* utility has sometimes been limited by its low strength [38]. In one study, it was combined with an advanced two-step transcriptional activation system (TSTA) to enhance cancer-specific gene expression in a panel of cancer cell lines *in vitro* and in an *in vivo* orthotopic liver tumor mouse model [39]. An intravenously delivered AAV2 vector carrying hTERT-driven firefly luciferase with the TSTA system led to liver tumor bioluminescence levels 18-fold

higher than delivery of only hTERT-driven luciferase, and 16-fold higher than using the standard TSTA system.

As mentioned earlier, Pandya *et al.* generated an AAV6-based mutant with enhanced transduction of DCs [30]. They also developed a chimeric promoter sufficiently small to fit into AAV vectors by combining different functional modules of the CD11c promoter, which is specific to DCs. Gene expression using this chimeric promoter (chmCd11c) was restricted to DCs, and delivery of the hPSA gene under its control to DCs resulted in a CTL response against human prostate adenocarcinoma cells, albeit 50% lower than when using the stronger yet ubiquitous chicken beta-actin (CBA) promoter.

Recently AAV8's strong murine liver tropism was combined with a liver-specific promoter and post-transcriptional regulation based on miR-122a to restrict gene expression to cancer cells in a murine model of metastatic hepatocarcinoma (HCC) [40]. MiR-122a, which is highly expressed in healthy liver tissue but downregulated in HCC, suppresses translation of mRNAs that harbor its target binding sequence. The HLP liver-specific promoter [41] was combined with tandem repeats of *miR-122a*-binding sequences inserted in the 3' untranslated region of the expression cassette. Systemic delivery of the resulting construct encoding firefly luciferase led to 40-fold lower liver expression compared to control vector without *miR-122a* elements. Furthermore, vector administration to mice bearing a subcutaneous HCC xenograft of miR-122a-negative SK-Hep1 cells led to tumor-restricted bioluminescence, with no luminescence from surrounding healthy liver tissue, confirming the combinatorial tumor tissue specificity of this vector and expression cassette.

3.5 AAV Delivery of Therapeutic Payloads in Preclinical Models of Cancer

In addition to efficiently transducing a variety of cancer cells *in vitro* [10-12], AAV has been increasingly employed to deliver therapeutic genes to *in vivo* preclinical tumor models. Over the last decade, the arsenal of delivered transgenes has greatly expanded, as have the types of cancer for which AAV vectors have been used. These transgenes can be divided into several categories: anti-angiogenesis genes, cytotoxic or suicide genes, cytokines for stimulating the immune system, tumor suppression and anti-tumor genes, DNA encoding small RNA's, antigens to stimulate antigen-presenting cells, and antibodies that block signaling.

Anti-Angiogenesis Therapy

Angiogenesis, the formation of new blood vessels from existing ones, is an important process for tumor nourishment, growth, and metastasis [42]. Consequently, inhibiting angiogenesis in tumors to reduce their progression and capacity to metastasize is a longstanding anti-cancer strategy. Multiple gene delivery approaches have been used to inhibit vascular endothelial growth factor (VEGF), a potent angiogenic growth factor, including using decoy receptors, monoclonal antibodies, and a combination of gene delivery with small molecule inhibitors. Mahendra *et al.* [43] used AAV2 to deliver a soluble splice variant of VEGF-Receptor-1 (sFlt1), a decoy that competitively inhibits VEGF-A binding to its endogenous receptor. Intramuscular AAV2-sFlt1 injection of vector to mice harboring a subcutaneous human ovarian cancer cell line (SKOV3.ip1) xenograft resulted in reduced tumor volume and in 83% survival rate, compared to no survival of

untreated mice, six weeks post tumor implantation. In an analogous study, intramuscular administration of AAV1-sFlt1 suppressed tumor growth and enhanced survival in a subcutaneous SHIN-3 ovarian cancer cell line xenograft model [44].

Soluble VEGFR1/R2, a chimeric VEGF receptor comprising domains of both VEGFR-1 and VEGFR-2, was combined with irradiated granulocyte-macrophage colony-stimulating factor (GM-CSF)-secreting tumor cell immunotherapy in mouse models of melanoma and colon carcinoma [45]. AAV8-sFVEGFR1/R2 was intravenously delivered to mice, followed by subcutaneous implantation of B16F10 melanoma tumor cells and later immunization with irradiated GM-CSF–secreting B16F10 (B16.GM) tumor cells. VEGR1/R2 delivery resulted in a mean survival time (MST) of 63 days, compared to 31 days for no treatment. This effect was further enhanced by combining vector delivery with B16.GM vaccination (MST of 93 days), which also led to increased numbers of activated DCs and T cells.

VEGF-C, which can mediate angiogenesis and metastasis to lymphatic vessels, has been targeted by delivering a secreted soluble VEGF-C decoy receptor, sVEGFR3-Fc, to melanoma and renal cell carcinoma mouse models [46]. Systemic portal vein administration of AAV2-sVEGFR3-Fc before subcutaneous implantation of A375-mln1 metastatic tumor cells had no effect on primary tumor growth, but inhibited metastasis to the lymph nodes, with only two out of seven mice developing lymph node metastases compared to all of nine mice in the control group. However, vector-mediated inhibition of metastasis to lung was less effective. Additionally, intramuscular injection of AAV2-sVEGFR3-Fc to the quadriceps inhibited lymph node metastasis in renal cell carcinoma (Caki-2) and prostate cancer models (PC-3) by 70% and 75%, respectively. Finally, intramuscular injection of AAV1-sVEGFR3 to mice bearing orthotopic endometrial cancer tumors (HEC1A) led to complete ablation of detectable lymph node and lung metastases compared to untreated mice [47].

In addition to VEGF receptors, other native inhibitors of angiogenesis have also been employed in anti-angiogenic gene delivery studies. Pigment epithelium-derived growth factor (PEDF) is a very potent inhibitor of angiogenesis that prevents the formation of new vessels from endothelial cells by interacting with VEGFR-1, without affecting the existent vasculature [48]. Intratumoral delivery of AAV2-PEDF to a mouse model of Lewis lung carcinoma (LCC) led to a 58% reduction in tumor size, reduced tumor microvessel density, increased tumor cell necrosis, and a 75% increase in MST compared to no treatment [49]. In a subsequent study, combining AAV2-PEDF with the chemotherapeutic drug cisplatin [50] prolonged survival by 150% and 50% compared to no treatment and either treatment alone, respectively. Investigators also reported greater tumor size reduction, tumor apoptosis, and tumor angiogenesis suppression compared to untreated mice or those receiving either treatment alone.

Monoclonal antibodies that block angiogenesis, widely used as a front-line treatment for many types of cancer, have been encoded into AAV vectors for sustained expression and therapeutic effects. Intravenous administration of AAV8-DC101 – encoding a neutralizing mAb against VEGFR2 – resulted in high antibody expression levels in serum, conferred protection against subcutaneous B16F10 melanoma and U87 glioblastoma tumors, and led to reduced tumor size (65% and 82% reduction, respectively) and long-term survival (10% and 80%, respectively) in both models [51]. Tumor angiogenesis was targeted in a DU 145 metastatic lung cancer model by

delivering AAVrh.10 encoding a murine mAb with a VEGF-A antigen recognition site equivalent to that of the humanized VEGF-A antibody bevacizumab. Intrapleural vector administration led to high levels of anti-VEGF-A mAb expression, which resulted in reduced growth (76%), vascularization (63%), and proliferation (74%) of metastatic lung tumors and subsequent over 2-fold longer mean survival of treated mice [52]. In another study, the same group intraperitoneally delivered AAVrh.10 packaged with bevacizumab to intraperitoneal models of ovarian carcinomatosis based on A2780 or SK-OV3 cells, eliciting 90% reduced A2780 tumor growth, 82% lower A2780 tumor angiogenesis, and prolonged survival (1.6-fold and 1.2-fold higher mean survival time in A2780 and SK-OV3 tumors, respectively) compared to untreated mice [53]. Additionally, the combination of vector delivery with chemotherapy drugs topotecan or paclitaxel generated further enhanced anti-tumor effects on A2780 xenografts (3.2-fold and 1.9-fold higher mean survival time, respectively, compared to untreated mice).

Endostatin and angiostatin, endogenous inhibitors of angiogenesis that prevent pro-angiogenic factors from interacting with endothelial cells [54], have been employed as protein therapies in clinical trials, motivating their use in gene therapies. Intratumoral delivery of AAV2-endostatin to mice carrying a subcutaneous human bladder cancer tumor (T24) yielded a 40% reduction in tumor volume and a 60% reduction in tumor angiogenesis, as well as enhanced tumor cell apoptosis [55]. The same group later combined endostatin with herpes simplex virus thymidine kinase (HSV-TK), a suicide gene that converts the pro-drug ganciclovir into a thymidine analog that is incorporated into and subsequently fragments DNA undergoing synthesis, for intratumor AAV2-mediated delivery to bladder cancer tumors [56]. This combination therapy led to three-fold slower tumor progression and a 60% reduction in tumor size compared to untreated mice, with either therapy individually producing a 40% reduction in size. Another group [57] delivered AAV2-angiostatin to a mouse liver cancer model based on intraportally injected EL-4 tumor cells previously transduced *in vitro* with AAV2-B7.1, a molecule that stimulates T-cells. Delivery of AAV2-angiostatin to mice vaccinated with B7.1-transduced cells suppressed tumor growth by 87% and greatly increased survival rates, with six of ten treated, vaccinated mice surviving for over 100 days, compared to median survival rates of 33, 42, and 25 days in untreated vaccinated mice, angiostatin-treated unvaccinated mice, and untreated, unvaccinated mice.

Isayeva *et al.* [58] studied the effect of co-delivering endostatin and angiostatin in an intraperitoneal mouse model of ovarian cancer (SKOV3.ip1). Intramuscular injection of bicistronic AAV2-angiostatin-endostatin (AAV2-E+A) resulted in a 50% reduction in tumor size, increased tumor cell apoptosis, decreased tumor angiogenesis, and 30% of mice surviving for over 150 days compared to control mice surviving an average of 45 days. In a subsequent study [59], combining intraperitoneal AAV2-E+A delivery with the chemotherapy drug taxol led to complete survival of 90% of dually-treated mice and a 90% reduction in tumor size compared to untreated mice. The same group extended this combinatorial approach to the transgenic adenocarcinoma of mouse prostate (TRAMP) prostate cancer model by intramuscularly delivering bicistronic AAV6 encoding endostatin and angiostatin [60]. Mice receiving AAV6-E+A at an early age (5 or 10 weeks old) had low grade, smaller tumors, and 60% of them survived longer than 60 weeks, compared to median survival times of 30-35 weeks for untreated mice or those receiving AAV6-E+A at older ages (>18 weeks), respectively. Endostatin has also been used in conjunction with another angiogenic inhibitor, thrombospodin-1 (TSP-1), in a mouse orthotopic pancreatic cancer model (AsPC-1) [61]. Intramuscular delivery of either AAV2-endostatin or AAV2-3TSR (the

antiangiogenic domain of TSP-1) prior to xenografting resulted in similar levels of protection, causing 45% lower tumor microvessel density and a 43% reduction in tumor size. Co-delivery of both vectors led to more marked effects in those parameters (65% and 62%, respectively) compared to either treatment alone.

Intramuscular delivery of AAV2-P125A-endostatin, an endostatin mutant with enhanced binding to endothelial cells and stronger anti-angiogenic effects, in an ovarian carcinoma mouse model (MA148) led to 72% smaller tumors and decreased angiogenesis, with a 46% reduction in the mean number of vessel nodes [62]. In a subsequent study [63], the same group delivered AAV2-P125A-endostatin in combination with the chemotherapy drug carboplatin to an orthotopic ovarian cancer model (MA148). This combination led to 25% higher median survival and 52% less vessel nodes compared to untreated mice.

A range of other antiangiogenic transgenes have been delivered with AAV vectors. AAV2 was used to deliver tissue factor pathway inhibitor (TFPI-2) – a suppressor of angiogenesis, tumor growth, and tumor cell invasiveness – to a glioblastoma mouse model (SNB19) [64]; kringle 5, a fragment of plasminogen with potent antiangiogenic properties, to a mouse model of ovarian cancer (MA148) [65]; and self-complementary cargoes encoding siRNAs against the unfolded protein response (UPR) proteins IRE1α, XBP-1, or ATF6 in a mouse breast cancer model (NeuT) with an AAV2 mutant with seven surface tyrosine to phenylalanine mutations [66]. Cai *et al.* [67] used AAV5 to deliver vasostatin – an endogenous inhibitor of angiogenesis – to a subcutaneous, orthotopic xenograft, and a spontaneous metastasis model of lung cancer (A549, LLC Lewis lung carcinoma, respectively). Finally, AAV8 encoding human plasminogen kringle 1-5, an inhibitor of angiogenesis, was administered to murine models of mouse melanoma (B16F1), mouse lung cancer (LLC), and human melanoma (A2058) [68]. Delivery of the described transgenes resulted in suppression of both angiogenesis and tumor growth.

Delivery of Cytotoxic or Suicide Genes

Suicide gene therapy has been broadly investigated as an anti-cancer therapy [69]. The most utilized system is the herpes simplex virus type 1 thymidine kinase (HSV-TK), which converts ganciclovir (GCV) into the toxic metabolite GCV-triphosphate within cells expressing the enzyme and also induces bystander toxicity to neighboring tumor cells [70]. Intratumoral administration of AAV2-HSV-TK under Dox-inducible Tet-On regulation to a mouse model of breast cancer (MCF-7) resulted in 75% suppression of tumor growth with only moderate toxicity [71]. In a subsequent study, the same group confirmed these results and elaborated on the therapeutic mechanism of the HSV-TK system in MCF-7 cells [72]. AAV2-mediated delivery of sc39TK, a hyperactive variant of HSV-TK with enhanced affinity for GCV, to HeLa cells that were later implanted into mice to generate subcutaneous tumors enabled 70% tumor growth suppression upon GCV administration [73].

Other cytotoxic genes have also been employed in AAV-mediated delivery to cancer cells. Kohlschütter *et al.* [12] used AAV2 to deliver diphtheria toxin A (DTA) and p53 upregulated modulator of apoptosis (PUMA) to HeLa cells, SiHa cervical carcinoma cells, and RPMI 8226 myeloma cells *in vitro*. DTA exerted a cytotoxic effect on all cell lines, whereas PUMA delivery cause cytotoxicity in HeLa and RPMI cells. They also used an AAV2 mutant they had previously

developed, RGDLGLS [34], to deliver DTA to mammary tumor cells from mice carrying the polyomavirus middle T antigen (PymT cells) and induced a 40% cytotoxicity.

Immunomodulation through Delivery of Cytokines

The delivery of stimulatory molecules such as cytokines can elicit an enhanced immune response against tumors. A widely used cancer therapeutic is tumor necrosis factor (TNF)-related apoptosis-inducing ligand (TRAIL), which elicits a strong apoptosis effect primarily in tumor cells, but not in normal tissue, by binding to death receptors [74]. Intraportal administration of AAV2-TRAIL in an orthotopic mouse model of lymphoma (EL-4) suppressed tumor growth by 95% and enhanced median survival by 92%, an effect of induced apoptosis in the tumor cells metastasizing to the liver [75]. The same group subsequently delivered AAV2-sTRAIL (soluble TRAIL) to a subcutaneous mouse model of human liver cancer (SMMC-7721) [76]. Oral or intraperitoneal administration of AAV2-sTRAIL suppressed tumor growth by 88% and 82%, respectively. This group also observed 82% tumor size suppression and 52% enhanced median survival when administering sTRAIL, packaged in AAV5, to mice bearing subcutaneous or orthotopic A549 lung adenocarcinoma tumors [77]. Another group [78] also delivered sTRAIL, packaged in AAV2, to an A549-based subcutaneous lung adenocarcinoma tumor model. Intratumor vector delivery led to 62% reduced tumor size, and systemic vector delivery before implantation of A549 cells lowered the frequency of tumor occurrence to 43% compared to 100% in untreated mice.

Intratumoral delivery of TRAIL, packaged in AAV2 under the control of the cancer-specific hTERT promoter, to a subcutaneous SMMC7721 HCC xenograft led to a 70% suppression of tumor growth and long-term survival, compared to a survival of 78-105 days in untreated mice [79]. They subsequently combined AAV2-hTERT-TRAIL and cisplatin in a subcutaneous BEL7404 HCC model, which resulted in 94% reduction in tumor size and complete survival [80]. In another study, intratumoral AAV2-hTERT-TRAIL delivery to an HCC SMMC7221 mouse model was combined with administration of the chemotherapeutic 5-fluorouracil (5-FU) [81]. Combination therapy led to a strong anti-tumor effect, with an 83% reduction in tumor growth compared to treatment with vector or 5-FU only (60% and 16% reduction, respectively). The same group [82] extended intratumoral delivery of AAV2-TRAIL, combined with cisplatin, to a subcutaneous mouse model of head and neck squamous cell carcinoma (HNSCC), resulting in 40% smaller tumors. In a different study, intracranial delivery of AAV2-interleukin-12 (IL-12), a potent immunostimulatory cytokine, in a RG2 rat model of glioblastoma led to enhanced TRAIL expression and microglia activation, 3.5-fold higher median survival time, and 30% reduced tumor volume [83].

Interferons (IFNs) are cytokines that induce antitumor effects that include interfering with cancer cell division and slowing tumor growth progression. Systemic administration of AAV8-hIFN-β to a mouse retroperitoneal xenograft of NB-1691 human neuroblastoma cells, by itself or combined with trichostatin, resulted in similar (90%) suppression of tumor growth relative to untreated or trichostatin-treated mice [84]. Maguire *et al.* [85] studied the protective effects of IFN-β expression against intracranial, orthotopic U87 xenografts of glioblastoma multiforme. Stereotactic delivery of AAVrh.8-IFN-β followed by cancer cell implantation prevented growth of glioma tumors, and even led to 100% survival against glioma challenge. Additionally, vector delivery into tumor-bearing mice led to regression of established tumors and subsequent complete survival. In another

study, AAV2-IFN-β under the control of the hTERT promoter reduced tumor growth by over 90% and enhanced survival in mouse models of colorectal cancer (SW620) and lung cancer (A549), with 87% and 83% long-term survival in treated mice, respectively [86]. Other interferons have been used in AAV-mediated delivery to cancer models, including intravenously administered AAV6-IFN-α to a B16F10 mouse model of metastatic melanoma, leading to a 60% reduction in the number of metastatic colonies and a modest enhancement in the survival of treated mice [87].

CD40-ligand (CD40L) is an immunostimulatory protein implicated in the activation of dendritic cells and induction of tumor cell apoptosis. Intratumor delivery of self-complementary AAV5-CD40L to subcutaneous A549 lung cancer tumors led to a 67% reduction in tumor size and 2.7-fold higher level of tumor cell apoptotic death [88]. Recently, self-complementary AAV5 vectors expressing a non-cleavable CD40L mutant were used to treat subcutaneous A549 lung cancer xenografts [89]. Intratumoral delivery of AAV5-CD40L and AAV5-CD40LM (i.e. mutant) reduced tumor size and increased apoptosis, with the CD40L mutant exhibiting greater effects than wild-type ligand (33% vs. 28% tumor reduction for wtCD40L).

Interleukins, another class of immunostimulatory molecules, have been employed in cancer gene therapies. Systemic delivery of AAV1 carrying melanoma differentiation-associated gene-7/interleukin-24 (mda-7/IL24), a cytokine capable of inducing tumor apoptosis and inhibiting tumor growth and metastasis, to a subcutaneous Ehrlich ascites tumor mouse model suppressed tumor growth by 63%, increased tumor cell apoptotic death, reduced tumor angiogenesis, and enhanced mean survival time by over 80% [90]. Likewise, intratumoral delivery of AAV2-IL24 to an orthotopic MHCC97-H HCC model increased apoptotic tumor cell death and inhibited tumor recurrence and metastasis in the liver and lung [91]. In another study, intramuscular delivery of AAV8-IL24 to a transgenic mouse model of mixed-lineage leukemia/AF4-positive acute lymphoblastic leukemia (MLL/AF4-positive ALL) reduced tumor angiogenesis by 57% [92].

Chang *et al.* [93] studied the delivery of IL-15, a cytokine capable of stimulating an immune response by inducing proliferation and activation of natural killer cells and T cells, to a BNL-h1 mouse model of metastatic HCC. Prophylactic intravenous delivery of AAV8 encoding an IL-15 superagonist followed by cancer cell implantation led to 82% lower tumor metastasis. Analogously, therapeutic delivery (vector delivered to tumor-bearing mice) led to both 80% lower tumor metastasis and enhanced mean survival by 41% with no apparent liver toxicity observed. Another group intramuscularly administered AAV2-IL15 to a transgenic model of SV40 T/t antigen-induced breast cancer prior to induction of breast cancer, which stimulated lymphokine-activated killer (LAK) cells, slowed tumor growth (tumor size reached 2500 mm^3 after 33 days vs. 20 days for control) and reduced final tumor size by 30% [94].

Other AAV-delivered immunostimulatory transgenes that have elicited anti-tumor effects include secondary lymphoid tissue chemokine (SLC), delivered preventatively and therapeutically by AAV2 to a Hepal-6 mouse liver cancer tumor model [95]; Nk4, delivered by AAV2 to a metastatic Lewis lung carcinoma (LLC) mouse model [96]; the cytokine LIGHT, delivered by AAV2 to a TC-1 mouse cervical cancer model [97]; the granulocyte-macrophage colony stimulation factor (GM-CSF) cytokine, delivered by AAV1 to a 9L tumor model [98]; and TNF-α, delivered by AAV2 to a U251 human glioma xenograft mouse model [99].

Delivery of Tumor Suppression and Repair Genes

Another anti-cancer gene therapy strategy is the delivery of transgenes and nucleic acids that can elicit tumor suppression or down-regulation of tumorigenic proteins (i.e. those overexpressed in tumor cells). Several groups have delivered dominant negative mutants of survivin, an anti-apoptotic protein overexpressed in most types of cancer. Tu *et al.* [100] used AAV2 to deliver the C84A survivin mutant, capable of inducing apoptosis, to SW1116 and Colo205 colon cancer cells that were then subcutaneously injected in nude mice, and they observed suppressed tumorigenesis and reduced tumor growth by 80% and 55%, respectively. Alternatively, intratumor therapeutic delivery inhibited the growth of previously established tumors by 81% and prolonged mean survival of treated mice by 75%. The same group [101] subsequently delivered another dominant-negative survivin mutant capable of inducing apoptosis and reducing tumor growth, T34A, to an HCT-116 human colon cancer mouse model using AAV2 and obtained similar results, with further enhanced therapeutic effects when combining AAV with oxaliplatin (62% of mice showing complete survival). Two other groups [102,103] also used AAV-mediated delivery of the C84A and T34A survivin mutants, respectively, for *in vivo* models of gastric cancer and observed reduced tumor growth, increased tumor cell apoptosis, and increased tumor sensitivity to 5-fluoracil.

The C-terminal fragment of the human telomerase reverse transcriptase (hTERTC27), which exerts an anti-tumor activity by inducing telomere dysfunction, was packaged in AAV2 and intratumorally delivered to a human glioblastoma multiforme U87-MG tumor xenograft mouse model [104]. The results were increased levels of tumor necrosis and apoptosis, increased infiltration of polymorphonuclear neutrophils into the tumor, reduced angiogenesis, and consequently an 83% reduction in tumor growth and two-fold higher median survival of treated mice. The same group then combined AAV2 and adenoviral vector delivery of hTERTC27 and obtained a synergistic therapeutic effect of 2.56-fold higher median survival compared to untreated mice [105].

A wide array of other anti-tumor transgenes have been delivered to preclinical cancer models using AAV vectors. These include AAV2-maspin to LNCaP and DU145 prostate cancer tumors [106]; AAV2-nm23H1 to SW626-M4 metastatic ovarian cancer tumors [107]; AAV2-HGFK1 (kringle 1 domain of human hepatocyte growth factor) to CT26 and Lovo colorectal carcinoma tumors [108]; AAV2-encoded anti-calcitonin ribozymes to an orthotopic implantation model and a transgenic model of prostate cancer [109]; AAV2-4EBP1 (eukaryotic translation initiation factor 4E-binding protein 1) to a K-ras^{LA1} lung cancer model [110]; AAV2-mediated delivery of the chemokine receptor CXC chemokine receptor 2 (CXCR2) C-tail sequence to an HPAC pancreatic tumor model [111]; AAV1 delivery of IL-24 and apoptotin to a HepG2 liver cancer model [112]; AAV2-TAP (alpha-tocopherol-associated protein) to PC-3 and LNCaP prostate cancer tumors [113]; delivery of trichosanthin, packaged in AAV3-S663V+T492V vectors, to HuH7 hepatocellular carcinoma (HCC) tumors [28]; AAV2-decorin to a U87MG glioblastoma multiforme model [114]; AAV2-cathelicidin to HT-29 colon cancer tumors [115]; AAV8-mediated delivery of Niemann-Pick type C2 (NPC2) to the N-methyltransferase knockout (Gnmt-/-) transgenic spontaneous HCC model [116]; and AAV9-mediated delivery of human Mullerian inhibiting substance (MIS, albumin leader Q425R MIS (LRMIS)) in a xenograft model of ovarian cancer [117]. Additionally, groups have delivered the p53 tumor suppressor gene, commonly mutated in cancerous cells, using AAV2 vectors to bladder cancer cells [118] and non-small cell lung cancer cells [119] *in vitro* and to an H358 bronchioalveolar carcinoma tumor model *in vivo* [120].

AAV Vectors Encoding Small RNAs

AAVs encoding RNA cargoes are another anti-cancer modality that has been employed in a variety of tumor models. Prophylactic administration of AAV2 encoding small hairpin RNA (shRNA) targeting Epstein-Barr virus (EBV) latent membrane protein-1 (LMP-1) to a C666-1 nasopharyngeal carcinoma (NPC) mouse model led to a 47% inhibition of tumor metastasis, though no effects on tumor growth were observed [121]. AAV2 encoding antisense RNA targeting the E7 oncogene from human papilloma virus 16 (HPV16) present in CaSki cervical cancer cells and subsequent implantation of these cells reduced tumor formation by 80% and inhibited the size of formed tumors by 79% compared to transplantation of uninfected cells [122]. Sun *et al.* [123] delivered AAV2 encoding shRNA targeting the androgen receptor (AR) gene to 22Rv1 prostate cancer xenografts. Among the group of AR-shRNAs that they screened, AAV2-ARHP8 suppressed tumor growth by 88% when delivered intratumorally, and systemic delivery of AAV2-ARHP8 caused elimination of xenografts. Intratumoral AAV2 encoding siRNA against Snail, a transcription factor involved in anti-apoptotic and chemoresistance upregulated in pancreatic cancer, to a PANC-1 xenograft model of pancreatic cancer suppressed tumor growth by 76% [124]. Subsequently, the same group delivered AAV encoding siRNA targeting the Slug gene, a suppressor of apoptosis, to an orthotopic QBC939 model of cholangiocarcinoma, a type of liver cancer [125]. Intratumoral injection of AAV2-SlugsiRNA led to 51% reduced tumor growth alone and complete tumor regression when combined with radiation treatment. Delivery of AAV2 encoding shRNA against FHL2 (four and a half LIM-only protein 2), a putative oncogene involved in various cellular processes including proliferation and migration, to a LoVo colon cancer xenograft led to 66% reduced tumor volume, an effect that was enhanced to a 95% reduction with co-administration of 5-FU [126]

Other AAV serotypes have also been employed for delivery of small RNA-encoding payloads. Delivery of AAV1 encoding shRNA against Hec1 (Highly Expressed in Cancer 1) to a U251 glioma xenograft mouse model increased tumor cell apoptosis but did not ultimately reduce tumor growth [127]. Systemic delivery of self-complementary AAV8 vectors encoding microRNA miR-26a, which becomes downregulated in HCC cells, to the tet-o-MYC, LAP-tTA bi-transgenic HCC mouse model resulted in high expression levels of miR-26a in the liver, reduced tumor occurrence, and 65% smaller average tumor size without any observed toxicity [128].

Delivery of Antigens for Stimulating Antigen-Presenting Cells (APCs)

Adeno-associated virus vectors have also been employed to deliver antigens to antigen-presenting cells and thereby elicit an immune response against tumor cells expressing that antigen, i.e. a tumor vaccine. An excellent example of AAV-mediated vaccination focused on antigens from human papilloma virus 16 (HPV16), which is associated with the development of cervical and anogenital cancer. Several groups have used AAV to express the HPV16 structural protein L1 and thereby induce anti-HPV neutralizing antibodies [129]. L1-based virus-like particles (VLPs), which are non-infectious and morphologically identical to HPV virions but do not carry any oncogenes, are safe vaccine agents that can elicit high titers of neutralizing antibodies. Liu *et al.* used intramuscularly delivered AAV2-HPV16L1 to elicit anti-L1 antibodies, then compared the resulting titers with those generated by either an AAV control vector, HPV16 VLPs composed of L1, naked DNA encoding L1, adenovirus coding for mGM-CSF, or a combination of AAV2 and adenovirus [129].

The antibody titer induced by AAV2-L1 delivery was 20% lower than that generated by VLPs; however, a single dose of combined AAV and adenovirus led to titers as high three doses of VLPs. AAV2-L1 delivery also led to accumulation of macrophages and DCs at levels comparable to VLP delivery.

Interestingly, a single dose of intranasal AAV5-mediated delivery of HPV16-L1 was sufficient to generate long-lasting, high titers of serum anti-L1 antibodies in mice, comparable to those generated by VLP delivery [130]. Additionally, vector delivery led to generation of mucosal antibodies in vaginal washes and to a long-term cellular immune response against HPV16. The same group subsequently investigated intranasal vaccination of mice by delivering an HPV16 L1/E7 fusion gene using AAV5, AAV8, or AAV9 vectors and showed serotypes 5 and 9 were most effective at generating neutralizing antibodies and a CTL response against HPV16 [131]. Moreover, the murine study was followed by successful intranasal vaccination of rhesus macaques using HP16 L1 delivered by AAV5 and AAV9 vectors, where the latter induced long lasting immunization [132]. Building upon their previous study of AAV-mediated vaccination against HPV16 [133], Liao *et al.* [134] developed vaccines against three HPV16 oncogenes – E5, E6, and E7 – that conferred immune protection against cervical cancer tumor growth. They used AAV2 to deliver a long peptide targeting HPV16 E5, E6, and E7 that induced an immune response against TC-1 cells, which express HPV16 proteins; vaccinated mice were protected from tumor growth for 300 days.

Various other antigens have been delivered using AAV vectors to preclinical cancer models for APC stimulation and antibody generation. AAV2 encoding a B-cell leukemia/lymphoma 1 (BCL1) idiotype led to the generation of anti-Id antibodies and protection against BCL1 cell-based tumors [135]. Intramuscular AAV2 packaged with the LMP2/1-hsp fusion gene, consisting of the Epstein-Barr virus latent membrane proteins 1 and 2 fused to heat shock protein as an adjuvant, to a tumor model based on SP2/0 cells expressing LMP2 led to a humoral and CTL response against LMP2-expressing tumor cells, 83% reduction in tumor growth, and long-term survival of 90% of treated animals [136]. In addition, intramuscular AAV6 encoding melanoma antigen Trp2 generated an antitumor response against B16.F10 tumors when combined with Toll-like receptor (TLR) agonists [137] The same group subsequently co-administered TLR agonists and AAV2 encoding carcinoembryonic antigen (CEA) to vaccinate mice against colon cancer cells, resulting in antitumor response against MC38 cells expressing CEA [138]. In another study investigating neu-expressing TUBO breast cancer tumors [139], intramuscular vaccination with AAV5-neu or AAV6-neu resulted in humoral and cell-mediated immune response, leading to 50% and 100% long-term survival, respectively. Similarly, oral vaccination led to 80% and 100% long-term survival with AAV5 and AAV6, respectively. Additionally, oral AAV6-neu vaccination also protected against re-challenge with TUBO tumor cells 320 days after original tumor cell implantation. Han *et al.* [140] used AAV2 to systemically deliver a soluble form of B and T lymphocyte attenuator (BTLA) in combination with a heat shock protein (HSP70) vaccine to a B16F1 mouse melanoma pulmonary metastasis model, which initially reduced metastatic foci but did not prevent late-stage metastatic melanoma. Conversely, prophylactic treatment caused enhanced innate and adaptive immune responses against tumor cells, leading to 80% inhibition of tumor formation and long-term survival of 83% of treated mice. One general challenge with prophylactic tumor vaccination with AAV, however, is that a single administration can lead to long-term neutralizing antibodies that cross-

react against multiple AAV serotypes, complicating subsequent AAV administrations to treat other conditions.

Delivery of Antibodies to Block Signaling

A number of anti-cancer monoclonal antibodies (mAbs) therapeutics have been developed to target cancer cells for immune system processing and presentation, to inhibit cancer cell growth and tumor progression by blocking antigens involved in tumor cellular processes such as migration, and to inhibit immunosuppressive signaling molecules and thereby boost anti-tumor immune responses. Adeno-associated virus vectors have been employed to deliver genes encoding such monoclonal antibodies for long-term expression in preclinical models.

Ho *et al.* [141] delivered 14E1, a murine antihuman epidermal growth factor (EGFR) antibody, by intramuscular administration of AAV1 vectors in the A431 human vulvar carcinoma xenograft model. Administration of vector prior to tumor cell xenografting completely inhibited or reduced tumor growth by 93% when administered 28 days before and 1 day after tumor cell implantation, respectively. Gene delivery also led to long-term survival, with a majority of mice showing complete tumor regression. Intratumorally injected AAV2 encoding adximab, a mouse-human chimeric antibody against death-receptor 5 (DR5), to mouse models of human liver cancer (SMMC7221) and colon cancer (HCT116) reduced tumor growth (58% and 40% reduction, respectively) and increased tumor cell apoptotic death (2-fold and 2.6-fold higher, respectively) in both models [142]. Finally, administration of an AAV9 vector encoding a monoclonal antibody against the glycolytic enzyme alpha-enolase (ENO1) prior to xenografting orthotopic CFPAC-1 pancreatic ductal adenocarcinoma (PDAC) tumors led to high concentrations of anti-ENO1 antibody in serum and a 95% reduction in lung metastases [143].

3.6 AAV Vectors in Cancer Clinical Trials

The promising results of adeno-associated virus vectors in preclinical models of cancer, coupled with their clinical successes for monogenic diseases [9], have motivated the translation of AAV vectors into oncology clinical trials.

A phase I trial performed between the Peking University School of Oncology and the Beijing Cancer Hospital and Institute [144] administered cytotoxic T lymphocytes (CTLs) that had been activated by dendritic cells (DCs) previously transduced with AAV2 vectors carrying carcinoembryonic antigen (CEA) to cancer patients who had failed to respond to standard treatments. From the 25 patients evaluated after treatment, 2 showed partial remission, 10 showed stable diseases, and 13 had progressive disease, with a resulting mean progression-free survival of 3.1 months. Importantly, no treatment-related serious adverse events were reported for any patients. Larger, randomized studies may follow.

A clinical trial (ClinicalTrials.gov Identifier:NCT02496273), led by Wu Changping, M.D. and Jiang Jingting, Ph.D. at The First People's Hospital of Changzhou in China, is investigating the clinical safety and efficacy of administering CEA-specific CTLs activated by DCs previously loaded with CEA via AAV2 transduction. This phase I clinical trial is focused on stage IV gastric

cancer patients, will monitor T cell populations and tumor progression, and initiated in January, 2016.

Another clinical trial (ClinicalTrials.gov Identifier: NCT02602249), developed by Beijing Doing Biomedical Co., Ltd in China, is similarly investigating the clinical safety and efficacy of administering CTLs specific for the Mucin 1 (MUC1) antigen, whose overexpression can be associated with cancer, to stage IV gastric cancer patients. MUC1-specific CTLs will be activated by DCs either loaded with MUC1 via AAV2 transduction or directly pulsed with a MUC1 peptide. This study is projected to be completed in June, 2018.

Finally, although not targeting cancer cells *per se*, another phase I clinical trial (ClinicalTrials.gov Identifier: NCT02446249) led by John A Chiorini, Ph.D. at the NIH is investigating the safety of using an AAV2-aquaporin (AAV-hAQP1) gene therapy for patients with irradiation-induced parotid salivary hypofunction (xerostomia), a condition that can develop in patients with a history of radiation therapy for head and neck cancer. The investigators have already completed a separate phase I clinical trial (06-D-0206) using adenovirus, where they showed safety and therapeutic efficacy of hAQP1 delivery to a single parotid gland. The study initiated in April, 2015, and the investigators will monitor therapeutic efficacy of the treatment by measuring parotid salivary gland output as well as safety through traditional clinical and immunological measures.

3.7 Future Prospects and Conclusions

AAV vectors have enjoyed increasing clinical success as a result of their excellent safety profile and high gene delivery efficacy. To date, over 130 clinical trials [6] have employed AAV vectors to treat conditions in a wide range of tissues, including muscle, eye, liver, central nervous system, heart, and lung diseases [9]. The approval of Glybera in the European Union and recent reports on clinical trials, including those for Sanfilippo B syndrome (Pasteur Institute, Phase I/II) and Leber's congenital amaurosis (Spark Therapeutics, Phase III), underscore the strong promise of AAV-mediated therapeutic gene delivery and foreshadow the development and approval of AAV gene therapies in the United States in the near future.

As presented in this review, AAV vectors, particularly AAV2, have been extensively used in a variety of preclinical models of cancer to deliver a wide array of transgenes, including anti-angiogenic factors, suicide genes, immunostimulatory genes and antigens, tumor suppressors, payloads encoding small interfering nucleic acids, and monoclonal antibodies. Despite the high prevalence of gene therapy clinical trials directed at cancer, AAV vectors have only recently entered this field, which has so far been focused on oncolytic viruses – including adenovirus, herpes simplex virus, and reovirus – and to a lesser extent, non-viral methods [145]. However, AAV vectors offer several complementary advantages that can be harnessed for anti-cancer therapies, including the potential for high efficiency transduction, the promise of vector engineering for targeted delivery, and gene expression in post-mitotic cells.

Due to their inability to replicate or efficiently integrate in transduced tumor cells, AAV vectors may have a limited potential for sustained oncolytic or pro-apoptotic effects, as evidenced by some *in vitro* and *in vivo* studies [146]. Instead, AAV vectors may be an excellent platform for eliciting protective anti-tumor effects via tumor suppression and immunostimulation – a strategy that

ongoing AAV cancer clinical trials are currently employing. Delivery of tumor-suppressive or stimulatory payloads – such as anti-angiogenic factors, monoclonal antibodies, cytokines, antigens for loading APCs, and immunomodulatory factors - would harness AAV's excellent safety and delivery properties, and, more importantly, would not require transduction of all tumor cells to induce an efficient therapeutic effect.

In particular, AAV vectors can deliver tumor-specific antigens to generate tumor-specific humoral and T cell-mediated responses – in efforts to vaccinate against the tumor – and this approach has been explored in both murine and non-human primate preclinical models that have strongly suggested the vector's potential against conditions like cervical cancer (HPV-L1) and prostate cancer (hPSA). Antigen delivery can also be employed in the *ex vivo* transduction of antigen-presenting cells like dendritic cells (DCs), which after being stimulated, loaded with the antigen, and reinjected into the patient, can elicit a CTL response against the tumor. Dendritic cell vaccines are safe and effective, and as explained above, mark some of the first AAV clinical trials directed at treating a type of cancer; this approach could potentially be extended to other types of cancer previously treated with DC vaccines, including melanoma, colon cancer, and prostate cancer [147].

Another important immunostimulatory strategy consists of augmenting anti-tumor cytotoxic T lymphocyte (CTL) responses by inhibiting negative immunoregulators such as CTLA-4 and PD-1 [148]. Blocking antibodies against CTLA-4, PD-1, and PD-1 Ligand 1 (PD-L1) have led to significant improvements in the treatment of various cancers (e.g. melanoma, renal cell carcinoma, lung cancer), and are either approved by the FDA (ipilimumab, anti-CTLA-4 approved for melanoma) or in advanced clinical trials [149]. AAV's gene transfer properties have already been exploited for the delivery of recombinant anti-angiogenesis monoclonal antibodies, including bevacizumab, to preclinical cancer models. AAV vectors could therefore be used to stimulate a CTL response by local delivery of blocking antibodies against CTLA-4 or PD-1. Long-term, sustained expression of these or other therapeutic antibodies could reduce overall dosage while increasing local expression levels, and consequently improve treatments for multiple indications such as non-Hodgkin's lymphoma, breast cancer, and colorectal cancer.

As another future direction, AAV vectors can benefit from further developments that would make them even more suitable gene delivery vehicles for cancer therapies. Novel vectors with selective tropism towards the tissue of interest, low off-target transduction, and the capacity to evade pre-existing neutralizing antibodies would promote high levels of gene expression, a requirement for a strong therapeutic effect. Furthermore, AAV vectors would strongly benefit from engineering for localization to primary and secondary tumors as well as to tumor initiating cells (sometimes regarded as "cancer stem cells"), which are resistant to traditional therapies and greatly contribute to the poor prognosis and post-therapy relapse of many cancers [2]. Vectors may also be engineered for specific transduction following different routes of administration – for example, systemic delivery, localized injection to post-mitotic non-tumor tissue for sustained transgene expression and secretion, or intratumoral administration – which can in turn influence gene delivery efficacy [150]. As previously discussed, directed evolution – which has successfully been applied to enhance existing vector properties or engineer entirely new and optimized properties for delivery to normal tissues –similarly offers strong potential for engineering novel AAV vectors for cancer therapies. Capsid engineering efforts can additionally be combined with the development of innovative

payloads that can provide tissue selectivity, strong expression, and maximization of genomic space for transgene delivery.

Finally, numerous studies presented in this review combined therapeutic gene delivery with traditional chemotherapy drugs or other therapeutic strategies to yield therapeutic effects greater than those elicited by either treatment alone. Thus, integrating AAV-mediated gene delivery with standard therapies (e.g. surgery, chemotherapy, radiotherapy) to develop novel anti-tumor treatment strategies offers strong promise in future cancer gene therapy studies.

3.8 Funding

JLSO has been supported by a Ford Foundation Fellowship, a National Science Foundation Graduate Fellowship, and two UC Berkeley's Graduate Division Fellowships. This work was also funded by R01EY022975.

Conflict of interest statement. DVS and JLSO are inventors on patents involving AAV directed evolution, and DS is the co-founder of an AAV gene therapy company.

3.9 References

1. Society, A.C. Cancer Facts & Figures 2015. (American Cancer Society, Atlanta, GA, 2015).
2. Venere, M., Fine, H.A., Dirks, P.B. & Rich, J.N. Cancer stem cells in gliomas: identifying and understanding the apex cell in cancer's hierarchy. *Glia* **59**, 1148-54 (2011).
3. Cross, D. & Burmester, J.K. Gene therapy for cancer treatment: past, present and future. *Clin Med Res* **4**, 218-27 (2006).
4. Simonelli, F. *et al.* Gene therapy for Leber's congenital amaurosis is safe and effective through 1.5 years after vector administration. *Mol Ther* **18**, 643-50 (2010).
5. Nathwani, A.C. *et al.* Adenovirus-associated virus vector-mediated gene transfer in hemophilia B. *N Engl J Med* **365**, 2357-65 (2011).
6. Indications Addressed by Gene Therapy Clinical Trials. Vol. 2015 (The Journal of Gene Medicine, www.wiley.co.uk/genmed/clinical).
7. Ledford, H. Cancer-fighting viruses win approval. *Nature* **526**, 622-3 (2015).
8. Giacca, M. & Zacchigna, S. Virus-mediated gene delivery for human gene therapy. *J Control Release* **161**, 377-88 (2012).
9. Kotterman, M.A. & Schaffer, D.V. Engineering adeno-associated viruses for clinical gene therapy. *Nat Rev Genet* **15**, 445-51 (2014).
10. Nicklin, S.A. *et al.* Transductional and transcriptional targeting of cancer cells using genetically engineered viral vectors. *Cancer Lett* **201**, 165-73 (2003).
11. Teschendorf, C., Emons, B., Muzyczka, N., Graeven, U. & Schmiegel, W. Efficacy of recombinant adeno-associated viral vectors serotypes 1, 2, and 5 for the transduction of pancreatic and colon carcinoma cells. *Anticancer Res* **30**, 1931-5 (2010).
12. Kohlschutter, J., Michelfelder, S. & Trepel, M. Novel cytotoxic vectors based on adeno-associated virus. *Toxins (Basel)* **2**, 2754-68 (2010).
13. Li, C., Bowles, D.E., van Dyke, T. & Samulski, R.J. Adeno-associated virus vectors: potential applications for cancer gene therapy. *Cancer Gene Ther* **12**, 913-25 (2005).
14. Shin, B.K. *et al.* Global profiling of the cell surface proteome of cancer cells uncovers an abundance of proteins with chaperone function. *J Biol Chem* **278**, 7607-16 (2003).
15. Buonaguro, L., Petrizzo, A., Tornesello, M.L. & Buonaguro, F.M. Translating tumor antigens into cancer vaccines. *Clin Vaccine Immunol* **18**, 23-34 (2011).
16. Novellino, L., Castelli, C. & Parmiani, G. A listing of human tumor antigens recognized by T cells: March 2004 update. *Cancer Immunol Immunother* **54**, 187-207 (2005).
17. Arap, W., Pasqualini, R. & Ruoslahti, E. Cancer treatment by targeted drug delivery to tumor vasculature in a mouse model. *Science* **279**, 377-80 (1998).
18. Hajitou, A. Targeted systemic gene therapy and molecular imaging of cancer contribution of the vascular-targeted AAVP vector. *Adv Genet* **69**, 65-82 (2010).
19. Grifman, M. *et al.* Incorporation of tumor-targeting peptides into recombinant adeno-associated virus capsids. *Mol Ther* **3**, 964-75 (2001).
20. Zhang, X. & Xu, W. Aminopeptidase N (APN/CD13) as a target for anti-cancer agent design. *Curr Med Chem* **15**, 2850-65 (2008).
21. Desgrosellier, J.S. & Cheresh, D.A. Integrins in cancer: biological implications and therapeutic opportunities. *Nat Rev Cancer* **10**, 9-22 (2010).
22. Shi, W. & Bartlett, J.S. RGD inclusion in VP3 provides adeno-associated virus type 2 (AAV2)-based vectors with a heparan sulfate-independent cell entry mechanism. *Mol Ther* **7**, 515-25 (2003).
23. Munch, R.C. *et al.* Displaying high-affinity ligands on adeno-associated viral vectors enables tumor cell-specific and safe gene transfer. *Mol Ther* **21**, 109-18 (2013).
24. Xie, Q. *et al.* The atomic structure of adeno-associated virus (AAV-2), a vector for human gene therapy. *Proc Natl Acad Sci U S A* **99**, 10405-10 (2002).

25. Schrodinger, LLC. The PyMOL Molecular Graphics System, Version 1.3r1. (2010).
26. Lee, H.S. *et al.* Acquisition of selective antitumoral effects of recombinant adeno-associated virus by genetically inserting tumor-targeting peptides into capsid proteins. *Oncol Lett* **2**, 1113-1119 (2011).
27. Cheng, B. *et al.* Development of optimized AAV3 serotype vectors: mechanism of high-efficiency transduction of human liver cancer cells. *Gene Ther* **19**, 375-84 (2012).
28. Ling, C. *et al.* Selective in vivo targeting of human liver tumors by optimized AAV3 vectors in a murine xenograft model. *Hum Gene Ther* **25**, 1023-34 (2014).
29. Sharma, P. & Allison, J.P. Immune checkpoint targeting in cancer therapy: toward combination strategies with curative potential. *Cell* **161**, 205-14 (2015).
30. Pandya, J., Ortiz, L., Ling, C., Rivers, A.E. & Aslanidi, G. Rationally designed capsid and transgene cassette of AAV6 vectors for dendritic cell-based cancer immunotherapy. *Immunol Cell Biol* **92**, 116-23 (2014).
31. Judd, J. *et al.* Tunable protease-activatable virus nanonodes. *ACS Nano* **8**, 4740-6 (2014).
32. Egeblad, M. & Werb, Z. New functions for the matrix metalloproteinases in cancer progression. *Nat Rev Cancer* **2**, 161-74 (2002).
33. Peng, K.W., Morling, F.J., Cosset, F.L., Murphy, G. & Russell, S.J. A gene delivery system activatable by disease-associated matrix metalloproteinases. *Hum Gene Ther* **8**, 729-38 (1997).
34. Michelfelder, S. *et al.* Successful expansion but not complete restriction of tropism of adeno-associated virus by in vivo biopanning of random virus display peptide libraries. *PLoS One* **4**, e5122 (2009).
35. Maguire, C.A. *et al.* Directed evolution of adeno-associated virus for glioma cell transduction. *J Neurooncol* **96**, 337-47 (2010).
36. Robson, T. & Hirst, D.G. Transcriptional Targeting in Cancer Gene Therapy. *J Biomed Biotechnol* **2003**, 110-137 (2003).
37. Rajendran, S. *et al.* Targeting of breast metastases using a viral gene vector with tumour-selective transcription. *Anticancer Res* **31**, 1627-35 (2011).
38. Kyo, S., Takakura, M., Fujiwara, T. & Inoue, M. Understanding and exploiting hTERT promoter regulation for diagnosis and treatment of human cancers. *Cancer Sci* **99**, 1528-38 (2008).
39. Watanabe, M. *et al.* Advanced two-step transcriptional amplification as a novel method for cancer-specific gene expression and imaging. *Oncol Rep* **26**, 769-75 (2011).
40. Della Peruta, M. *et al.* Preferential targeting of disseminated liver tumors using a recombinant adeno-associated viral vector. *Hum Gene Ther* **26**, 94-103 (2015).
41. McIntosh, J. *et al.* Therapeutic levels of FVIII following a single peripheral vein administration of rAAV vector encoding a novel human factor VIII variant. *Blood* **121**, 3335-44 (2013).
42. Al-Husein, B., Abdalla, M., Trepte, M., Deremer, D.L. & Somanath, P.R. Antiangiogenic therapy for cancer: an update. *Pharmacotherapy* **32**, 1095-111 (2012).
43. Mahendra, G. *et al.* Antiangiogenic cancer gene therapy by adeno-associated virus 2-mediated stable expression of the soluble FMS-like tyrosine kinase-1 receptor. *Cancer Gene Ther* **12**, 26-34 (2005).
44. Takei, Y. *et al.* Suppression of ovarian cancer by muscle-mediated expression of soluble VEGFR-1/Flt-1 using adeno-associated virus serotype 1-derived vector. *Int J Cancer* **120**, 278-84 (2007).
45. Li, B. *et al.* Vascular endothelial growth factor blockade reduces intratumoral regulatory T cells and enhances the efficacy of a GM-CSF-secreting cancer immunotherapy. *Clin Cancer Res* **12**, 6808-16 (2006).
46. Lin, J. *et al.* Inhibition of lymphogenous metastasis using adeno-associated virus-mediated gene transfer of a soluble VEGFR-3 decoy receptor. *Cancer Res* **65**, 6901-9 (2005).
47. Takahashi, K. *et al.* Suppression of lymph node and lung metastases of endometrial cancer by muscle-mediated expression of soluble vascular endothelial growth factor receptor-3. *Cancer Sci* **104**, 1107-11 (2013).

48. Cai, J., Jiang, W.G., Grant, M.B. & Boulton, M. Pigment epithelium-derived factor inhibits angiogenesis via regulated intracellular proteolysis of vascular endothelial growth factor receptor 1. *J Biol Chem* **281**, 3604-13 (2006).
49. He, S.S. *et al.* AAV-mediated gene transfer of human pigment epithelium-derived factor inhibits Lewis lung carcinoma growth in mice. *Oncol Rep* **27**, 1142-8 (2012).
50. He, S.S. *et al.* Enhanced efficacy of combination therapy with adenoassociated virus-delivered pigment epithelium-derived factor and cisplatin in a mouse model of Lewis lung carcinoma. *Mol Med Rep* **9**, 2069-76 (2014).
51. Fang, J. *et al.* Stable antibody expression at therapeutic levels using the 2A peptide. *Nat Biotechnol* **23**, 584-90 (2005).
52. Watanabe, M., Boyer, J.L. & Crystal, R.G. AAVrh.10-mediated genetic delivery of bevacizumab to the pleura to provide local anti-VEGF to suppress growth of metastatic lung tumors. *Gene Ther* **17**, 1042-51 (2010).
53. Xie, Y. *et al.* AAV-mediated persistent bevacizumab therapy suppresses tumor growth of ovarian cancer. *Gynecol Oncol* **135**, 325-32 (2014).
54. Folkman, J. Angiogenesis inhibitors: a new class of drugs. *Cancer Biol Ther* **2**, S127-33 (2003).
55. Pan, J.G., Zhou, X., Zeng, G.W. & Han, R.F. Suppression of bladder cancer growth in mice by adeno-associated virus vector-mediated endostatin expression. *Tumour Biol* **32**, 301-10 (2011).
56. Pan, J.G., Zhou, X., Zeng, G.W. & Han, R.F. Potent antitumour activity of the combination of HSV-TK and endostatin armed oncolytic adeno-associated virus for bladder cancer in vitro and in vivo. *J Surg Oncol* **105**, 249-57 (2012).
57. Sun, X. *et al.* Anti-angiogenic therapy subsequent to adeno-associated-virus-mediated immunotherapy eradicates lymphomas that disseminate to the liver. *Int J Cancer* **113**, 670-7 (2005).
58. Isayeva, T., Ren, C. & Ponnazhagan, S. Recombinant adeno-associated virus 2-mediated antiangiogenic prevention in a mouse model of intraperitoneal ovarian cancer. *Clin Cancer Res* **11**, 1342-7 (2005).
59. Isayeva, T., Ren, C. & Ponnazhagan, S. Intraperitoneal gene therapy by rAAV provides long-term survival against epithelial ovarian cancer independently of survivin pathway. *Gene Ther* **14**, 138-46 (2007).
60. Isayeva, T., Chanda, D., Kallman, L., Eltoum, I.E. & Ponnazhagan, S. Effects of sustained antiangiogenic therapy in multistage prostate cancer in TRAMP model. *Cancer Res* **67**, 5789-97 (2007).
61. Zhang, X., Xu, J., Lawler, J., Terwilliger, E. & Parangi, S. Adeno-associated virus-mediated antiangiogenic gene therapy with thrombospondin-1 type 1 repeats and endostatin. *Clin Cancer Res* **13**, 3968-76 (2007).
62. Subramanian, I.V., Ghebre, R. & Ramakrishnan, S. Adeno-associated virus-mediated delivery of a mutant endostatin suppresses ovarian carcinoma growth in mice. *Gene Ther* **12**, 30-8 (2005).
63. Subramanian, I.V. *et al.* Adeno-associated virus-mediated delivery of a mutant endostatin in combination with carboplatin treatment inhibits orthotopic growth of ovarian cancer and improves long-term survival. *Cancer Res* **66**, 4319-28 (2006).
64. Yanamandra, N. *et al.* Recombinant adeno-associated virus (rAAV) expressing TFPI-2 inhibits invasion, angiogenesis and tumor growth in a human glioblastoma cell line. *Int J Cancer* **115**, 998-1005 (2005).
65. Bui Nguyen, T.M., Subramanian, I.V., Xiao, X., Nguyen, P. & Ramakrishnan, S. Adeno-associated virus-mediated delivery of kringle 5 of human plasminogen inhibits orthotopic growth of ovarian cancer. *Gene Ther* **17**, 606-15 (2010).
66. Ruan, Q. *et al.* Development of an anti-angiogenic therapeutic model combining scAAV2-delivered siRNAs and noninvasive photoacoustic imaging of tumor vasculature development. *Cancer Lett* **332**, 120-9 (2013).

67. Cai, K.X. *et al.* Suppression of lung tumor growth and metastasis in mice by adeno-associated virus-mediated expression of vasostatin. *Clin Cancer Res* **14**, 939-49 (2008).
68. Kuo, C.H. *et al.* Development of recombinant AAV2/8 carrying kringle domains of human plasminogen for sustained expression and cancer therapy. *Hum Gene Ther* (2015).
69. Kroeger, K.M. *et al.* Gene therapy and virotherapy: novel therapeutic approaches for brain tumors. *Discov Med* **10**, 293-304 (2010).
70. Chen, C.Y. *et al.* Effect of herpes simplex virus thymidine kinase expression levels on ganciclovir-mediated cytotoxicity and the "bystander effect". *Hum Gene Ther* **6**, 1467-76 (1995).
71. Li, Z.B., Zeng, Z.J., Chen, Q., Luo, S.Q. & Hu, W.X. Recombinant AAV-mediated HSVtk gene transfer with direct intratumoral injections and Tet-On regulation for implanted human breast cancer. *BMC Cancer* **6**, 66 (2006).
72. Zeng, Z.J. *et al.* The cell death and DNA damages caused by the Tet-On regulating HSV-tk/GCV suicide gene system in MCF-7 cells. *Biomed Pharmacother* **68**, 887-92 (2014).
73. Kim, J.Y. *et al.* Persistent anti-tumor effects via recombinant adeno-associated virus encoding herpes thymidine kinase gene monitored by PET-imaging. *Oncol Rep* **25**, 1263-9 (2011).
74. Griffith, T.S. *et al.* TRAIL gene therapy: from preclinical development to clinical application. *Curr Gene Ther* **9**, 9-19 (2009).
75. Ma, H. *et al.* Recombinant adeno-associated virus-mediated TRAIL gene therapy suppresses liver metastatic tumors. *Int J Cancer* **116**, 314-21 (2005).
76. Ma, H., Liu, Y., Liu, S., Xu, R. & Zheng, D. Oral adeno-associated virus-sTRAIL gene therapy suppresses human hepatocellular carcinoma growth in mice. *Hepatology* **42**, 1355-63 (2005).
77. Shi, J. *et al.* Overexpression of soluble TRAIL induces apoptosis in human lung adenocarcinoma and inhibits growth of tumor xenografts in nude mice. *Cancer Res* **65**, 1687-92 (2005).
78. Yoo, J. *et al.* Adeno-associated virus-mediated gene transfer of a secreted form of TRAIL inhibits tumor growth and occurrence in an experimental tumor model. *J Gene Med* **8**, 163-74 (2006).
79. Wang, Y. *et al.* Potent antitumor effect of TRAIL mediated by a novel adeno-associated viral vector targeting to telomerase activity for human hepatocellular carcinoma. *J Gene Med* **10**, 518-26 (2008).
80. Wang, Y. *et al.* The efficacy of combination therapy using adeno-associated virus-TRAIL targeting to telomerase activity and cisplatin in a mice model of hepatocellular carcinoma. *J Cancer Res Clin Oncol* **136**, 1827-37 (2010).
81. Zhang, Y. *et al.* AAV-mediated TRAIL gene expression driven by hTERT promoter suppressed human hepatocellular carcinoma growth in mice. *Life Sci* **82**, 1154-61 (2008).
82. Jiang, M. *et al.* Synergistic antitumor effect of AAV-mediated TRAIL expression combined with cisplatin on head and neck squamous cell carcinoma. *BMC Cancer* **11**, 54 (2011).
83. Chiu, T.L., Wang, M.J. & Su, C.C. The treatment of glioblastoma multiforme through activation of microglia and TRAIL induced by rAAV2-mediated IL-12 in a syngeneic rat model. *J Biomed Sci* **19**, 45 (2012).
84. Hamner, J.B. *et al.* The efficacy of combination therapy using adeno-associated virus--interferon beta and trichostatin A in vitro and in a murine model of neuroblastoma. *J Pediatr Surg* **43**, 177-82; discussion 182-3 (2008).
85. Maguire, C.A. *et al.* Preventing growth of brain tumors by creating a zone of resistance. *Mol Ther* **16**, 1695-702 (2008).
86. He, L.F. *et al.* Suppression of cancer growth in mice by adeno-associated virus vector-mediated IFN-beta expression driven by hTERT promoter. *Cancer Lett* **286**, 196-205 (2009).
87. Ren, C. *et al.* Therapeutic potential of mesenchymal stem cells producing interferon-alpha in a mouse melanoma lung metastasis model. *Stem Cells* **26**, 2332-8 (2008).
88. Wu, J.Q., Zhao, W.H., Li, Y., Zhu, B. & Yin, K.S. Adeno-associated virus mediated gene transfer into lung cancer cells promoting CD40 ligand-based immunotherapy. *Virology* **368**, 309-16 (2007).

89. Xu, W. *et al.* Self-complementary adeno-associated virus 5-mediated gene transduction of a novel CD40L mutant confers direct antitumor effects in lung carcinoma. *Mol Med Rep* **11**, 482-8 (2015).
90. Tahara, I. *et al.* Systemic cancer gene therapy using adeno-associated virus type 1 vector expressing MDA-7/IL24. *Mol Ther* **15**, 1805-11 (2007).
91. Yang, Y.J. *et al.* Targeted IL-24 gene therapy inhibits cancer recurrence after liver tumor resection by inducing tumor cell apoptosis in nude mice. *Hepatobiliary Pancreat Dis Int* **8**, 174-8 (2009).
92. Tamai, H. *et al.* AAV8 vector expressing IL24 efficiently suppresses tumor growth mediated by specific mechanisms in MLL/AF4-positive ALL model mice. *Blood* **119**, 64-71 (2012).
93. Chang, C.M. *et al.* Treatment of hepatocellular carcinoma with adeno-associated virus encoding interleukin-15 superagonist. *Hum Gene Ther* **21**, 611-21 (2010).
94. Yiang, G.T. *et al.* Immunotherapy for SV40 T/t antigen-induced breast cancer by recombinant adeno-associated virus serotype 2 carrying interleukin-15 in mice. *Int J Mol Med* **29**, 809-14 (2012).
95. Liang, C.M. *et al.* Local expression of secondary lymphoid tissue chemokine delivered by adeno-associated virus within the tumor bed stimulates strong anti-liver tumor immunity. *J Virol* **81**, 9502-11 (2007).
96. Buhles, A. *et al.* Anti-metastatic effects of viral and non-viral mediated Nk4 delivery to tumours. *Genet Vaccines Ther* **7**, 5 (2009).
97. Maitituoheti, M. *et al.* Adeno-associated virus-mediated local delivery of LIGHT suppresses tumorigenesis in a murine cervical cancer model. *J Immunother* **34**, 581-7 (2011).
98. Driessens, G. *et al.* Development of a successful antitumor therapeutic model combining in vivo dendritic cell vaccination with tumor irradiation and intratumoral GM-CSF delivery. *Cancer Immunol Immunother* **60**, 273-81 (2011).
99. Ma, H. *et al.* Effect and mechanism of Mitomycin C combined with recombinant adeno-associated virus type II against glioma. *Int J Mol Sci* **15**, 1-14 (2014).
100. Tu, S.P. *et al.* Gene therapy for colon cancer by adeno-associated viral vector-mediated transfer of survivin Cys84Ala mutant. *Gastroenterology* **128**, 361-75 (2005).
101. Xue, Z. *et al.* Adeno-associated virus-mediated survivin mutant Thr34Ala cooperates with oxaliplatin to inhibit tumor growth and angiogenesis in colon cancer. *Oncol Rep* **25**, 1039-46 (2011).
102. Weng, Y., Fei, B., Chi, A.L. & Cai, M. Inhibition of gastric cancer cell growth in vivo by overexpression of adeno-associated virus-mediated survivin mutant C84A. *Oncol Res* **20**, 411-7 (2013).
103. Dang, S.C. *et al.* Overexpression of Survivin mutant Thr34Ala induces apoptosis and inhibits gastric cancer growth. *Neoplasma* **62**, 81-7 (2015).
104. Ng, S.S. *et al.* A novel glioblastoma cancer gene therapy using AAV-mediated long-term expression of human TERT C-terminal polypeptide. *Cancer Gene Ther* **14**, 561-72 (2007).
105. Gao, Y. *et al.* Development of recombinant adeno-associated virus and adenovirus cocktail system for efficient hTERTC27 polypeptide-mediated cancer gene therapy. *Cancer Gene Ther* **15**, 723-32 (2008).
106. Watanabe, M. *et al.* Adeno-associated virus 2-mediated intratumoral prostate cancer gene therapy: long-term maspin expression efficiently suppresses tumor growth. *Hum Gene Ther* **16**, 699-710 (2005).
107. Li, J. *et al.* Inhibition of ovarian cancer metastasis by adeno-associated virus-mediated gene transfer of nm23H1 in an orthotopic implantation model. *Cancer Gene Ther* **13**, 266-72 (2006).
108. Nie, B. *et al.* AAV-HGFK1 and Ad-p53 cocktail therapy prolongs survival of mice with colon cancer. *Mol Cancer Ther* **7**, 2855-65 (2008).

109. Shah, G.V. *et al.* Calcitonin promotes in vivo metastasis of prostate cancer cells by altering cell signaling, adhesion, and inflammatory pathways. *Endocr Relat Cancer* **15**, 953-64 (2008).
110. Chang, S.H. *et al.* Aerosol delivery of eukaryotic translation initiation factor 4E-binding protein 1 effectively suppresses lung tumorigenesis in K-rasLA1 mice. *Cancer Gene Ther* **20**, 331-5 (2013).
111. Wang, S. *et al.* CXCR2 macromolecular complex in pancreatic cancer: a potential therapeutic target in tumor growth. *Transl Oncol* **6**, 216-25 (2013).
112. Yuan, L., Zhao, H., Zhang, L. & Liu, X. The efficacy of combination therapy using adeno-associated virus-mediated co-expression of apoptin and interleukin-24 on hepatocellular carcinoma. *Tumour Biol* **34**, 3027-34 (2013).
113. Zhu, B. *et al.* Cross-talk of alpha tocopherol-associated protein and JNK controls the oxidative stress-induced apoptosis in prostate cancer cells. *Int J Cancer* **132**, 2270-82 (2013).
114. Ma, H.I. *et al.* Intratumoral decorin gene delivery by AAV vector inhibits brain glioblastomas and prolongs survival of animals by inducing cell differentiation. *Int J Mol Sci* **15**, 4393-414 (2014).
115. Cheng, M. *et al.* Cathelicidin suppresses colon cancer development by inhibition of cancer associated fibroblasts. *Clin Exp Gastroenterol* **8**, 13-29 (2015).
116. Liao, Y.J. *et al.* Niemann-Pick Type C2 protein regulates liver cancer progression via modulating ERK1/2 pathway: Clinicopathological correlations and therapeutical implications. *Int J Cancer* (2015).
117. Pepin, D. *et al.* AAV9 delivering a modified human Mullerian inhibiting substance as a gene therapy in patient-derived xenografts of ovarian cancer. *Proc Natl Acad Sci U S A* **112**, E4418-27 (2015).
118. Ruifa, H., Liwei, L., Binxin, L. & Ximing, L. Additional gene therapy with rAAV-wt-p53 enhanced the efficacy of cisplatin in human bladder cancer cells. *Urol Int* **77**, 355-61 (2006).
119. Neukirchen, J. *et al.* The proteasome inhibitor bortezomib acts differently in combination with p53 gene transfer or cytotoxic chemotherapy on NSCLC cells. *Cancer Gene Ther* **14**, 431-9 (2007).
120. Qazilbash, M.H., Xiao, X., Seth, P., Cowan, K.H. & Walsh, C.E. Cancer gene therapy using a novel adeno-associated virus vector expressing human wild-type p53. *Gene Ther* **4**, 675-82 (1997).
121. Li, X. *et al.* Recombinant adeno-associated virus mediated RNA interference inhibits metastasis of nasopharyngeal cancer cells in vivo and in vitro by suppression of Epstein-Barr virus encoded LMP-1. *Int J Oncol* **29**, 595-603 (2006).
122. Wu, S. *et al.* Reversal of the malignant phenotype of cervical cancer CaSki cells through adeno-associated virus-mediated delivery of HPV16 E7 antisense RNA. *Clin Cancer Res* **12**, 2032-7 (2006).
123. Sun, A. *et al.* Adeno-associated virus-delivered short hairpin-structured RNA for androgen receptor gene silencing induces tumor eradication of prostate cancer xenografts in nude mice: a preclinical study. *Int J Cancer* **126**, 764-74 (2010).
124. Zhang, K. *et al.* Knockdown of snail sensitizes pancreatic cancer cells to chemotherapeutic agents and irradiation. *Int J Mol Sci* **11**, 4891-2 (2010).
125. Zhang, K. *et al.* Slug inhibition upregulates radiation-induced PUMA activity leading to apoptosis in cholangiocarcinomas. *Med Oncol* **28 Suppl 1**, S301-9 (2011).
126. Wu, Y. *et al.* A novel colon cancer gene therapy using rAAVmediated expression of human shRNA-FHL2. *Int J Oncol* **43**, 1618-26 (2013).
127. Li, L. *et al.* Development of recombinant adeno-associated virus vectors carrying small interfering RNA (shHec1)-mediated depletion of kinetochore Hec1 protein in tumor cells. *Gene Ther* **14**, 814-27 (2007).
128. Kota, J. *et al.* Therapeutic microRNA delivery suppresses tumorigenesis in a murine liver cancer model. *Cell* **137**, 1005-17 (2009).

129. Liu, D.W. *et al.* Co-vaccination with adeno-associated virus vectors encoding human papillomavirus 16 L1 proteins and adenovirus encoding murine GM-CSF can elicit strong and prolonged neutralizing antibody. *Int J Cancer* **113**, 93-100 (2005).
130. Kuck, D. *et al.* Intranasal vaccination with recombinant adeno-associated virus type 5 against human papillomavirus type 16 L1. *J Virol* **80**, 2621-30 (2006).
131. Nieto, K. *et al.* Combined prophylactic and therapeutic intranasal vaccination against human papillomavirus type-16 using different adeno-associated virus serotype vectors. *Antivir Ther* **14**, 1125-37 (2009).
132. Nieto, K. *et al.* Intranasal vaccination with AAV5 and 9 vectors against human papillomavirus type 16 in rhesus macaques. *Hum Gene Ther* **23**, 733-41 (2012).
133. Zhou, L. *et al.* Long-term protection against human papillomavirus e7-positive tumor by a single vaccination of adeno-associated virus vectors encoding a fusion protein of inactivated e7 of human papillomavirus 16/18 and heat shock protein 70. *Hum Gene Ther* **21**, 109-19 (2010).
134. Liao, S. *et al.* A novel "priming-boosting" strategy for immune interventions in cervical cancer. *Mol Immunol* **64**, 295-305 (2015).
135. Cesco-Gaspere, M., Zentilin, L., Giacca, M. & Burrone, O.R. Boosting anti-idiotype immune response with recombinant AAV enhances tumour protection induced by gene gun vaccination. *Scand J Immunol* **68**, 58-66 (2008).
136. Pan, J. *et al.* Recombinant adeno-associated virus encoding Epstein-Barr virus latent membrane proteins fused with heat shock protein as a potential vaccine for nasopharyngeal carcinoma. *Mol Cancer Ther* **8**, 2754-61 (2009).
137. Triozzi, P.L., Aldrich, W. & Ponnazhagan, S. Regulation of the activity of an adeno-associated virus vector cancer vaccine administered with synthetic Toll-like receptor agonists. *Vaccine* **28**, 7837-43 (2010).
138. Triozzi, P.L., Aldrich, W. & Ponnazhagan, S. Inhibition and promotion of tumor growth with adeno-associated virus carcinoembryonic antigen vaccine and Toll-like receptor agonists. *Cancer Gene Ther* **18**, 850-8 (2011).
139. Steel, J.C. *et al.* Oral vaccination with adeno-associated virus vectors expressing the Neu oncogene inhibits the growth of murine breast cancer. *Mol Ther* **21**, 680-7 (2013).
140. Han, L. *et al.* AAV-sBTLA facilitates HSP70 vaccine-triggered prophylactic antitumor immunity against a murine melanoma pulmonary metastasis model in vivo. *Cancer Lett* **354**, 398-406 (2014).
141. Ho, D.T. *et al.* Growth inhibition of an established A431 xenograft tumor by a full-length anti-EGFR antibody following gene delivery by AAV. *Cancer Gene Ther* **16**, 184-94 (2009).
142. Lv, F. *et al.* Adeno-associated virus-mediated anti-DR5 chimeric antibody expression suppresses human tumor growth in nude mice. *Cancer Lett* **302**, 119-27 (2011).
143. Principe, M. *et al.* Targeting of surface alpha-enolase inhibits the invasiveness of pancreatic cancer cells. *Oncotarget* **6**, 11098-113 (2015).
144. Di, L. *et al.* Clinical safety of induced CTL infusion through recombinant adeno-associated virus-transfected dendritic cell vaccination in Chinese cancer patients. *Clin Transl Oncol* **14**, 675-81 (2012).
145. Amer, M.H. Gene therapy for cancer: present status and future perspective. *Mol Cell Ther* **2**, 27 (2014).
146. Hadaczek, P., Mirek, H., Berger, M.S. & Bankiewicz, K. Limited efficacy of gene transfer in herpes simplex virus-thymidine kinase/ganciclovir gene therapy for brain tumors. *J Neurosurg* **102**, 328-35 (2005).
147. Palucka, K. & Banchereau, J. Cancer immunotherapy via dendritic cells. *Nat Rev Cancer* **12**, 265-77 (2012).
148. Dougan, M. & Dranoff, G. Immune therapy for cancer. *Annu Rev Immunol* **27**, 83-117 (2009).

149. Kyi, C. & Postow, M.A. Checkpoint blocking antibodies in cancer immunotherapy. *FEBS Lett* **588**, 368-76 (2014).
150. Fumoto, S., Kawakami, S., Hashida, M. & Nishida, K. *Targeted Gene Delivery: Importance of Administration Routes*, (2013).

Chapter 4: In Vivo Directed Evolution of Adeno-Associated Virus Vectors for Glioblastoma Multiforme Tumor-Initiating Cells

This chapter is the product of a collaboration with the Sanjay Kumar Laboratory in the Department of Bioengineering at U.C. Berkeley

4.1 Introduction

Glioblastoma multiforme (GBM), a grade IV astrocytoma, is both the most virulent and the most frequent of adult glial tumors[1], with an incidence of 3-4 new cases per 100,000 people each year[2]. In contrast to lower grade tumors that are localized and tend to have favorable prognosis, GBM tumors are diffuse and highly invasive, and thus result in poor prognosis[3]. Conventional treatment of this high-grade glioma includes concomitant surgical resection, chemotherapy, and radiation. However, even with this aggressive intervention, median survival post-diagnosis is frequently less than 1 year, and most patients have an overall survival of less than two years[4,5].

One property of GBM that greatly influences its poor prognosis is the existence of highly invasive, therapy-resistant cells – termed tumor-initiating cells (TICs) – that can re-initiate tumor formation after therapy is discontinued. These TICs are also involved in GBM invasiveness, as they migrate into the brain parenchyma as either single cells or small groups of cells, sometimes infiltrating the whole brain[6] and initiating the formation of secondary tumors that further contribute to poor survival[7]. Imaging studies have shown that infiltrating tumor cells course through white matter tracts in "normal" brain parenchyma, a process that obviates the ability to delineate between normal brain tissue and the tumor and thus renders successful surgical resection virtually impossible. TICs – which display "stem cell-like" qualities such as self-renewal, expression of "stemness" markers including nestin and CD133, and the capacity to differentiate into more mature GBM tumor cells[1] – also exhibit resistance to standard therapies due to their slow cycling rates[8], ability to activate DNA damage responses[9], and increased expression of anti-apoptotic and drug resistance genes[10]. Because of these features, TICs should be taken into account in GBM therapies. In particular, successful targeting of these cells along with other tumor cells could enable enhanced clinical efficacy and eventually longer survival times in patients afflicted with this highly aggressive and invasive disease.

Xenografts of GBM TICs offer a more accurate recapitulation of cancer biology compared to more traditionally cultured and xenografted cancer cell lines, which have been the typical models for human cancer biology and therapeutic development. In fact, the phenotypic and genetic characteristics of cancer cell lines extensively passaged *in vitro* often do not correspond to those found within a primary human tumor[11]. In general, this has led to poorly predictive therapeutic screening models and an incomplete understanding of tumor cell biology[12]. This is also the case for glioblastoma models, where GBM cells lines subjected to extensive *in vitro* passaging fail to generate xenograft models with genomic and phenotypic features present in the original tumor[13], yielding for example well-segregated rather than highly invasive tumors and an inaccurate representation of GBM cellular heterogeneity[14]. In contrast, preclinical models based on primary and early passage GBM TICs can recapitulate the biology of the tumors from which they were derived[15]. In particular, GBM models generated by xenografting TICs isolated from patient GBMs

into immunocompromised mice develop into GBMs that accurately match the biological characteristics of the primary tumors, including tumor invasiveness, heterogeneity (e.g. mix of TICs and differentiated GBM tumor cells), genetic properties, and susceptibility to chemotherapy and antiangiogenic treatment[16,17]. We therefore propose to develop novel gene therapy strategies harnessing xenografts of primarily-cultured GBM TICs derived from glioblastoma patient resections[8,18] that we have previously studied and characterized[19] .

Gene therapy investigations for glioma have employed retroviral, adenoviral, vaccinia, and herpes virus-based vectors[20]. These have been utilized for suicide gene therapy[21], immunotherapy[22], oncolytic therapy[23], and other cargoes[24]. However, currently approved oncolytic therapies can require direct intratumoral administration and are still early in development, and immunotherapies such as CART-T have shown strong responses in leukemias with a clear tumor-associated antigen but limited success for solid tumors and antigens that are also expressed in host cells (leading to graft vs. host disease)[25]. Furthermore, preclinical and clinical development of other vectors and cargoes has been hindered by low gene delivery efficiency due to anatomical barriers including the blood-brain barrier (BBB), limited dispersion of vectors from a local intracranial administration site, poor gene delivery efficiency to tumor cells, and the inability to access and target tumor cells and TICs that have disseminated throughout the brain parenchyma. Therefore, the development of novel gene delivery vectors that can address these challenges is of utmost importance for potential cancer gene therapies.

Adeno-associated viruses (AAV) are non-pathogenic parvoviruses with a 4.7 kb double-stranded DNA genome encoding two genes: *rep*, which encodes enzymes that mediate viral DNA replication, and *cap*, which encodes the viral capsid that serves as the viral gene delivery vehicle. AAV vectors have a strong safety profile[26], can mediate delivery to a number of tissues, and as a result have enjoyed increasing success in human clinical trials[27-35] for monogenic disease targets including Leber's congenital amaurosis type 2[32], choroideremia[33], hemophilia B[29], and familial lipoprotein lipase deficiency (LPLD)[34]. Moreover, the first regulatory approved gene therapy product in Western nations (in the EU in 2012) uses an AAV1 vector to treat LPLD[35].

As we have recently reviewed[36], AAV vectors have also been harnessed for delivery of an extensive repertoire of transgenes in preclinical models of cancer and, more recently, clinical trials involving certain cancers[37]. However, the natural versions of AAVs utilized in these studies suffer from numerous shortcomings that render this success difficult to extend to the majority of human diseases. As we have reviewed[38], barriers for AAV and other vectors include high titer neutralizing antibodies due to prior exposure of the majority of the human population to natural AAVs, poor biodistribution to important tissue targets, poor spread within those tissues, an inability to target specific cells, and poor efficiency on those cells. Moreover, AAV vectors experience a number of delivery and transport barriers for CNS gene delivery – including biodistribution to the central nervous system (CNS), the BBB, and intraparenchymal and intratumoral transport to the primary and diffuse secondary tumors – and once they arrive they do not display strong intrinsic cell tropism for glioma cells. Thus, it would highly desirable to develop AAV vectors that upon administration via an optimal route of administration – such as systemic injection – are capable of overcoming these delivery barriers.

Directed evolution is a powerful, high-throughput approach that was initially applied to generate antibodies with enhanced binding affinity and enzymes with improved catalytic activity[39]. Our group first developed and has since broadly implemented directed evolution to create novel, optimized lentiviral and AAV vectors[40-49]. Importantly, this work has also included the *in vivo* directed evolution of AAV for enhanced tissue spread and infection of non-permissive cell types[43,44]. We have thus developed an *in vivo* directed evolution selection strategy to create AAV vectors for efficient gene delivery to GBM tumor cells and TICs after systemic administration. Here, we describe the methodology for this stringent selection strategy and the initial characterization of their infectivity. We also describe on-going experiments to validate their *in vivo* gene delivery properties, as well as their efficacy in delivering a therapeutic agent that can inhibit tumor growth and progression and thereby extend the survival of our animal models. The resulting AAV vectors will have the potential to enable new, potent therapies to treat highly invasive and malignant GBM tumors, as well as help establish a paradigm for engineering optimized AAV against other cancer targets.

4.2 Results

In vitro directed evolution of AAV libraries for infectivity on cultured GBM TICs

It has been well-established that natural AAVs are ineffective on GBM cell lines[50-54], and to confirm this with GBM TICs, natural AAV serotypes (AAV1-6, 8, 9) encoding the green fluorescent protein (GFP) were packaged and incubated with cells at a multiplicity of infection (MOI) of 10,000 viral genomes/cell (Figure 4.1). This high MOI mediated only very low or modest transduction of GBM cells and confirmed the need for the engineering of the AAV capsid for delivery to GBMs, as task we set out to do via directed evolution.

Like its natural counterpart, directed evolution involves iterative genetic diversification and selective pressure to create and isolate genetic variants with enhanced properties. Importantly, the approach does not require preexisting structural and mechanistic knowledge of virus-cell interactions (i.e. why natural AAVs do not infect GBMs well) in order to achieve greatly improved function. It relies instead on the generation of a diverse gene pool or library and development of a phenotypic selection that yields therapeutically relevant properties. We have previously generated a large (~100 million) library of novel AAV *cap* variants utilizing using a range of molecular approaches, including error-prone polymerase chain reaction (PCR)[47], saturation mutagenesis of key regions, DNA shuffling[48], ancestral reconstruction[55], and insertion of a string of seven random amino acids into the capsid of natural serotypes[56] or within other libraries including the ancestral library[55] and a computationally-guided DNA shuffling library (Ojala, D.S. et al., *in preparation*). These genetic libraries are then packaged such that each virus particle is composed of a variant capsid protein shell that surrounds the viral genome encoding that mutant capsid. Functional selections are performed on these pools, and with each round the *cap* variants responsible for the desired functional changes are recovered (e.g. by PCR), repackaged, and re-selected. After a suitable number of rounds, individual AAV variants are isolated, characterized, and harnessed for therapeutic gene delivery in disease models.

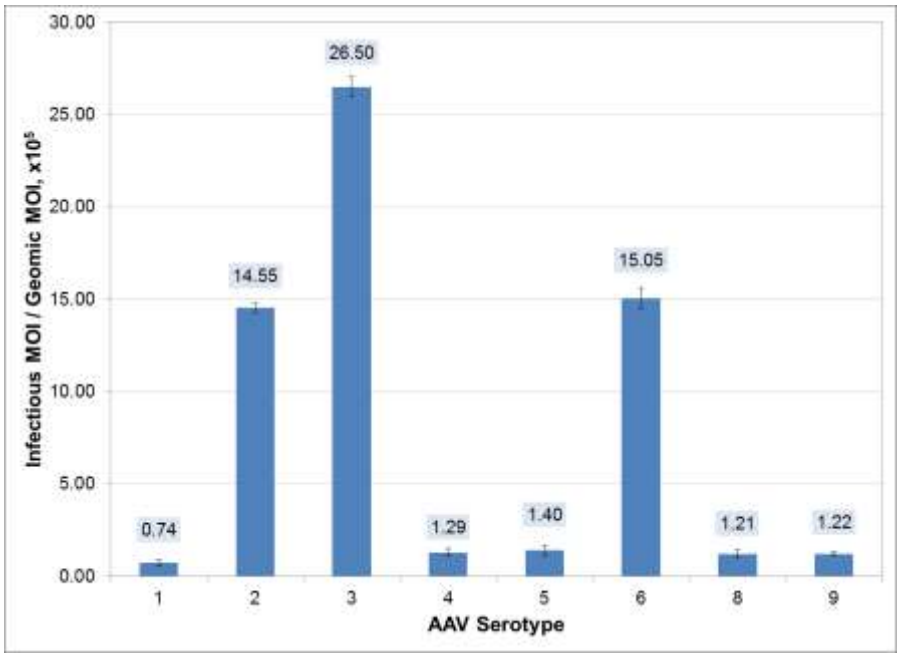

Figure 4.1. Ratio of infectious to genomic MOI (x 10^5) of natural AAV serotypes on GBM TICs. Cultured cells were transduced with vectors packaged with a self-complementary CMV-GFP cassette at a genomic MOI of 10,000 viral genomes/cell. The fraction of GFP-positive cells was quantified by flow cytometry 72 hours later. Data presented as mean±SEM, *n*=3.

We therefore initiated directed evolution using all of the AAV libraries mentioned in the prior paragraph, as well as error-prone libraries of the AAV3 and AAV6 *cap* genes (based on Figure 4.1)[47]. As an initial step to prime for *in vivo* infectivity on TICs, we performed three rounds of AAV library selection *in vitro* on TIC cultures from GBM patient surgical resections[8]. Specifically, GBM cells were first infected with AAV libraries at an initial genomic MOI of 10,000, and successful virions were recovered by superinfecting the cells with adenovirus type 5 to induce AAV replication and rescue[57]. The stringency of selection was then elevated by decreasing the genomic MOI to 1,000 and 100 in the second and third round of infection, respectively. After completing three rounds of *in vitro* selection, the primed libraries were packaged and we proceeded with an *in vivo* selection.

Generation of reporter GBM TICs for in vivo selection

Our GBM animal model involves xenotransplantation of human primary GBM TICs into non-obese diabetic/severe combined immunodeficient gamma (NSG) mice[19], which are stereotactically injected intracranially with TICs into their striatum[8]. To enable monitoring of xenografted tumor cells and their progression into tumors, we stably transduced these GBM TICs so they constitutively express a firefly luciferase gene, which does not affect tumor properties[58] but enables live monitoring of tumor progression using bioluminescence imaging (BLI)[59], as well as mCherry[60], a fluorescent protein previously used to monitor cancer cells[61] and that will facilitate both the *in vivo* AAV selection and downstream histology. Confirmation of bioluminescence and fluorescence of transduced cells is shown for a representative mouse in Figure B.1.

In vivo directed evolution strategy

We hypothesized that selection for the capacity to transduce GBMs *in vivo* would result in vectors capable of infecting both TICs as well as bulk tumor cells that would have differentiated between the time of xenografting and virus administration. For the first round of our *in vivo* directed evolution, depicted in Figure 4.2, we intravenously injected, four weeks post-xenotransplantation and confirmed tumor presence (Figure B.1), the combined *in vitro* selected libraries of AAV particles. Two weeks after virus administration, brain tissue was recovered, and cells were dissociated using the neurosphere assay[18]. Cells expressing mCherry were sorted through FACS and the DNA extracted from cells was used for PCR amplification of viral genomes. Recovered *cap* sequences were cloned into the replication competent AAV packaging plasmid pSub2, further diversified using error-prone PCR[47] (and subsequently recloned into pSub2), and packaged into AAV particles for further selection. A total of three rounds of *in vivo* selection were conducted.

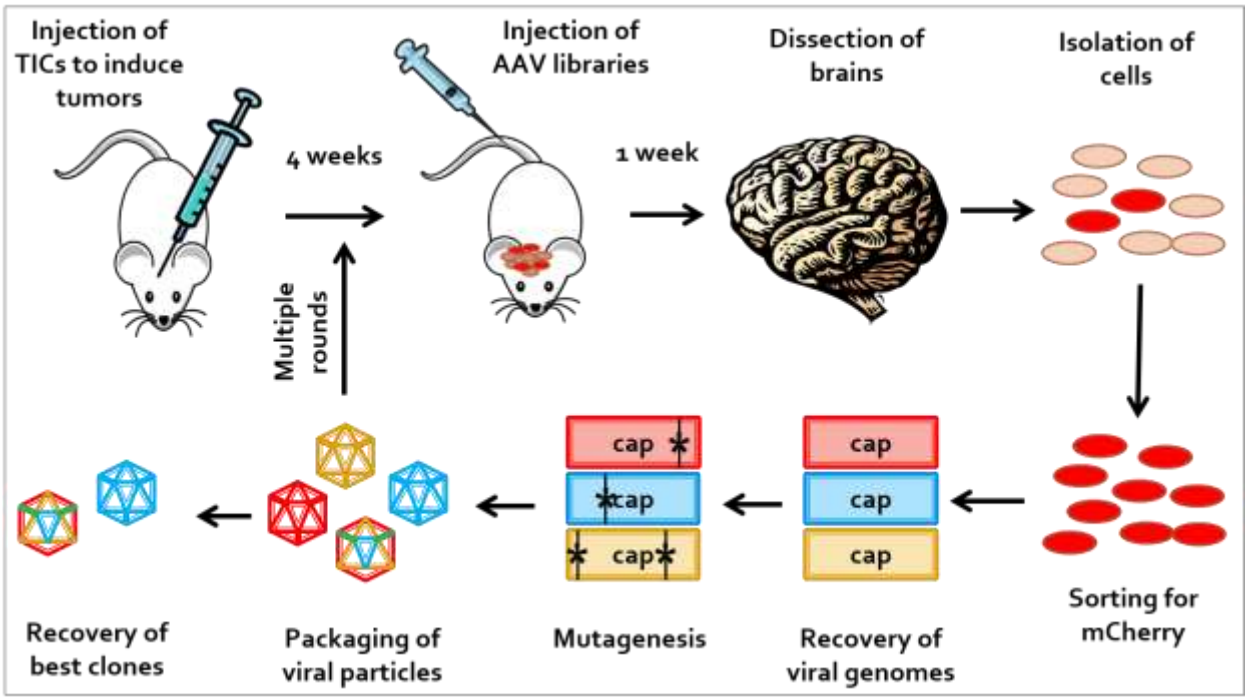

Figure 4.2. Depiction of in vivo AAV directed evolution scheme. TICs are intracranially injected in immunocompromised mice and over the course of 4 weeks are allowed to expand into tumors that harbor both TICs as well as differentiated tumor cells. AAV libraries are then administered intravenously, and one week later GBM cells are recovered using fluorescence-activated cell sorting (FACS) for mCherry expression. Viral genomes that have successfully arrived in GBM cells are then recovered using PCR primers designed to specifically amplify *cap* sequences. Recovered sequences are diversified using error-prone PCR and then packaged into viral particles that will enter further rounds of selection until convergence is achieved and the best clones are recovered.

Convergence of AAV libraries upon selected variants

After three rounds of in vivo selection and recovery, 22 *cap* genes were sequenced. Interestingly, every single clone was a seven-amino acid insertion (7mer) (Figure 4.3a) into a capsid clone derived from either our ancestral AAV library[55] or a computationally-guided AAV DNA shuffling

library (SCHEMA library; Ojala, D.S. et al., *in preparation*). In particular, three 7mer sequences were recovered. The most prominent 7mer sequence was (SSARASA, clone name SGA1), found in 9 of the 22 clones, where it was present in the context of an ancestral AAV *cap* gene. The residue identities at the positions diversified during the ancestral library construction are presented in Table B.1; this clone additionally contains the mutations A70S and P148S. The location of the 7mer sequence, which may confer novel properties upon this AAV vector, is depicted in Figure 4.3 in the crystal structure of AAV1 (4.3b), the most homologous natural serotype with a solved structure; the modeled depiction (4.3c) shows the predicted structure of the 7mer insertion.

Figure 4.3 Distribution of 7mer insertions and predicted crystal structure of SGA1 clone. After three rounds of selection, convergence was achieved upon three different 7mer insertion sequences (a). The crystal structure of AAV1 (b) was used to predict the structure of variant SGA1 (c), which is of ancestral origin and therefore shares the most homology with AAV1. The 7mer insertion is depicted in magenta.

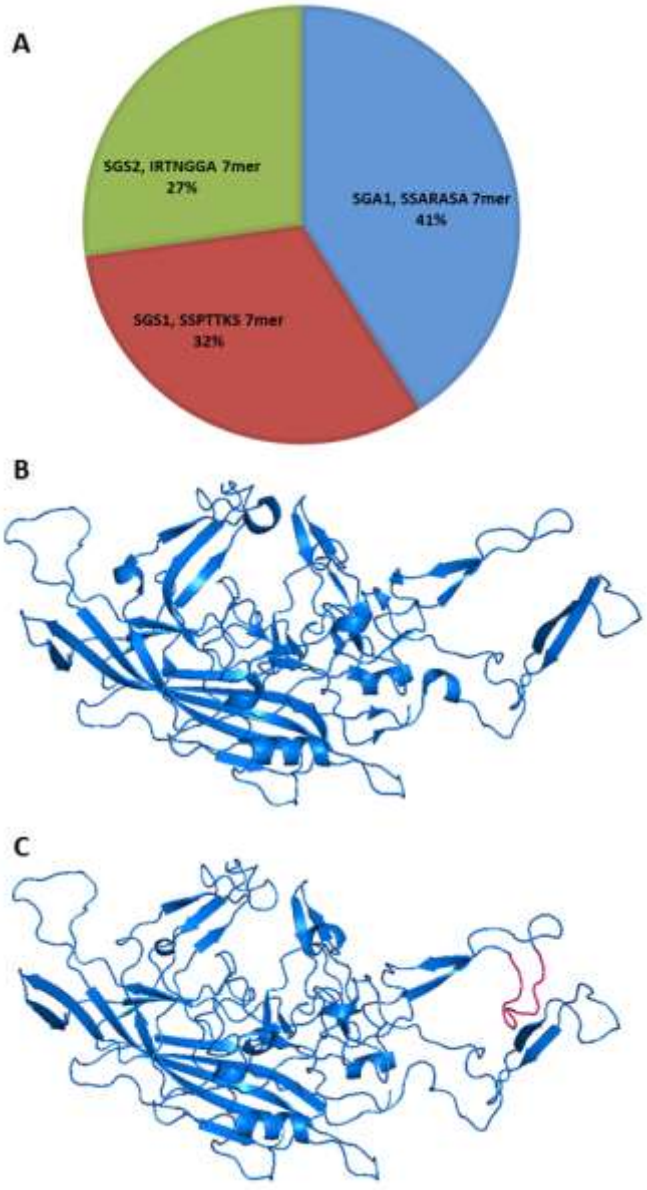

The second most abundant 7mer sequence, (SSPTTKS), was present in 7/22 clones, which are derived from a SCHEMA DNA shuffling library. Briefly, the library was generated by fragmenting the *cap* genes from AAV natural serotypes 2, 4, 5, 6, 8, and 9 into "blocks" such that the break points between blocks would minimize the disruptions of protein-protein contacts within monomers and at the full multimeric capsid assembly (Ojala, D.S. et al., *in preparation*). Clones that come from this library can thus be characterized by describing the AAV natural serotype present in each block (Table B.2). All recovered SCHEMA clones with the (SSARASA) 7mer insertion shared the following string of blocks: AAV2;F110L-AAV2;L129F,P135G,V136A-AAV6/AAV9-AAV8-AAV2-AAV2-AAV2, with a few individual ones having certain mutations including T415S, T567A, and A674T. The representative clone, named SGS1, had the string AAV2;F110L-AAV2;L129F,P135G,V136A-AAV6-AAV8-AAV2-AAV2-AAV2 and no additional mutations.

Finally, the third most abundant 7mer insertion was (IRTNGGA), present in 6/22 clones, all of which also came from the SCHEMA library. Five of these shared the same backbone sequence, AAV2;F110L-AAV2;L129F,P135G,V136A-AAV9-AAV8-AAV2-AAV9-AAV9, (Table B.2) which was used as the representative clone SGS2; the remaining clone had AAV2 present in its last two blocks instead of AAV9. The sequences of the three chosen evolved vectors are described in Table B.3.

In vitro characterization of evolved clones

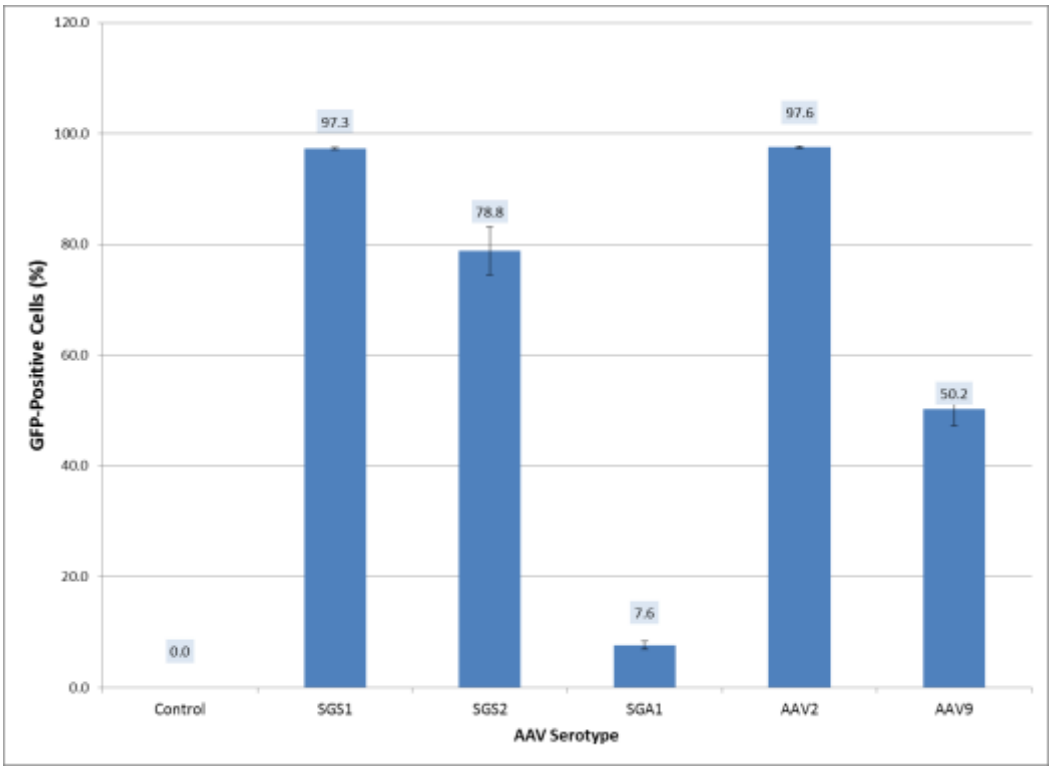

Figure 4.4 Infectivity of evolved AAV clones on L0 tumor initiating cells. Cultured cells were transduced with vectors packaged with a self-complementary CMV-GFP cassette at a genomic MOI of 4,000 viral genomes/cell. The fraction of GFP-positive cells was quantified by flow cytometry 72 hours later. Data presented as mean±SEM, *n*=3.

As an initial characterization step, we investigated the gene delivery properties of our *in vivo* evolved vectors on cultured GBM TICs *in vitro*. The three clones were packaged as high titer, iodixanol-purified recombinant AAV (rAAV) vectors encoding green fluorescent protein (GFP), as were the natural serotypes AAV2 and AAV9. GBM clones SGA1, SGS1, and SGS2 had similar packaging efficiencies as AAV2 and AAV9 (Table 4.1). GFP-encoding viral particles were used to infect GBM TICs at a multiplicity of infection (MOI) of 4,000 viral genomes/cell (Figure 4.4), showing that GBM clones mediated highly efficient gene delivery to TICs. Having confirmed the *in vitro* infectivity of the evolved clones, we set out to characterize their efficacy at mediating *in vivo* gene delivery to GBM TICs and tumor cells.

AAV Serotype	Genomic titer (vg/mL)
SGS1	2.32E+11
SGS2	1.90E+10
SGA1	7.90E+11
AAV2	1.95E+11
AAV9	4.91E+11

Table 4.1. Genomic titers of evolved AAV clones and natural serotypes. The viral genomic titers of the recovered particles were measured by quantitative PCR as previously described[49].

4.3 *In vivo* characterization of evolved vectors

Vector tropism

AAV vector tropism and biodistribution must be well characterized before implementation into gene therapy applications. To quantify gene delivery efficiency at the single cell level, AAV vectors packaged with GFP[43,44] can be administered to mice bearing GBMs expressing mCherry, enabling histology with dual label analysis.

GBM clones SGA1, SGS1, and SGS2 and AAV9 (a serotype capable of penetrating the BBB after systemic administration[62-64] that will be used as a benchmark) were packaged to encode GFP under the strong, ubiquitous CAG promoter, and administered systemically via tail-vein injection to tumor-bearing mice. Immunohistochemistry of the harvested tissues, which is currently ongoing, will enable the quantification of gene delivery at a single-cell level. Since these AAVs will have been strongly selected for tropism to GBMs, we anticipate that they will be selective to tumors rather than being diluted into other cells and tissues.

Vector biodistribution

Biodistribution, or the range of tissues a vector can localize to and transduce upon systemic administration, is an important gene delivery property that we will also study. Using methods we have previously described[48], GBM clones SGA1, SGS1, and SGS2 as well as AAV9 are currently being packaged using a luciferase reporter gene and will be systemically administered via tail-vein injection. We will validate and quantify results with *in vitro* bioluminescence on the harvested tissues[48].

Therapeutic gene delivery

In addition to studying the delivery properties of selected vectors, we are also interested in evaluating their therapeutic potential by delivering genetic cargos that can inhibit tumor growth and progression and extend the survival of our animal models. There are many potential options for anti-glioblastoma payloads targeting a wide spectrum of molecular targets[65] including: angiogenesis[66], EGFR signaling[67], mechanotransductive signaling[19], and immunostimulation through immune checkpoint blockade[68]. To benchmark against literature, we will use one of the most common approaches of gene therapy against cancer in the preclinical and clinical settings[66] - the delivery of cDNA encoding an anti-angiogenesis agent. Specifically, AAV-mediated delivery of cDNA encoding the anti-VEGF monoclonal antibody bevacizumab (i.e. Avastin) has previously been investigated preclinical cancer models[69-71]. This therapeutic monoclonal antibody reduces angiogenesis by binding to forms of vascular endothelial growth factor (VEGF) and inhibiting their interaction with VEGF receptors. It is the most widely used angiogenic inhibitor in the clinic for the treatment of many types of cancer[66,72], including glioblastoma[73].

We will study whether the *in vivo* expression of bevacizumab can alter and suppress tumor initiation and progression and prolong survival relative to the administration of WT vectors and lack of treatment. GBM clones SGA1, SGS1, and SGS2 are being packaged with cDNA encoding bevacizumab and purified as previously described[44]. They will be assayed for therapeutic gene delivery by systemic administration in mice bearing GBMs that express luciferase, and compared to wild-type (WT) AAV9 delivery and untreated mice (total of five experimental groups). We will monitor tumor progression *in vivo* through BLI, which can be detected over background before physical symptoms are presented and is correlated to tumor size[74]. We will also perform subsequent histological analyses to study tumor cell numbers, degree of tumor cell infiltration into brain parenchyma, transgene expression levels, and degree of tumor-induced angiogenesis[19].

4.4 Discussion

Glioma, the most common brain tumor in adults, develops as a result of aberrant growth and invasion of transformed astrocytic cells. Even with aggressive treatment, survival is very poor due in part to the presence of therapy-resistant tumor-initiating cells (TICs), which are highly migratory and invasive and thus render complete surgical tumor removal impossible. While effective therapeutic payloads exist, specific, efficient and non-invasive gene delivery to tumor cells still represents a major challenge in the field. Engineering therapies that target glioma tumor cells and TICs may enable enhanced efficacy and as a result longer clinical survival times in patients afflicted with this disease. In this project, we focused on development of gene therapy strategies for glioblastoma multiforme (GBM), an aggressive form of glioma, based on the targeting of AAV vectors to GBM tumor cells and TICs.

Adeno-associated virus (AAV) has emerged as a safe and promising vector for gene delivery applications. Unfortunately, natural AAVs are incapable of trafficking to GBM tumors and mediating high efficiency gene delivery upon systemic administration, and mechanistic knowledge of virus-GBM interactions are entirely insufficient to enable rational design of improved vectors. However, our AAV directed evolution approach[40-49,55,75,76] has enabled the direct *in vivo* selection of AAVs to overcome tissue and cellular barriers that are representative of clinical GBMs, including transporting from circulation to brain, trafficking through the BBB and spread into the brain parenchyma[77], and transduction of GBM and TICs.

Our strategy included several important features that selected for AAV variants that mediate high efficiency gene delivery to accurate representations of GBMs. Our GBM animal model involves the xenotransplantation of human primary GBM TICs into non-obese diabetic/severe combined immunodeficient gamma (NSG) mice[19], which are stereotactically injected with TICs into their striatum[8]. This animal model derived from primary GBM cells can recapitulate the hallmarks of actual tumors - including the invasive and migratory ability of GBM to invade parenchymal tissues and to initiate the formation of secondary tumors – and thus represents the transport barriers that vectors encounter clinically**.**

The convergence of the initial library (~100 million variants) to several clones with seven amino-acid (7mer) peptide insertions into the *cap* gene underscores both the power of *in vivo* directed evolution and the promise that these variants will have advantageous properties. For example, our laboratory previously conducted an *in vivo* directed evolution scheme for enhanced retinal gene delivery that yielded 7m8, a novel AAV variant with a 7mer peptide insertion (LGETTRP) into loop 4 of AAV2, that mediates robust pan-retinal transgene expression after intravitreal injection into adult mice, far higher than its parental AAV2 serotype[44]. Moreover, this 7m8 variant also resulted in more efficient transgene delivery to the retina of non-human primates (NHP) after intravitreal administration into the macaque eye, substantially better than the AAV2 natural serotype (and the AAV2 quadruple tyrosine mutant 4YF)[44]. The 7mer insertions in the three evolved clones may similarly be partially responsible for the transport and transduction properties of the GBM vectors. To investigate this possibility, future work can include the *in vitro* and *in vivo* analysis of the corresponding *cap* genes without the presence of their respective 7mers. Further vector characterization will also involve receptor binding studies, as we have previously studied[55], to compare the receptor affinities of the GBM vectors with that of the natural serotypes, which include affinity for N- and O-linked sialic acids, heparan sulfate proteoglycans, and galactose. Preliminary studies (Figure B.2) show that transduction by the most prominent clone, SGA1, is dependent on the recently discovered AAV receptor (AAVR, also known as KIAA0319L)[78].

To study the efficacy at therapeutic gene delivery of the evolved vectors, we are delivering a timely anti-tumor therapeutic payload: a therapeutic anti-angiogenesis cargo that may result in local reduction of tumor growth (bevacizumab). In addition to studies of AAV-mediated delivery of bevacizumab[69-71], AAV vectors have been utilized long-term expression of other monoclonal antibodies in various preclinical models of cancer. These include the delivery of a murine antihuman epidermal growth factor (EGFR) antibody in AAV1 vectors to a human vulvar carcinoma xenograft model[79], delivery of AAV2 encoding a mouse-human chimeric antibody against death-receptor 5 (DR5) to mouse models of human liver and colon cancer[80], and the administration of AAV9 vectors encoding a monoclonal antibody against the glycolytic enzyme

alpha-enolase (ENO1) to models of pancreatic ductal adenocarcinoma (PDAC) tumors[81]. Our engineered vectors could therefore serve as platforms for the delivery of other monoclonal antibodies against gliomas.

In fact, our work can lay the groundwork for future therapies based on AAV-mediated, localized immune checkpoint blockade. In future studies, we are interested in delivering the soluble extracellular part of programmed cell death 1 (sPD-1), a very promising glioblastoma therapeutic modality[68], and assessing the resulting transgene expression levels as a proof-of-concept delivery to GBM tumors using the developed vectors. The ability of the engineered vectors to mediate localized, GBM gene expression would offer significant improvements over current delivery methods for bevacizumab and anti-PD-1 protein therapies, which to date have involved systemic administration. First, high local levels of these molecules may mediate higher therapeutic efficacy. Second, systemic administration of these molecules has side effects. Systemic bevacizumab can cause significant cardiovascular complications, proteinuria, and gastrointestinal perforation[82-85], whereas systemic anti-PD-L1 antibodies have been associated with inflammation and auto-immune adverse events in clinical trials[86,87]. Localized expression of these molecules would thus likely reduce their associated toxicities and overall enhance their safety profile. If this work is successful, full comparisons between protein vs. gene therapy approaches will be explored in future work, as well as potential combinations with traditional approaches such as small molecule chemotherapies.

Our engineered vectors could also be employed to package alternate payloads in addition to monoclonal antibodies. For example, they can be packaged with cargoes for shRNA-mediated downregulation of other molecular targets that could also confer a therapeutic effect, such as the neurotrophin receptors Tropomyosin receptor kinase B and C (TrkB, TrkC), which enhance TIC viability and whose downregulation decreases TIC growth without being deleterious to the mature brain[88 89]; shRNA-mediated downregulation of targets could be explored individually[90] or in a multiplexed manner[91].

In summary, we applied an *in vivo* directed evolution strategy to engineer novel AAV-based vectors for efficient and effective therapeutic gene delivery to glioblastoma multiforme tumors and tumor-initiating cells. Our system relied on an animal model capable of representing the hallmarks of GBM and a selective and stringent selection strategy, which enabled us to select for novel variants with enhanced gene delivery properties that are capable of localizing to the CNS and transducing GBM TICs upon systemic administration. We are currently in our final stages of characterizing the gene delivery properties and the therapeutic potential of the evolved variants. The resulting greatly improved gene delivery vehicles will have the potential to enable new, potent therapies to treat highly invasive and malignant GBM tumors, as well as help establish a paradigm for engineering optimized AAV against other cancer targets.

4.5 Materials and Methods

Cell culture

L0 human glioblastoma tumor initiating cells classified as the Classical subtype of GBM[92], which were used throughout the whole study, were kindly provided by Dr. Brent Reynolds (University

of Florida, Gainesville), and propagated in neurosphere assay growth conditions[93] as we have previously described[94], with serum-free media (Neurocult NS-A Proliferation kit, Stem Cell Technologies) that contained epidermal growth factor (EGF, 20 ng/ml, R&D), basic fibroblast growth factor (bFGF, 10 ng/ml, R&D), and heparin (0.2% diluted in phosphate buffered saline, Sigma). Lentiviral vectors encoding firefly luciferase and mCherry were packaged as previously described[95]. L0 cells were stably transduced with concentrated viral particles and culture medium was changed 24h post-transduction. Luciferase activity was assayed in vitro with the Firefly Luciferase Assay System (Promega) by using a single-sample luminometer (70% sensitivity, 2s measurement delay, 10s measurement read). Expression of mCherry was confirmed with microscopy, and mCherry-positive cells were sorted using fluorescence-activated cell sorting (FACS, U.C. Berkeley Flow Cytometry Facility, Berkeley, CA).

Library construction and vector packaging

AAV vector libraries were produced as previously described[44,47]. Replication competent AAV was then packaged and purified by iodixanol density centrifugation as previously described[48,49]. DNase-resistant genomic titers were obtained via quantitative real time PCR using a Bio-Rad iCycler (Bio-Rad, Hercules, CA) and Taqman probe (Biosearch Technologies, Novato, CA)[48]. To perform *in vitro* infectivity studies of natural AAV serotypes and evolved clones, recombinant AAV (rAAV) vectors were packaged with a self-complementary CMV-GFP cassette using the transient transfection method previously described[48,49]. Cells were seeded in 24-well plates at a density of 25,000 cells per well. One day after seeding, cells were infected with rAAV at the indicated genomic MOI ($n = 3$). For all studies, the fraction of GFP-expressing cells 72 hours post-infection was quantified via flow cytometry using a Beckman Coulter FC500 analytical cytometer (UC Berkeley Stem Cell Center, Berkeley, CA).

In vitro directed evolution

Cells were seeded in 6-well tissue culture plates at a density of 1×10^5 cells per well. One day after seeding, cells were infected with replication competent AAV libraries at genomic MOIs of 10,000 (Round 1), 1,000 (Round 2), and 100 (Round 3). After 24 hours of exposure, cells were superinfected with adenovirus serotype 5 (Ad5). Approximately 48 hours later, cytopathic effect was observed, and virions were harvested by three freeze/thaw steps followed by treatment with Benzonase nuclease (1 unit/mL) (Sigma-Aldrich) at 37 °C for 30 minutes. Viral lysates were then incubated at 56°C for 30 minutes to inactivate Ad5. The viral genomic titer was determined as described above. To analyze *cap* sequences, AAV viral genomes were extracted after the third round of evolution, amplified by PCR, and sequenced at the UC Berkeley DNA Sequencing Facility.

GBM animal model

Female 8-week-old nonobese diabetic/severe combined immunodeficient g (NSG) mice (NOD.Cg-Prkdc(scid)Il2rg(tm1Wjl)/SzJ, Jackson Laboratories 005557) were implanted intracranially with 200,000 L0 TICs (expressing both mCherry and firefly luciferase) according to a previously established protocol[92]. For the in vivo directed evolution, approximately 10^{11} DNase-resistant particles were injected into the tail vein of tumor-bearing mice four weeks post-tumor

cell implantation. Two weeks later, animals were euthanized, brain and tumor tissue were recovered, and cells were dissociated using the neurosphere assay as previously described[18]. mCherry-expressing cells were sorted through FACS with a BD Influx Sorter (UC Berkeley Flow Cytometry Facility, Berkeley, CA). DNA extracted from cells[96] was used for PCR amplification of viral genomes, which were cloned and packaged for future rounds as described above. All animal procedures were approved by the Office of Laboratory Animal Care at the University of California, Berkeley and conducted in accordance with NIH guidelines on laboratory animal care.

Molecular Modeling

The amino acid residues were inserted into the Protein Data Bank (PDB) file 3NG9 (AAV1) after position D590 with Maestro software. This data file was submitted to SWISS MODEL homology mode, with settings to build a monomer by using the 3NG9 structure for comparison. The generated PDB structure file was submitted to Viper (Scripps) for transforming to Viper convention and for assembly of the full capsid.

4.6 Acknowledgements

We are grateful to Professor Brent Reynolds (University of Florida) for kindly providing the L0 human glioblastoma tumor-initiating cells and to Professor Ronald G. Crystal for kindly providing the expression cassette for packaging bevacizumab in AAV. We are also grateful to Professor Jan E. Carette for providing the AAVR-knockout HeLa cell line used in AAVR receptor binding studies, and to Vijay S. Reddy (Scripps Institute) for assembly of the full SGA1 capsid.

4.7 Funding

JLSO has been supported by a Ford Foundation Fellowship, a National Science Foundation Graduate Fellowship, and two U.C. Berkeley Graduate Division Fellowships.

Conflict of interest statement. DVS and JLSO are inventors on patents involving AAV directed evolution, and DS is the co-founder of an AAV gene therapy company.

4.8 References

1. Ray-Chaudhury, A. Pathology of Glioblastoma Multiforme. *Glioblastoma: Molecular Mechanisms of Pathogenesis and Current Therapeutic Strategies*, 77-84 (2010).
2. Louis, D.N. *et al.* The 2007 WHO classification of tumours of the central nervous system. *Acta Neuropathologica* **114**, 97-109 (2007).
3. Vescovi, A.L., Galli, R. & Reynolds, B.A. Brain tumour stem cells. *Nat Rev Cancer* **6**, 425-36 (2006).
4. Nakada, M. *et al.* Molecular targets of glioma invasion. *Cell Mol Life Sci* **64**, 458-78 (2007).
5. Stupp, R. *et al.* Radiotherapy plus concomitant and adjuvant temozolomide for glioblastoma. *N Engl J Med* **352**, 987-96 (2005).
6. Welsh, C.T. Molecular Mechanisms of Pathogenesis in Glioblastoma and Current Therapeutic Strategies. *Glioblastoma: Molecular Mechanisms of Pathogenesis and Current Therapeutic Strategies*, 85-93 (2010).
7. Venere, M., Fine, H.A., Dirks, P.B. & Rich, J.N. Cancer stem cells in gliomas: identifying and understanding the apex cell in cancer's hierarchy. *Glia* **59**, 1148-54 (2011).
8. Deleyrolle, L.P. *et al.* Evidence for label-retaining tumour-initiating cells in human glioblastoma. *Brain* **134**, 1331-43 (2011).
9. Bao, S. *et al.* Glioma stem cells promote radioresistance by preferential activation of the DNA damage response. *Nature* **444**, 756-60 (2006).
10. Sakariassen, P.O., Immervoll, H. & Chekenya, M. Cancer stem cells as mediators of treatment resistance in brain tumors: status and controversies. *Neoplasia* **9**, 882-92 (2007).
11. Deschavanne, P.J. & Fertil, B. A review of human cell radiosensitivity in vitro. *Int J Radiat Oncol Biol Phys* **34**, 251-66 (1996).
12. Lee, J. *et al.* Tumor stem cells derived from glioblastomas cultured in bFGF and EGF more closely mirror the phenotype and genotype of primary tumors than do serum-cultured cell lines. *Cancer Cell* **9**, 391-403 (2006).
13. Taillandier, L., Antunes, L. & Angioi-Duprez, K.S. Models for neuro-oncological preclinical studies: solid orthotopic and heterotopic grafts of human gliomas into nude mice. *J Neurosci Methods* **125**, 147-57 (2003).
14. Bonavia, R., Inda, M.M., Cavenee, W.K. & Furnari, F.B. Heterogeneity maintenance in glioblastoma: a social network. *Cancer Res* **71**, 4055-60 (2011).
15. Xie, Q. *et al.* A highly invasive human glioblastoma pre-clinical model for testing therapeutics. *J Transl Med* **6**, 77 (2008).
16. Singh, S.K. *et al.* Identification of human brain tumour initiating cells. *Nature* **432**, 396-401 (2004).
17. Wang, H. *et al.* miR-33a promotes glioma-initiating cell self-renewal via PKA and NOTCH pathways. *J Clin Invest* **124**, 4489-502 (2014).
18. Azari, H. *et al.* Purification of immature neuronal cells from neural stem cell progeny. *PLoS One* **6**, e20941 (2011).
19. Wong, S.Y. *et al.* Constitutive activation of myosin-dependent contractility sensitizes glioma tumor-initiating cells to mechanical inputs and reduces tissue invasion. *Cancer Res* (2015).
20. Pulkkanen, K.J. & Yla-Herttuala, S. Gene therapy for malignant glioma: current clinical status. *Mol Ther* **12**, 585-98 (2005).
21. Kroeger, K.M. *et al.* Gene therapy and virotherapy: novel therapeutic approaches for brain tumors. *Discov Med* **10**, 293-304 (2010).
22. Lowenstein, P.R. Immunology of viral-vector-mediated gene transfer into the brain: an evolutionary and developmental perspective. *Trends Immunol* **23**, 23-30 (2002).

23. Aghi, M. & Martuza, R.L. Oncolytic viral therapies - the clinical experience. *Oncogene* **24**, 7802-16 (2005).
24. Jin, S. & Ye, K. Nanoparticle-mediated drug delivery and gene therapy. *Biotechnol Prog* **23**, 32-41 (2007).
25. Tobias, A., Ahmed, A., Moon, K.S. & Lesniak, M.S. The art of gene therapy for glioma: a review of the challenging road to the bedside. *J Neurol Neurosurg Psychiatry* **84**, 213-22 (2013).
26. Berns, K.I. & Linden, R.M. The cryptic life style of adeno-associated virus. *Bioessays* **17**, 237-45 (1995).
27. Testa, F. *et al.* Three-year follow-up after unilateral subretinal delivery of adeno-associated virus in patients with Leber congenital Amaurosis type 2. *Ophthalmology* **120**, 1283-91 (2013).
28. Dalkara, D. & Sahel, J.A. Gene therapy for inherited retinal degenerations. *C R Biol* **337**, 185-92 (2014).
29. Nathwani, A.C. *et al.* Adenovirus-associated virus vector-mediated gene transfer in hemophilia B. *N Engl J Med* **365**, 2357-65 (2011).
30. Ohmori, T., Mizukami, H., Ozawa, K., Sakata, Y. & Nishimura, S. New approaches to gene and cell therapy for hemophilia. *J Thromb Haemost* **13 Suppl 1**, S133-42 (2015).
31. Carpentier, A.C. *et al.* Effect of alipogene tiparvovec (AAV1-LPL(S447X)) on postprandial chylomicron metabolism in lipoprotein lipase-deficient patients. *J Clin Endocrinol Metab* **97**, 1635-44 (2012).
32. Jacobson, S.G. *et al.* Gene therapy for leber congenital amaurosis caused by RPE65 mutations: safety and efficacy in 15 children and adults followed up to 3 years. *Arch Ophthalmol* **130**, 9-24 (2012).
33. MacLaren, R.E. *et al.* Retinal gene therapy in patients with choroideremia: initial findings from a phase 1/2 clinical trial. *Lancet* **383**, 1129-37 (2014).
34. Stroes, E.S. *et al.* Intramuscular administration of AAV1-lipoprotein lipase S447X lowers triglycerides in lipoprotein lipase-deficient patients. *Arterioscler Thromb Vasc Biol* **28**, 2303-4 (2008).
35. Gaudet, D. *et al.* Efficacy and long-term safety of alipogene tiparvovec (AAV1-LPLS447X) gene therapy for lipoprotein lipase deficiency: an open-label trial. *Gene Ther* **20**, 361-9 (2013).
36. Santiago-Ortiz, J.L. & Schaffer, D.V. Adeno-associated virus (AAV) vectors in cancer gene therapy. *J Control Release* (2016).
37. Di, L. *et al.* Clinical safety of induced CTL infusion through recombinant adeno-associated virus-transfected dendritic cell vaccination in Chinese cancer patients. *Clin Transl Oncol* **14**, 675-81 (2012).
38. Kotterman, M.A. & Schaffer, D.V. Engineering adeno-associated viruses for clinical gene therapy. *Nat Rev Genet* **15**, 445-51 (2014).
39. Romero, P.A. & Arnold, F.H. Exploring protein fitness landscapes by directed evolution. *Nat Rev Mol Cell Biol* **10**, 866-76 (2009).
40. Excoffon, K.J. *et al.* Directed evolution of adeno-associated virus to an infectious respiratory virus. *Proc Natl Acad Sci U S A* **106**, 3865-70 (2009).
41. Jang, J.H. *et al.* An evolved adeno-associated viral variant enhances gene delivery and gene targeting in neural stem cells. *Mol Ther* **19**, 667-75 (2011).
42. Asuri, P. *et al.* Directed evolution of adeno-associated virus for enhanced gene delivery and gene targeting in human pluripotent stem cells. *Mol Ther* **20**, 329-38 (2012).
43. Klimczak, R.R., Koerber, J.T., Dalkara, D., Flannery, J.G. & Schaffer, D.V. A novel adeno-associated viral variant for efficient and selective intravitreal transduction of rat Muller cells. *PLoS One* **4**, e7467 (2009).
44. Dalkara, D. *et al.* In vivo-directed evolution of a new adeno-associated virus for therapeutic outer retinal gene delivery from the vitreous. *Sci Transl Med* **5**, 189ra76 (2013).

45. Dalkara, D. *et al.* AAV mediated GDNF secretion from retinal glia slows down retinal degeneration in a rat model of retinitis pigmentosa. *Mol Ther* **19**, 1602-8 (2011).
46. Koerber, J.T. *et al.* Molecular evolution of adeno-associated virus for enhanced glial gene delivery. *Mol Ther* **17**, 2088-95 (2009).
47. Koerber, J.T., Maheshri, N., Kaspar, B.K. & Schaffer, D.V. Construction of diverse adeno-associated viral libraries for directed evolution of enhanced gene delivery vehicles. *Nat Protoc* **1**, 701-6 (2006).
48. Koerber, J.T., Jang, J.H. & Schaffer, D.V. DNA shuffling of adeno-associated virus yields functionally diverse viral progeny. *Mol Ther* **16**, 1703-9 (2008).
49. Maheshri, N., Koerber, J.T., Kaspar, B.K. & Schaffer, D.V. Directed evolution of adeno-associated virus yields enhanced gene delivery vectors. *Nat Biotechnol* **24**, 198-204 (2006).
50. Maguire, C.A. *et al.* Directed evolution of adeno-associated virus for glioma cell transduction. *J Neurooncol* **96**, 337-47 (2010).
51. Wollmann, G., Tattersall, P. & van den Pol, A.N. Targeting human glioblastoma cells: comparison of nine viruses with oncolytic potential. *J Virol* **79**, 6005-22 (2005).
52. Thorsen, F. *et al.* Adeno-associated virus (AAV) serotypes 2, 4 and 5 display similar transduction profiles and penetrate solid tumor tissue in models of human glioma. *J Gene Med* **8**, 1131-40 (2006).
53. Huszthy, P.C. *et al.* Widespread dispersion of adeno-associated virus serotype 1 and adeno-associated virus serotype 6 vectors in the rat central nervous system and in human glioblastoma multiforme xenografts. *Hum Gene Ther* **16**, 381-92 (2005).
54. Harding, T.C. *et al.* Enhanced gene transfer efficiency in the murine striatum and an orthotopic glioblastoma tumor model, using AAV-7- and AAV-8-pseudotyped vectors. *Hum Gene Ther* **17**, 807-20 (2006).
55. Santiago-Ortiz, J. *et al.* AAV ancestral reconstruction library enables selection of broadly infectious viral variants. *Gene Ther* (2015).
56. Muller, O.J. *et al.* Random peptide libraries displayed on adeno-associated virus to select for targeted gene therapy vectors. *Nat Biotechnol* **21**, 1040-6 (2003).
57. Berns, K.I. & Giraud, C. Biology of adeno-associated virus. *Curr Top Microbiol Immunol* **218**, 1-23 (1996).
58. Tiffen, J.C., Bailey, C.G., Ng, C., Rasko, J.E. & Holst, J. Luciferase expression and bioluminescence does not affect tumor cell growth in vitro or in vivo. *Mol Cancer* **9**, 299 (2010).
59. Nogawa, M. *et al.* Monitoring luciferase-labeled cancer cell growth and metastasis in different in vivo models. *Cancer Lett* **217**, 243-53 (2005).
60. Shaner, N.C. *et al.* Improved monomeric red, orange and yellow fluorescent proteins derived from Discosoma sp. red fluorescent protein. *Nat Biotechnol* **22**, 1567-72 (2004).
61. Pfister, W., Blick, T., Kok, S.F., Polekhina, G. & Waltham, M. High-dose antioxidants as potential anti-osteolytic and palliative therapies for breast cancer bone metastasis. *Bone* **48**, S53-S53 (2011).
62. Foust, K.D. *et al.* Intravascular AAV9 preferentially targets neonatal neurons and adult astrocytes. *Nat Biotechnol* **27**, 59-65 (2009).
63. Shen, F. *et al.* Intravenous delivery of adeno-associated viral vector serotype 9 mediates effective gene expression in ischemic stroke lesion and brain angiogenic foci. *Stroke* **44**, 252-4 (2013).
64. Shen, F. *et al.* Inhibition of pathological brain angiogenesis through systemic delivery of AAV vector expressing soluble FLT1. *Gene Ther* (2015).
65. Choi, J.W., Schroeder, M.A., Sarkaria, J.N. & Bram, R.J. Cyclophilin B supports Myc and mutant p53-dependent survival of glioblastoma multiforme cells. *Cancer Res* **74**, 484-96 (2014).
66. Samant, R.S. & Shevde, L.A. Recent advances in anti-angiogenic therapy of cancer. *Oncotarget* **2**, 122-34 (2011).

67. Newton, H.B. Overview of the Molecular Genetics and Molecular Chemotherapy of GBM. *Glioblastoma: Molecular Mechanisms of Pathogenesis and Current Therapeutic Strategies*, 1-42 (2010).
68. Preusser, M., Lim, M., Hafler, D.A., Reardon, D.A. & Sampson, J.H. Prospects of immune checkpoint modulators in the treatment of glioblastoma. *Nat Rev Neurol* **11**, 504-14 (2015).
69. Xie, Y. *et al.* AAV-mediated persistent bevacizumab therapy suppresses tumor growth of ovarian cancer. *Gynecol Oncol* **135**, 325-32 (2014).
70. Watanabe, M., Boyer, J.L. & Crystal, R.G. AAVrh.10-mediated genetic delivery of bevacizumab to the pleura to provide local anti-VEGF to suppress growth of metastatic lung tumors. *Gene Ther* **17**, 1042-51 (2010).
71. Hicks, M.J. *et al.* Genetic modification of neurons to express bevacizumab for local anti-angiogenesis treatment of glioblastoma. *Cancer Gene Ther* **22**, 1-8 (2015).
72. Vasudev, N.S. & Reynolds, A.R. Anti-angiogenic therapy for cancer: current progress, unresolved questions and future directions. *Angiogenesis* **17**, 471-94 (2014).
73. Rahmathulla, G., Hovey, E.J., Hashemi-Sadraei, N. & Ahluwalia, M.S. Bevacizumab in high-grade gliomas: a review of its uses, toxicity assessment, and future treatment challenges. *Onco Targets Ther* **6**, 371-89 (2013).
74. Hawes, J.J. & Reilly, K.M. Bioluminescent approaches for measuring tumor growth in a mouse model of neurofibromatosis. *Toxicol Pathol* **38**, 123-30 (2010).
75. Koerber, J.T., Jang, J.H., Yu, J.H., Kane, R.S. & Schaffer, D.V. Engineering adeno-associated virus for one-step purification via immobilized metal affinity chromatography. *Hum Gene Ther* **18**, 367-78 (2007).
76. Koerber, J.T. & Schaffer, D.V. Transposon-based mutagenesis generates diverse adeno-associated viral libraries with novel gene delivery properties. *Methods Mol Biol* **434**, 161-70 (2008).
77. Watkins, S. *et al.* Disruption of astrocyte-vascular coupling and the blood-brain barrier by invading glioma cells. *Nat Commun* **5**, 4196 (2014).
78. Pillay, S. *et al.* An essential receptor for adeno-associated virus infection. *Nature* **530**, 108-12 (2016).
79. Ho, D.T. *et al.* Growth inhibition of an established A431 xenograft tumor by a full-length anti-EGFR antibody following gene delivery by AAV. *Cancer Gene Ther* **16**, 184-94 (2009).
80. Lv, F. *et al.* Adeno-associated virus-mediated anti-DR5 chimeric antibody expression suppresses human tumor growth in nude mice. *Cancer Lett* **302**, 119-27 (2011).
81. Principe, M. *et al.* Targeting of surface alpha-enolase inhibits the invasiveness of pancreatic cancer cells. *Oncotarget* **6**, 11098-113 (2015).
82. Hansel, T.T., Kropshofer, H., Singer, T., Mitchell, J.A. & George, A.J. The safety and side effects of monoclonal antibodies. *Nat Rev Drug Discov* **9**, 325-38 (2010).
83. Economopoulou, P., Kotsakis, A., Kapiris, I. & Kentepozidis, N. Cancer therapy and cardiovascular risk: focus on bevacizumab. *Cancer Manag Res* **7**, 133-43 (2015).
84. Brandes, A.A., Bartolotti, M., Tosoni, A., Poggi, R. & Franceschi, E. Practical management of bevacizumab-related toxicities in glioblastoma. *Oncologist* **20**, 166-75 (2015).
85. Tahover, E. *et al.* An observational cohort study of bevacizumab and chemotherapy in metastatic colorectal cancer patients: safety and efficacy with analysis by age group. *Target Oncol* **10**, 55-63 (2015).
86. Brahmer, J.R. *et al.* Safety and activity of anti-PD-L1 antibody in patients with advanced cancer. *N Engl J Med* **366**, 2455-65 (2012).
87. Teply, B.A. & Lipson, E.J. Identification and management of toxicities from immune checkpoint-blocking drugs. *Oncology (Williston Park)* **28 Suppl 3**, 30-8 (2014).
88. Lawn, S. *et al.* Neurotrophin signaling via TrkB and TrkC Receptors promote the growth of Brain Tumor Initiating Cells. *J Biol Chem* (2014).

89. Bergami, M. *et al.* Deletion of TrkB in adult progenitors alters newborn neuron integration into hippocampal circuits and increases anxiety-like behavior. *Proc Natl Acad Sci U S A* **105**, 15570-5 (2008).
90. Borel, F., Kay, M.A. & Mueller, C. Recombinant AAV as a platform for translating the therapeutic potential of RNA interference. *Mol Ther* **22**, 692-701 (2014).
91. Xia, X.G., Zhou, H. & Xu, Z. Multiple shRNAs expressed by an inducible pol II promoter can knock down the expression of multiple target genes. *Biotechniques* **41**, 64-8 (2006).
92. Wong, S.Y. *et al.* Constitutive activation of myosin-dependent contractility sensitizes glioma tumor-initiating cells to mechanical inputs and reduces tissue invasion. *Cancer Res* **75**, 1113-22 (2015).
93. Deleyrolle, L.P. *et al.* Determination of somatic and cancer stem cell self-renewing symmetric division rate using sphere assays. *PLoS One* **6**, e15844 (2011).
94. Wong, R.K., Hubschman, S. & Tsui, I. Reactivation of retinopathy of prematurity after ranibizumab treatment. *Retina* **35**, 675-80 (2015).
95. Yang, L. *et al.* Engineered lentivector targeting of dendritic cells for in vivo immunization. *Nat Biotechnol* **26**, 326-34 (2008).
96. Arad, U. Modified Hirt procedure for rapid purification of extrachromosomal DNA from mammalian cells. *Biotechniques* **24**, 760-2 (1998).

Appendix A: Supplementary Material for Chapter 2

This appendix contains material adapted from a manuscript published as

J. Santiago-Ortiz*, D. Ojala*, O. Westesson, J. Weinstein, S. Wong, A. Steinsapir, S. Kumar, I. Holmes, D. Schaffer. AAV Ancestral Reconstruction Library Enables Selection of Broadly Infectious Viral Variants. *Gene Therapy* **22**, 934-946 (2015).

* Indicates co-first authors.

A.1 Supplementary Figures and Tables

Figure A.1. Full phylogenetic tree for AAV ancestral sequence reconstruction. Curly braced numbers indicate clade posterior probabilities. The phylogenetic tree graphic was generated in Dendroscope.

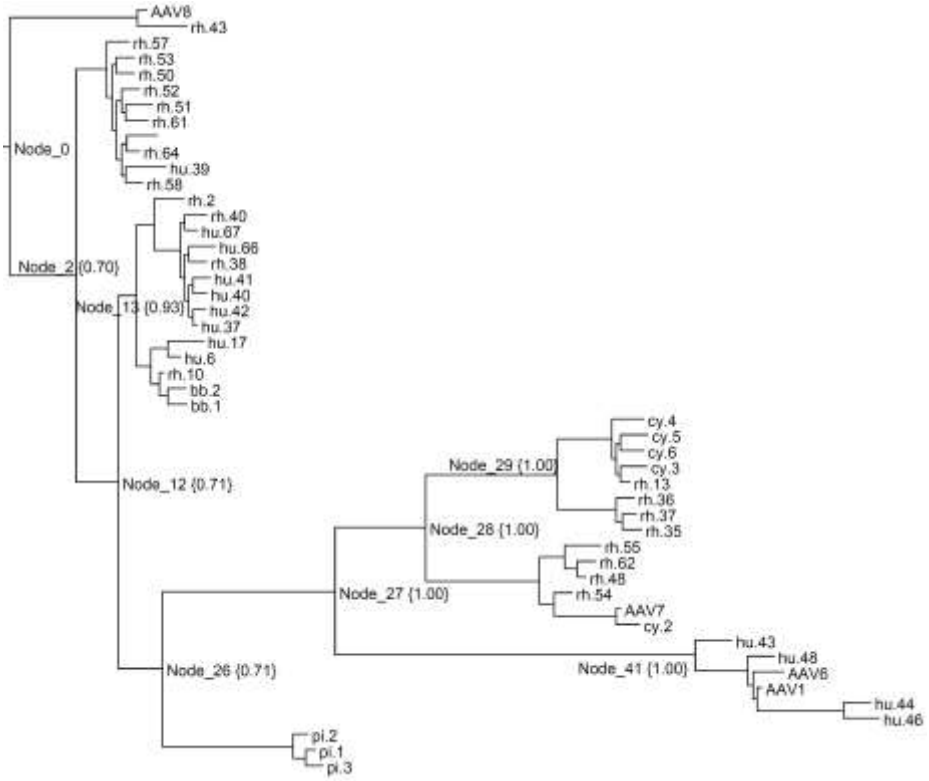

Figure A2. **Amino acid sequences of the ancestral AAV (a) *cap* and (b) AAP reading frames**. Variable residues are labeled with a bold, underlined letter X. In the AAP sequence, the shifted reading frame results in four variable residues corresponding to AAP positions 88, 90, 91, and 92.

a)

MAADGYLPDWLEDNLSEGIREWWDLKPGAPKPKANQQKQDDGRGLVLPGYKYLGPFNGLDKGEPVNAA
DAAALEHDKAYDQQLKAGDNPYLRYNHADAEFQERLQEDTSFGGNLGRAVFQAKKRVLEPLGLVEEGA
KTAPGKKRPVEPSPQRSPDSSTGIGKKGQQPAKKRLNFGQTGDSESVPDPQPLGEPPAGPSGLGSGTMAAG
GGAPMADNNEGADGVGNASGNWHCDSTWLGDRVITTSTRTWALPTYNNHLYKQISS**X**S**X**G**X**TNDNHYF
GYSTPWGYFDFNRFHCHFSPRDWQRLINNNWGFRPKRLNFKLFNIQVKEVTTNDGVTTIANNLTSTVQVFS
DSEYQLPYVLGSAHQGCLPPFPADVFMIPQYGYLTLNNGSQAVGRSSFYCLEYFPSQMLRTGNNFTFSYTF
EDVPFHSSYAHSQSLDRLMNPLIDQYLYYL**X**RTQSTGGTAG**XX**ELLFSQ**X**GP**XX**MS**X**QAKNWLPGPCYRQ
QRVSKTL**X**QNNNSNFAWTGATKYHLNGR**X**SLVNPGVAMATHKDDE**X**RFFPSSGVLIFGK**X**GAG**X**NNT**X**L
XNVM**X**T**X**EEEIKTTNPVATE**X**YGVVA**X**NLQSSNTAP**X**TG**X**VNSQGALPGMVWQNRDVYLQGPIWAKIPH
TDGNFHPSPLMGGFGLKHPPPQILIKNTPVPANPP**XX**F**XX**AKFASFITQYSTGQVSVEIEWELQKENSKRWN
PEIQYTSNYAKS**X**NVDFAV**XXX**GVY**X**EPRPIGTRYLTRNL

b)

LATQSQSPTLNLSENHQQAPLVWDLVQWLQAVAHQWQTITKAPTEWVMPQEIGIAIPHGWATESSPPAPEP
GPCPPTTTTSTSKSPV**X**R**XXX**PTTTTTSATAPPGGILTSTDSTATSHHVTGSDSSTTTGDSGPRDSTSSSSTSRS
RRSRRMTASRPSLITLPARFRSFRTRNTSCRTSSALRTRAACLRSRRTSS

Figure A.3. Alignment of the ancestral AAV *cap* protein with natural serotypes. Capsid amino acids were aligned using the Geneious program (Biomatters). Colored amino acids represent disagreements with the reference ancestral *cap* sequence. The variable positions in the ancestral library are annotated in black and designated with the letter X.

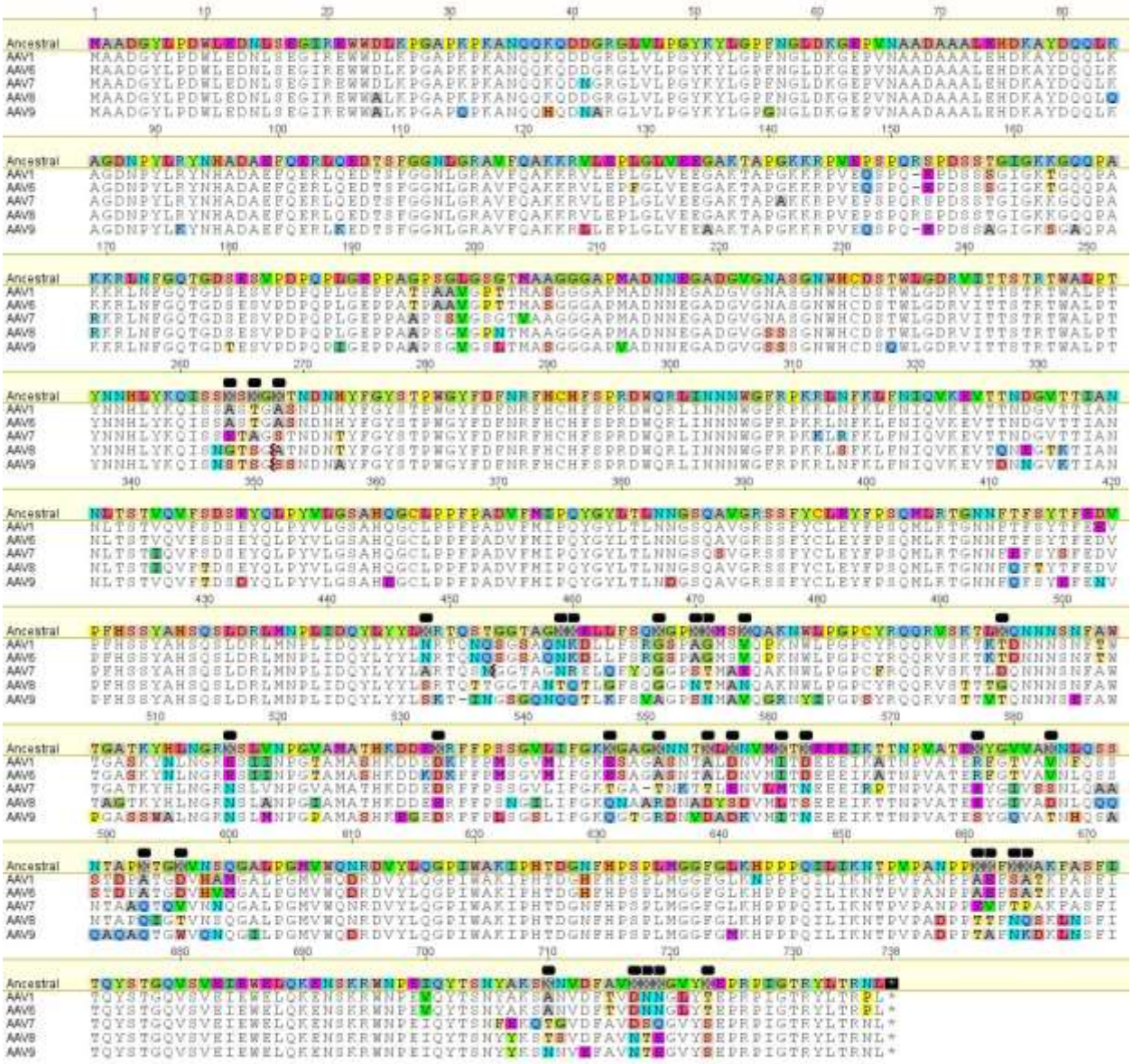

Figure A.4. **Dominant amino acids at variable positions after three rounds of selection**. A heat map was generated based on the frequency of the most common amino acid at each position in the different libraries. The dominant amino acid and frequency at each position were determined based on sequencing results from individual clones (n =14).

Amino acid	C2C12 round 3	293T round 3	IB3 round 3	GBM round 3	B16 round 3
264	Q, 69%.	Q, 53%.	A, 73%.	A, 47%.	Q, 50%.
266	S, 100%.	S, 59%.	S, 87%.	S, 80%.	A, 57%.
268	S, 100%.	S, 76%.	S, 100%.	S, 93%.	S, 100%.
448	S, 56%.	S, 50%.	A, 53%.	A, 67%.	A, 71%.
459	N, 56%.	T, 88%.	T, 100%.	T, 80%.	T, 93%.
460	R, 81%.	R, 88%.	R, 93%.	R, 87%.	R, 93%.
467	A, 69%.	A, 53%.	A, 67%.	A, 73%.	A, 79%.
470	S, 69%.	S, 88%.	S, 93%.	S, 93%.	S, 92%.
471	N, 88%.	T, 65%.	N, 67%.	N, 53%.	N, 57%.
474	A, 100%.	A, 100%.	A, 93%.	A, 100%.	A, 86%.
495	S, 94%.	S, 71%.	S, 87%.	S, 87%.	S, 86%.
516	D, 100%.	D, 100%.	D, 100%.	D, 100%.	D, 100%.
533	D, 50%.	D, 94%.	D, 80%.	D, 100%.	D, 86%.
547	Q, 100%.	Q, 82%.	Q, 100%.	Q, 93%.	Q, 79%.
551	A, 75%.	A, 82%.	A, 87%.	A, 80%.	A, 93%.
555	T, 50%.	A, 82%.	A, 73%.	T, 67%.	T, 57%.
557	E, 63%.	E, 59%.	E, 73%.	E, 100%.	E, 86%.
561	M, 94%.	M, 82%.	M, 100%.	M, 73%.	M, 57%.
563	S, 75%.	S, 59%.	S, 100%.	N, 60%.	S, 71%.
577	Q, 100%.	Q, 88%.	Q, 100%.	Q, 100%.	Q, 86%.
583	S, 100%.	S, 88%.	S, 100%.	S, 100%.	S, 86%.
593	A, 50%.	Q, 53%.	A, 60%.	A, 53%.	V, 43%.
596	T, 69%.	A, 67%.	A, 73%.	A, 67%.	A, 71%.
661	A, 69%.	A, 53%.	A, 67%.	A, 80%.	A, 86%.
662	V, 88%.	V, 60%.	V, 60%.	V, 67%.	V, 64%.
664	T, 56%.	T, 73%.	T, 87%.	T, 87%.	T, 86%.
665	P, 88%.	P, 73%.	P, 73%.	P, 73%.	P, 71%.
710	T, 100%.	T, 80%.	T, 100%.	T, 87%.	T, 100%.
717	N, 69%.	N, 80%.	N, 93%.	N, 71%.	N, 93%.
718	N, 50%.	N, 47%.	S, 67%.	N, 60%.	S, 71%.
719	E, 100%.	E, 67%.	E, 93%.	E, 93%.	E, 93%.
723	S, 94%.	T, 62%.	S, 60%.	S, 71%.	S, 93%.

Figure A.5. Change in amino acid frequency at variable positions between rounds three and six of selection. The percent change in amino acid frequency between the third and sixth round of selection on each cell line was calculated. If the identity of the dominant amino acid did not change, the increase (blue) or decrease (red) in frequency is displayed. If selection resulted in a change in amino acid identity at that position, the new amino acid and frequency is shown (yellow).

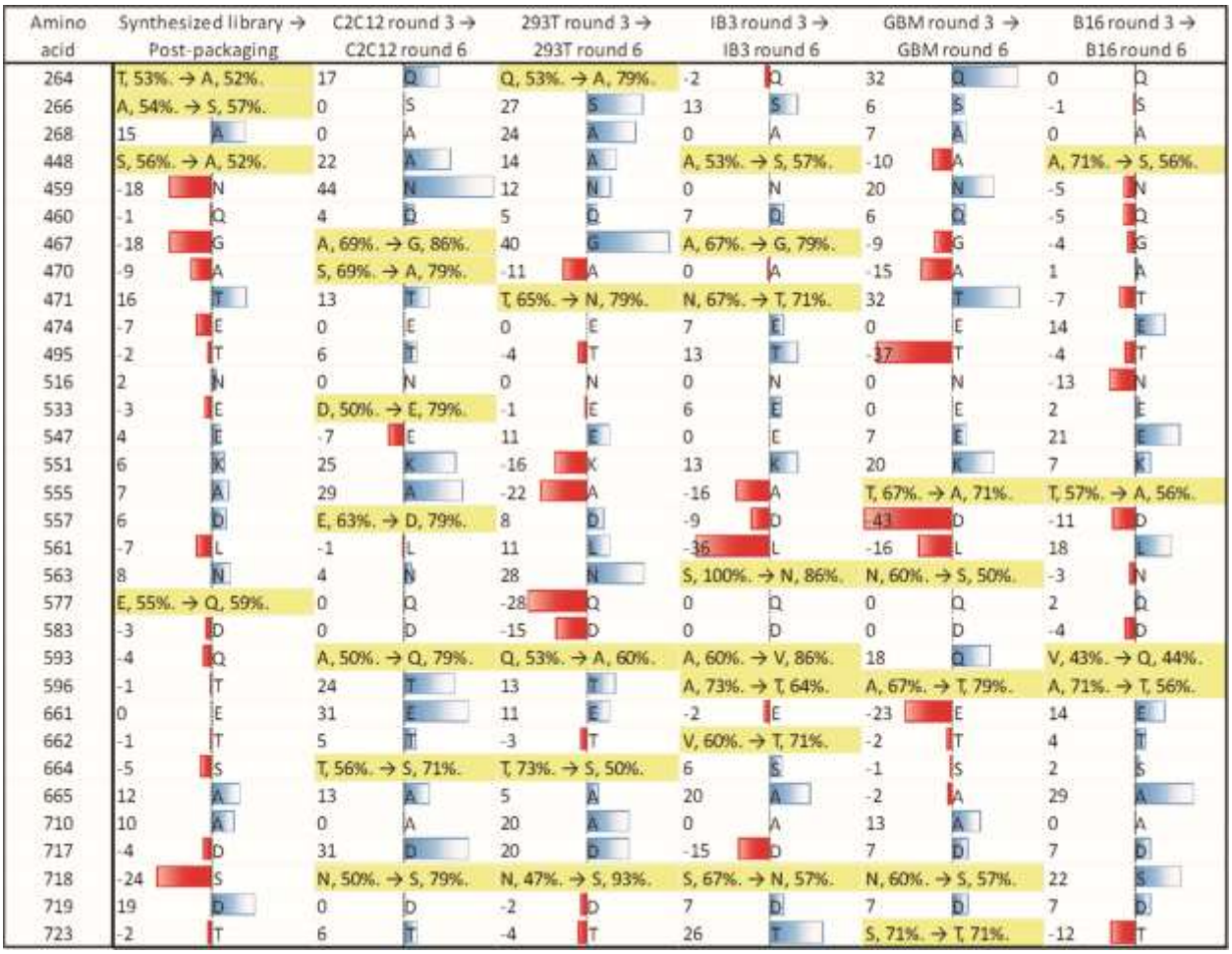

Amino acid	Synthesized library → Post-packaging	C2C12 round 3 → C2C12 round 6	293T round 3 → 293T round 6	IB3 round 3 → IB3 round 6	GBM round 3 → GBM round 6	B16 round 3 → B16 round 6
264	T, 53%. → A, 52%.	17 Q	Q, 53%. → A, 79%.	-2 Q	32 Q	0 Q
266	A, 54%. → S, 57%.	0 S	27 S	13 S	6 S	-1 S
268	15 A	0 A	24 A	0 A	7 A	0 A
448	S, 56%. → A, 52%.	22 A	14 A	A, 53%. → S, 57%.	-10 A	A, 71%. → S, 56%.
459	-18 N	44 N	12 N	0 N	20 N	-5 N
460	-1 Q	4 Q	5 Q	7 Q	6 Q	-5 Q
467	-18 G	A, 69%. → G, 86%.	40 G	A, 67%. → G, 79%.	-9 G	-4 G
470	-9 A	S, 69%. → A, 79%.	-11 A	0 A	-15 A	1 A
471	16 T	13 T	T, 65%. → N, 79%.	N, 67%. → T, 71%.	32 T	-7 T
474	-7 E	0 E	0 E	7 E	0 E	14 E
495	-2 T	6 T	-4 T	13 T	-37 T	-4 T
516	2 N	0 N	0 N	0 N	0 N	-13 N
533	-3 E	D, 50%. → E, 79%.	-1 E	6 E	0 E	2 E
547	4 E	-7 E	11 E	0 E	7 E	21 E
551	6 K	25 K	-16 K	13 K	20 K	7 K
555	7 A	29 A	-22 A	-16 A	T, 67%. → A, 71%.	T, 57%. → A, 56%.
557	6 D	E, 63%. → D, 79%.	8 D	-9 D	-43 D	-11 D
561	-7 L	-1 L	11 L	-36 L	-16 L	18 L
563	8 N	4 N	28 N	S, 100%. → N, 86%.	N, 60%. → S, 50%.	-3 N
577	E, 55%. → Q, 59%.	0 Q	-28 Q	0 Q	0 Q	2 Q
583	-3 D	0 D	-15 D	0 D	0 D	-4 D
593	-4 Q	A, 50%. → Q, 79%.	Q, 53%. → A, 60%.	A, 60%. → V, 86%.	18 Q	V, 43%. → Q, 44%.
596	-1 T	24 T	13 T	A, 73%. → T, 64%.	A, 67%. → T, 79%.	A, 71%. → T, 56%.
661	0 E	31 E	11 E	-2 E	-23 E	14 E
662	-1 T	5 T	-3 T	V, 60%. → T, 71%.	-2 T	4 T
664	-5 S	T, 56%. → S, 71%.	T, 73%. → S, 50%.	6 S	-1 S	2 S
665	12 A	13 A	5 A	20 A	-2 A	29 A
710	10 A	0 A	20 A	0 A	13 A	0 A
717	-4 D	31 D	20 D	-15 D	7 D	7 D
718	-24 S	N, 50%. → S, 79%.	N, 47%. → S, 93%.	S, 67%. → N, 57%.	N, 60%. → S, 57%.	22 S
719	19 D	0 D	-2 D	7 D	7 D	7 D
723	-2 T	6 T	-4 T	26 T	S, 71%. → T, 71%.	-12 T

Figure A.6. Glycan dependency of ancestral libraries and select ancestral variants. a) The transduction efficiency of ancestral libraries (after six rounds of selection) and select AAV variants C4, C7, and G4 carrying self-complimentary CMV-GFP was quantified by flow cytometry 72 hours after infection. For the libraries, infections were carried out at a genomic MOI of 2,000 (Pro5, Lec1, Lec2) and 50,000 (CHO-K1, pgsA). For select clones from the Round 6 C2C12 (C4, C7) and GBM (G4) libraries, infections were carried out at a genomic MOI of 500 (Pro5, Lec1, Lec2) and 13,000 (CHO-K1, pgsA) to ensure an adequate number of GFP positive cells for analysis. The CHO-K1/pgsA comparison examines heparan sulfate proteoglycan dependence, while Pro5/Lec1 and Pro5/Lec2 probe sialic acid dependence. Data are presented as mean ± SEM, $n = 3$. AL, ancestral library.

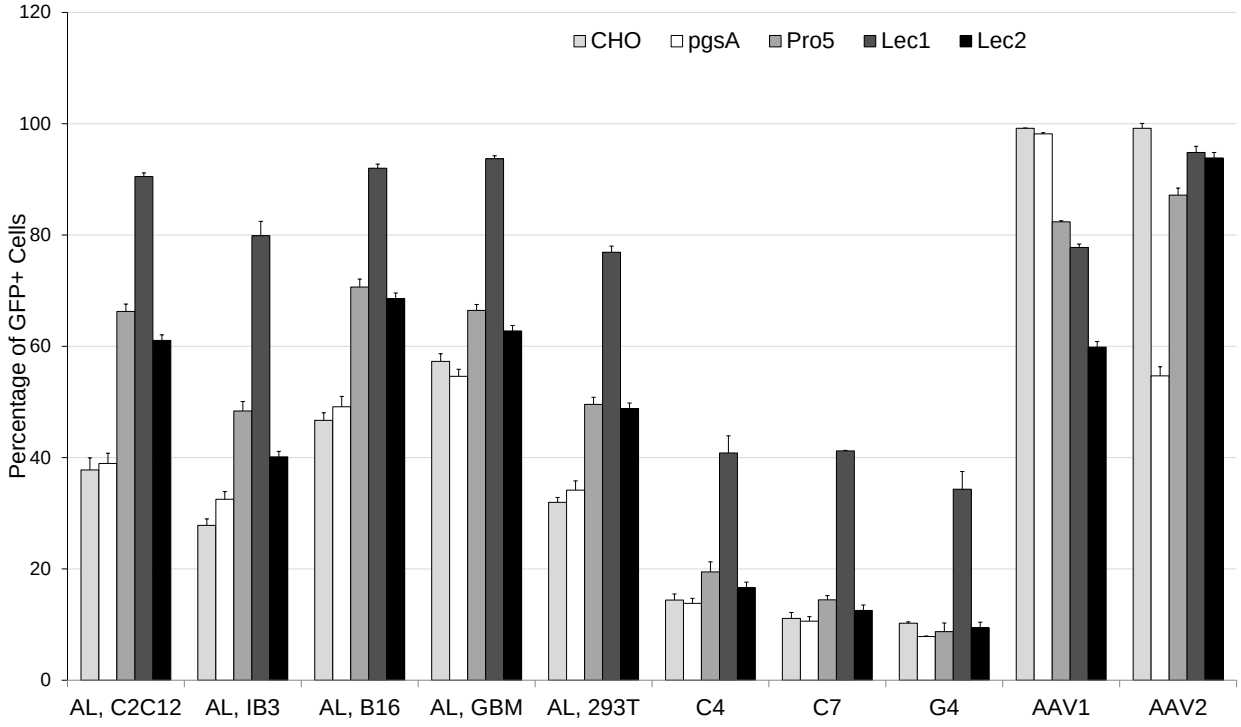

Figure A.7. Ancestral AAV libraries are neutralized by human intravenous immunoglobulin (IVIG) *in vitro*. Recombinant round 6 ancestral AAV libraries and AAV1 were packaged with a self-complimentary CMV-GFP cassette, incubated for one hour at 37°C with serial dilutions of heat-inactivated IVIG, then used to infect HEK293T cells at a genomic MOI of 2,000 (*n*=3). The fraction of GFP expressing cells was quantified by flow cytometry 72 hours later. Data are presented as mean ± SEM, *n* = 3. AL, ancestral library.

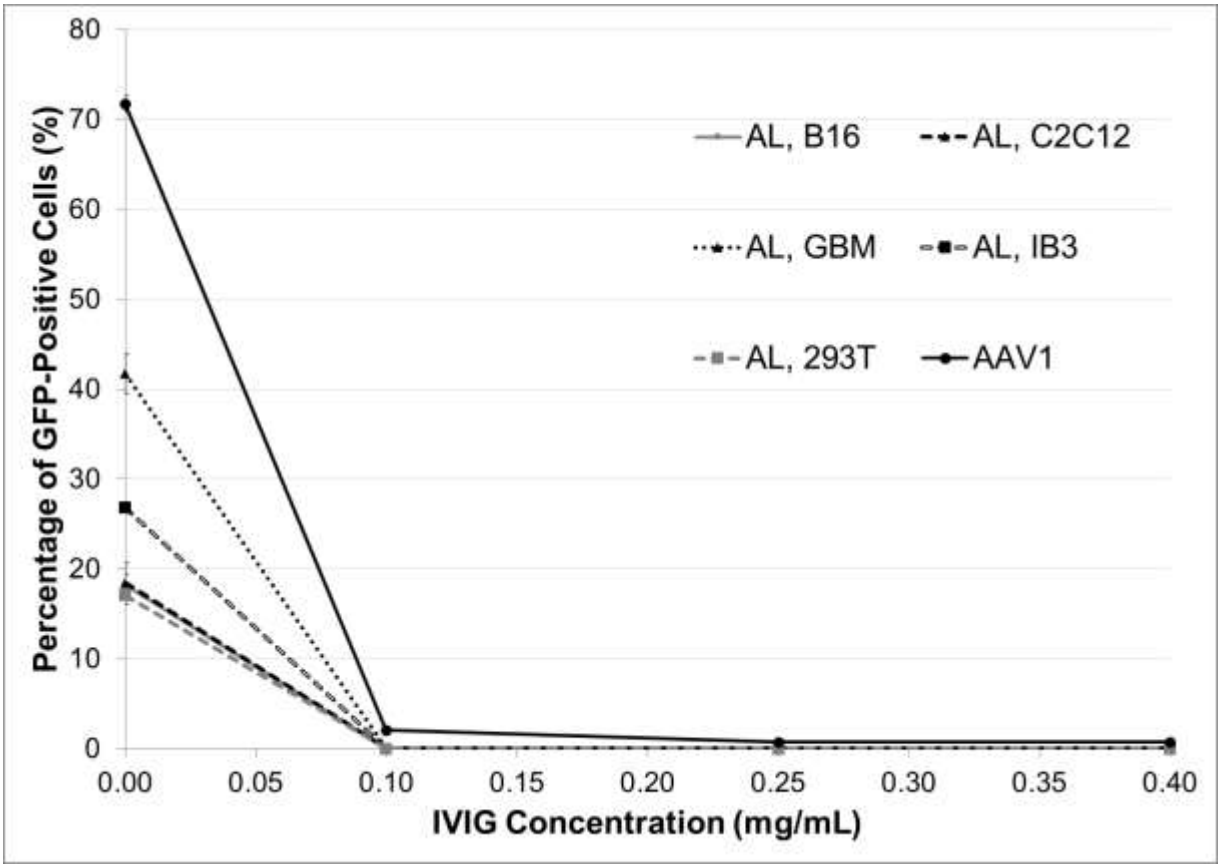

Table A.1. Selection stringency applied in ancestral AAV library selections.

Round of Selection	Genomic Multiplicity of Infection
1	5,000
2	500
3	250
4	250
5	50
6	25

Table A.2. Identities of the 32 variable amino acids present in the candidate ancestral clones evaluated *in vivo*.

Amino Acid	Ancestral AAV Clone		
	C4	**C7**	**G4**
264	A	Q	A
266	S	S	S
268	S	S	S
448	A	S	A
459	N	N	T
460	R	R	R
467	G	G	G
470	S	A	S
471	N	N	N
474	A	A	A
495	S	S	T
516	D	D	D
533	D	E	D
547	E	Q	Q
551	A	A	A
555	A	T	A
557	E	D	D
561	L	M	I
563	N	S	N
577	Q	Q	Q
583	S	S	S
593	A	Q	A
596	A	T	T
661	A	A	T
662	T	V	V
664	T	S	S
665	P	P	P
710	T	T	T
717	N	N	N
718	N	S	S
719	E	E	E
723	S	S	T

Appendix B: Supplementary Material for Chapter 4

B.1 Supplementary Figures and Tables

Figure B.1. Stable transduction of L0 cells with firefly luciferase and mCherry. (A) Bioluminescence imaging of a representative tumor-bearing mouse after transplantation of luciferase-expressing GBM TICs. Image taken 14 minutes after administration of D-luciferin four weeks post-surgery. (B) FACS-sorting of mCherry-expressing cells (P3) dissociated from the brain of a tumor-bearing mouse. Gating for control cells is depicted as P2 (bottom left).

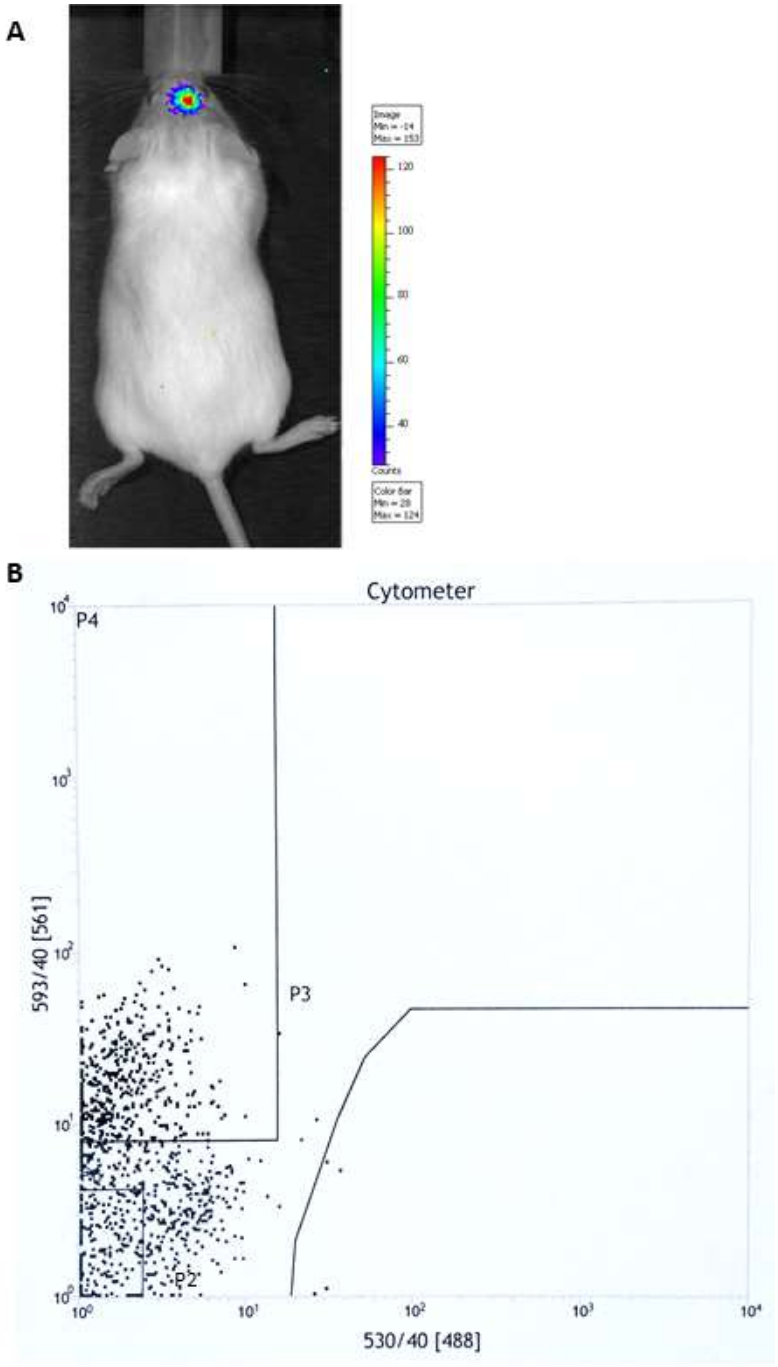

Figure B.2. Transduction by clone SGA1 is dependent on AAVR receptor. SGA1 encoding GFP was used to infect wild-type HeLa cells and an AAVR-knockout HeLa cell line (courtesy of Professor Jan E. Carette). Knockout of AAVR ablated AAV infection, showing that transduction with this clone is AAVR-dependent.

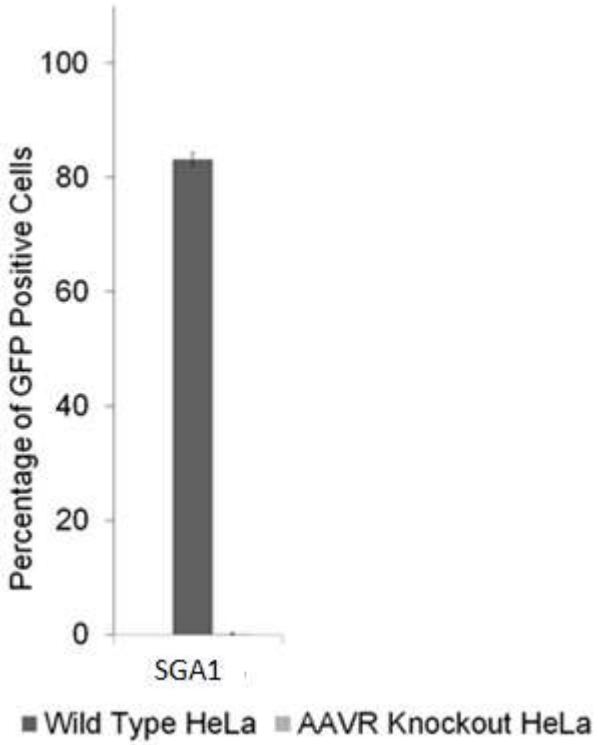

Table B.1. Residue identities at the diversified positions for the ancestral clone SGA1.

Residue Number	SGA1 (SSARASA); Also contains A70S and P148S point mutations
264	A
266	S
268	S
448	A
459	T
460	R
467	A
470	S
471	N
474	A
495	S
516	D
533	D
547	Q
551	A
555	T
557	E
561	L
563	N
577	Q
583	D
593	L
596	A
661	A
662	V
664	T
665	A
710	T
717	N
718	N
719	E
723	S

Table B.2. Description of recovered clones SGS1, and SGS2.

Clone Name	Block 1	Block 2	Block 3	Block 4	Block 5	Block 6	Block 7	Block 8
SGS1	AAV2; F110L	AAV2; L129F, P135G, V136A	AAV6	AAV8	AAV2	AAV2	AAV2	AAV2
SGS2	AAV2; F110L	AAV2; L129F, P135G, V136A	AAV9	AAV8	AAV2	AAV2	AAV9	AAV9

Table B.3. Primary sequences of recovered clones SGA1, SGS1, and SGS2.

Clone Name	Sequence
SGA1	MAADGYLPDWLEDNLSEGIREWWDLKPGAPKPKANQQKQDDGRGLVLPGYKYLGPF NGLDKGEPVNAADSAALEHDKAYDQQLKAGDNPYLRYNHADAEFQERLQEDTSFGGN LGRAVFQAKKRVLEPLGLVEEGAKTAPGKKRPVESSPQRSPDSSTGIGKKGQQPAKKRL NFGQTGDSESVPDPQPLGEPPAGPSGLGSGTMAAGGGAPMADNNEGADGVGNASGNW HCDSTWLGDRVITTSTRTWALPTYNNHLYKQISSASSGSTNDNHYFGYSTPWGYFDFNR FHCHFSPRDWQRLINNNWGFRPKRLNFKLFNIQVKEVTTNDGVTTIANNLTSTVQVFSD SEYQLPYVLGSAHQGCLPPFPADVFMIPQYGYLTLNNGSQAVGRSSFYCLEYFPSQMLR TGNNFTFSYTFEDVPFHSSYAHSQSLDRLMNPLIDQYLYYLARTQSTGGTAGTRELLFSQ AGPSNMSAQAKNWLPGPCYRQQRVSKTLSQNNNSNFAWTGATKYHLNGRDSLVNPGV AMATHKDDEDRFFPSSGVLIFGKQGAGANNTTLENVMLTNEEEIKTTNPVATEQYGVV ADNLQSSNTATGSSARASAGLSPLTGAVNSQGALPGMVWQNRDVYLQGPIWAKIPHTD GNFHPSPLMGGFGLKHPPPQILIKNTPVPANPPAVFTAAKFASFITQYSTGQVSVEIEWEL QKENSKRWNPEIQYTSNYAKSTNVDFAVNNEGVYSEPRPIGTRYLTRNL
SGS1	MAADGYLPDWLEDTLSEGIRQWWKLKPGPPPPKPAERHKDDSRGLVLPGYKYLGPFNG LDKGEPVNEADAAALEHDKAYDRQLDSGDNPYLKYNHADAEFQERLKEDTSLGGNLG RAVFQAKKRVLEPFGLVEEGAKTAPGKKRPVEHSPVEPDSSSGTGKAGQQPARKRLNF GQTGDADSVPDPQPLGQPPAAPSGLGTNTMATGSGAPMADNNEGADGVGNSSGNWHC DSTWMGDRVITTSTRTWALPTYNNHLYKQISSQSGASNDNHYFGYSTPWGYFDFNRFH CHFSPRDWQRLINNNWGFRPKRLNFKLFNIQVKEVTTNDGVTTIANNLTSTVQVFTDSE YQLPYVLGSAHQGCLPPFPADVFMIPQYGYLTLNNGSQAVGRSSFYCLEYFPSQMLRTG NNFQFSYTFEDVPFHSSYAHSQSLDRLMNPLIDQYLYYLSRTNTPSGTTTQSRLQFSQAG ASDIRDQSRNWLPGPCYRQQRVSKTSADNNNSEYSWTGATKYHLNGRDSLVNPGPAM ASHKDDEEKFFPQSGVLIFGKQGSEKTNVDIEKVMITDEEEIRATNPVATEQYGSVSTNL QRGNLASSPTTKSARQAATADVNTQGVLPGMVWQDRDVYLQGPIWAKIPHTDGHFHP SPLMGGFGLKHPPPQILIKNTPVPANPSTTFSAAKFASFITQYSTGQVSVEIEWELQKENS KRWNPEIQYTSNYNKSVNVDFTVDTNGVYSEPRPIGTRYLTRNL

SGS2	MAADGYLPDWLEDTLSEGIRQWWKLKPGPPPPKPAERHKDDSRGLVLPGYKYLGPFNG LDKGEPVNEADAAALEHDKAYDRQLDSGDNPYLKYNHADAEFQERLKEDTSLGGNLG RAVFQAKKRVLEPFGLVEEGAKTAPGKKRPVEHSPVEPDSSSGTGKAGQQPARKRLNF GQTGDADSVPDPQPLGQPPAAPSGLGTNTMATGSGAPMADNNEGADGVGNSSGNWHC DSTWMGDRVITTSTRTWALPTYNNHLYKQISSQSGASNDNHYFGYSTPWGYFDFNRFH CHFSPRDWQRLINNNWGFRPKRLNFKLFNIQVKEVTDNNGVKTIANNLTSTVQVFTDSE YQLPYVLGSAHQGCLPPFPADVFMIPQYGYLTLNNGSQAVGRSSFYCLEYFPSQMLRTG NNFQFTYTFEDVPFHSSYAHSQSLDRLMNPLIDQYLYYLSRTNTPSGTTTQSRLQFSQAG ASDIRDQSRNWLPGPCYRQQRVSKTSADNNNSEYSWTGATKYHLNGRDSLVNPGPAM ASHKDDEEKFFPQSGVLIFGKQGSEKTNVDIEKVMITDEEEIRTTNPVATEQYGSVSTNL QRGNLAIRTNGGAARQAATADVNTQGVLPGMVWQDRDVYLQGPIWAKIPHTDGNFHP SPLMGGFGMKHPPPQILIKNTPVPADPPTAFNKDKLNSFITQYSTGQVSVEIEWELQKEN SKRWNPEIQYTSNYYKSNNVEFAVNTEGVYSEPRPIGTRYLTRNL